Ministry of Education and Science of the Russian Federation
Federal Independent Educational Institution
“NATIONAL RESEARCH TOMSK POLYTECHNIC UNIVERSITY”

School ………………………………………………………….. Nuclear Science and Engineering
Direction of training (Specialty)…… ………………………... Nuclear Physics and Technology
Division……………………………………….. Nuclear Power Plant Installations and Operation

APPROVED BY:
Head of the Division

_____ _______ ____________
(Signature) (Date) (Full name)

ASSIGNMENT

for the Master’s Thesis completion

In the form:

Master’s thesis

(Master’s Thesis)

For a student:

Group	Full name
0АМ6И	Afornu Bright Kwame

Topic of the work:

Simulation of Cone Beam X-ray Computed Tomography and the Development of Reconstruction Algorithm for NDT Applications in the Nuclear Industry	
Approved by the order of the Head (date, number)	

Deadline for completion of the Master’s Thesis:	

TERMS OF REFERENCE:

Initial data for work *(the name of the object of research or design; performance or load; mode of operation (continuous, periodic, cyclic, etc.); type of raw material or material of the product; requirements for the product, product or process; special requirements to the features of the operation of the object or product in terms of operational safety, environmental impact, energy costs; economic analysis, etc.).*	Object of research – algorithm of 3D tomographic analysis Type of the algorithm – Filtered back-projection algorithm Beam pattern – parallel and cone beam Application – NDT and 3D analysis

List of the issues to be investigated, designed and developed *(analytical review of literary sources in order to elucidate the achievements of world science and technology in the field under consideration, the formulation of the problem of research, design, construction, the content of the procedure of the research, design, construction, discussion of the performed work results, the name of additional sections to be developed; work conclusion).*	**Theoretical aspect** 1. History and general understanding of X-ray radiography and tomography 2. Study of x-ray interactions with matter 3. Study of contrast types more specifically on absorption contrast 4. Tomographic setups involving parallel and conical beams 5. X-ray tomography applications in NDT **Practical aspect** 1. Python programming language training 2. Implementation of standard data collection scheme for parallel beam 3. Implementation of reconstruction algorithm parallel beam and filtering 4. Mathematical interpretation of conical (fan) pattern 5. Implementation of fan beam pattern 6. Reconstruction of fan beam pattern 7. Comparing the results of the parallel and conical (fan) pattern reconstruction.
List of graphic material *(with an exact indication of mandatory drawings)*	Block scheme of the developed algorithm

Advisors on the sections of the Master's Thesis
(with indication of sections)

Chapter	**Advisor**
Introduction	Dmitry Sednev, School of NDT and security, Deputy director for development
Literature review	Dmitry Sednev, School of NDT and security, Deputy director for development
Theoretical aspect of the reconstruction	Dmitry Sednev, School of NDT and security, Deputy director for development
Practical aspect of the reconstruction	Dmitry Sednev, School of NDT and security, Deputy director for development
Social responsibility	Dr. Dan A. Verigin, School of nuclear science and engineering, Division for nuclear-fuel cycle, senior lecturer
Financial management	Timur R. Rakhimov, School of engineering entrepreneurship, associate professor
Summary	Dr. Dan A. Verigin, School of nuclear science and engineering, Division for nuclear-fuel cycle, senior lecturer

Date of issuance of the assignment for Master's Thesis completion according to a line schedule	08 September 2017

The task was issued by the Head:

Position	Full name	Academic degree, academic status	Signature	Date
Deputy director for development	Dmitry Sednev Andreevich	PhD		

The assignment was accepted for execution by the student:

Group	Full name	Signature	Date
0AM6И	Afornu Bright Kwame		

Ministry of Education and Science of the Russian Federation
Federal Independent Educational Institution
“NATIONAL RESEARCH TOMSK POLYTECHNIC UNIVERSITY”

School ………………………………………………………….. Nuclear Science and Engineering
Direction of training (Specialty)…………………………………..... NPP Installations and Operation
Level of education ………………………………………...masters
Division …………………………………………… Nuclear Power Plant Installations and Operation
Period of completion…………………………………………… (fall/spring semester 2017/2018)

Form of presenting the work:

Master’s Thesis

(Master’s Thesis)

SCHEDULED COURSE ASSESSMENT CALENDAR
for the Master’s Thesis completion

Deadline for completion of the Master’s Thesis:	

Assessment date	**Title of section (module) / type of work (research)**	**Maximum score of the section (module)**
Sep 2017 – Dec 2017	Theoretical aspects of X-Ray tomography and it’s applications	
Jan 2018 – Feb 2018	Learning Python programming, training course	
Mar 2018 – May 2018	Simulations and algorithm development	

Made by professor:

Position	**Full name**	**Academic degree, academic status**	**Signature**	**Date**
Deputy director for development	Sednev D.A.			

AGREED:

Head of the Division	**Full name**	**Academic degree, academic status**	**Signature**	**Date**
Nuclear Power Plant Installations and Operation	Gorunov A.G.			

Ministry of Education and Science of the Russian Federation

Federal Independent Educational Institution
"NATIONAL RESEARCH TOMSK POLYTECHNIC UNIVERSITY"

School…………………………………………………………..Nuclear Science an Engineering

Direction of training (Specialty)……………………………….. Nuclear Physics and Technology

Division……………………………………….... Nuclear Power Plant Installations and Operation

MASTER'S THESIS

Topic of the work
Simulation of Cone Beam X-ray Computed Tomography and the Development of Reconstruction Algorithm for NDT Applications in the Nuclear Industry

UDC____________

Student

Group	Full name	Signature	Date
0AM6И	Afornu Bright Kwame		

Scientific Supervisor

Position	Full name	Academic degree, academic rank	Signature	Date
Deputy director for development	Dmitry Sednev Andreevich	PhD		

ADVISORS:

Section "Financial Management, Resource Efficiency and Resource Saving"

Position	Full name	Academic degree, academic rank	Signature	Date
Associate professor	Timur R. Rakhimov	PhD Economics		

Section "Social Responsibility"

Position	Full name	Academic degree, academic rank	Signature	Date
Senior lecturer	Dr. Dan A. Verigin	Associate professor		

ADMIT TO DEFENSE:

Head of the Division	Full name	Academic degree, academic rank	Signature	Date
Director	Oleg Dolmatov	Professor		

Tomsk – 2018

ABSTRACT

The master's dissertation consists of (147) pages; 79 figures; 17 tables; 47 references and 2 appendixes.

Keywords: simulations, cone beam, tomography, nuclear, industries, computed, X-rays, reconstruction, algorithm, development.

The objective of this study is to develop a reconstruction algorithm to directly simulate data acquired from cone beam x-ray tomography set-up.

The purpose of the study is to reduce the complexities involved in the rebinning algorithm and to make these codes easily available to industries involved in its applications.

Coding and simulations performed in this research were conducted with the use of the python programming software and ATOM IDE. Moreover, ANSYS Spaceclaim and ImageJ were used for flattening, handling and designing of phantoms involved.

As a result of the research, the goal was achieved with the mathematical, numerical, geometrical and algorithmic understanding of the propagation of fan beam as a subset of conical beam.

The degree of implementation of the developed algorithm for cone (fan) beam became a success through comparison of the results with the parallel reconstruction approach where same reconstruction images were obtained to prove the accuracy of the generated codes.

Possible Application areas of these codes generated includes the nuclear industries, heavy mechanical machine building industries where tomographic testing are conducted with the projection of cone beam x-rays from high energy particle accelerators. Also, it can be extended to medical imaging reconstruction involving cone beam for data acquisition purposes.

However, the knowledge acquisition in training workers in the research was economically efficient when conducted in the university than in a research institute and a working environment.

Table of Contents

ASSIGNMENT FOR THE SECTION "FINANCIAL MANAGEMENT, RESOURCE EFFICIENCY AND RESOURCE SAVING"

To the student:

Group	Name
0АМ6И	Afornu Bright Kwame

Institute	Nuclear Science and Engineering	**Department of**	Nuclear Power Plant
Education Level	Masters	**Direction/ specialty**	NPP Installations and Operation

<table>
<tr><td colspan="2">References for "Financial management, resource efficiency and resource conservation":</td></tr>
<tr><td>1. The cost of research: Logistics, energy, financial, information and human</td><td>According to manual provided</td></tr>
<tr><td>2. Norms and standards resource consumption</td><td>According to manual provided</td></tr>
<tr><td>3. used the tax system, tax rates, deductions, discounting and credit</td><td>According to manual provided</td></tr>
<tr><td colspan="2">The list of questions for study, design and development:</td></tr>
<tr><td>1. Evaluation of commercial and innovative potential STI</td><td>Implement at least 1 option from the list (1-6) below:
1. Potential consumers of research results
2. Analysis of competitive technical solutions from the perspective of resource efficiency and resource savings
3. Technology QUAD
4. FAST-analysis
5. Diagram Ishikawa
6. SWOT-analysis
Perform
• Evaluation of the project readiness for commercialization
• Methods for the commercialization of scientific and technological research</td></tr>
<tr><td>2. Development of the charter of scientific and technical project</td><td>• Objectives and outcomes of the project.
• The organizational structure of the project.
• Identification of possible alternatives</td></tr>
</table>

3. *Project management planning: the structure and schedule of the budget, risk and procurement organization*	• The structure of the work within the framework of scientific research • Determination of the complexity of work • Scheduling scientific research • The budget of the scientific and technical research (STR)
4. *Defining resource, financial, economic efficiency*	• Integral financial efficiency indicator • Integral resource-efficiency indicator • Integral total efficiency indicator • Comparative project efficiency indicator
List of graphic material	
1. *Segmentation of the market* 2. *Estimation of competitiveness of technical solutions* 3. *FAST-Chart* 4. *SWOT Matrix* 5. *Schedule and budget of the project* 6. *Assessment resource, financial and economic efficiency of the project*	

Date of issue of assignment	

Assignment given by consultant:

Position	Name	degree	Signature	Date
Associate Professor	**Timur R. Rakhimov**	**PhD Economics**		

Assignment received by student for implementation:

Group	Name	Signature	Date
0AM6И	Afornu Bright Kwame		

ASSIGNMENT FOR THE SECTION "SOCIAL RESPONSIBILITY"

To the student:

Group	Full name
ОАМ6И	Afornu Bright Kwame

School	National Research Tomsk Polytechnic University (TPU)	**Department**	**Nuclear Power Plant**
Degree	Masters	**Specialization**	Nuclear Power Plants Installations and Operations

Input data to the "social responsibility":	
1. *Describe workplace (work area) for occurrence of:*	– Harmful factors of the environment (microclimate, illumination, noise, vibration, electro-magnetic fields, ionizing radiation); – dangerous factors of environment factors (electrical, fire and explosive nature).
2. *Acquaintance and selection of legislative and normative documents on the topic*	– electrical safety; – fire and explosion safety; – labor protection requirements when working on a PC. – radiation safety
The list of subjects to study, design and develop:	
1. *Analysis of the identified harmful factors of the environment in the following sequence:*	– The effect of the factor on the human body; – Reduction of permissible standards with the required dimensionality (with reference to the relevant normative and technical document); – Proposed remedies (collective and individual).
2. *Analysis of identified hazards of the environment:*	– Electrical safety (including static electricity, protective equipment); – fire and explosion safety (causes, preventive measures, primary fire extinguishing agents).
Date of issue of the task for the section according to the schedule	

Task issued by consultant:

Position	Full name	Scientific degree, rank	Signature	date
Dr.	Dan A. Verigin	PhD		

The task was accepted by the student:

Group	Full name	Signature	date
ОАМ6И	Afornu Bright Kwame		

Introduction

In recent times, the advancement in research and technology in the field of computed tomography is now applicable not only in the medical imaging and diagnosis as used to be in the past decades. The application has now cut across to other disciplines such as industrial and engineering applications. This work was based on the applicability in the determination of defects in industrial and engineering materials known as non-destructive testing. However, this happens to be one of the most accurate and reliable technique of defect inspections and it is continually improved both in terms of software and hardware to yield an optimized result.

In industrial environment, such as the nuclear industry and many others, where various engineering components are constructed to stand the shocks and stress during their time of campaign, they are required to be well tested to ensure that they are free from defects before mounted to serve the purpose of which they've been built for. Moreover, during their campaign, they are also required to be investigated from time to time to avoid any catastrophic situation that may spring up from both the internal and external defects or cracks in the various components of the reactor vessels, steam generators, turbines, condensers, and many others.

Currently, there exist several non-destructive techniques, such as the visual measuring testing, acoustic monitoring, capillary testing, eddy current testing, ultrasonic testing, magnetic particle testing, radiation testing and many more. The radiation testing is a kind of testing which is based on the interaction of ionizing penetrating gamma and x-ray radiation with a controlled object accompanied by the transformation of the radiation image into a visible format on a memory device. This then formed the basis of tomography. Tomography is simply the accumulation of the 2-dimensional slices of images from several directions to form a 3-dimensional image due to alterations in the algorithms involved during the reconstruction stage. However, the radiation testing still stands out as one of the surfaces, subsurface and internal inspecting techniques. It also gives much information on the object of interest and the test results can be repeated severally. Despite its merits, it also has some disadvantages that need to be taking more seriously, for instance, it remains the most dangerous non-destructive testing techniques in history due to the involvement of radiation.

To detect defects in industrial materials, there are two major steps to arrive at the result. Firstly, the data acquisition stage which involves the setting up of equipment for projecting the radiation through the object of interest and registering the radiation absorbed data from the detector onto a computer unit. Secondly, the data collected are processed using codes with specific reconstruction algorithms to generate the image out of the data and this procedure is known as the reconstruction stage.

In the nuclear industry, there exist thousands of equipment of varied sizes which are liable to any kind of defects. Small and medium sizes of nuclear reactor components, spare parts and many others can be tested with the conventional x-ray tomography technique which can handle those sizes. However, large scale industrial objects such as the reactor vessels, steam generator vessels, pressurizers, condensers, turbines, emergency core cooling systems and many others of such sizes cannot be tested using the conventional set-up, since these sizes and weight cannot be rotated with the current rotational stage available. The figure 1 below is an example of such reactor components.

Figure 1 – Reactor vessel under construction in Atomenergomash

Figure 2 – Partially designed Reactor vessel in Atomenergomash

Hence, it requires the use of particle accelerators such as the modern betatrons that are designed to generate high energy x-ray beam to scan through such large industrial components. With the use of different data acquisition approach such as the translational based data acquisition technique, it is possible to acquire the necessary data required to process and reconstruct the image expected. However, x-rays projected from betatrons area not in the usual parallel beam pattern but in a conical beam shape. Therefore, this requires that the conical beam pattern undergoes rebinning to arrive at the fan beam or the parallel beam pattern which would simplify the reconstruction algorithm to be implemented. Rebinning is a process where by a conical beam is taking into fan beam shape and reformatted into parallel beam projections. This mathematical and algorithmic conversion sometimes alters the final reconstructed image by losing some qualities in the data.

Therefore, many industries that employs the rebinning approach prefer to use an algorithm that can process the cone beam data directly to obtain the image in order to avoid data loss and the other complications associated with the rebinning algorithm processes.

The main of objective of this research work would be focused on building a reconstruction algorithm which is capable of direct image reconstruction from the cone beam data acquired to obtain the final image to avoid the limitations that would be incurred during rebinning. Moreover, there are other algorithms of this kind already in existence but are very rare and expensive. Hence, success achieved in this research would help the nuclear industries, machine building industries, hospitals and many other industries that uses the cone beam x-ray computed tomography set-ups and data generated from betatrons to have access to these codes to enhance productivity and to reduce the time involved in the acquisition and processing of data. Hence, the theme "Simulation of Cone Beam X-ray Computed Tomography and the Development of Reconstruction Algorithm for NDT Applications in the Nuclear Industry".

Chapter 1 Literature review

1.1 History of x-ray radiography / tomography

The genesis of x-ray radiography was a coincidental discovery by a German professor of physics called Wilhelm Conrad Röntgen. This discovery took place on Friday 8th of November 1895 during an experiment which was based on the phenomena of light, and the emissions given by discharging electrical current in a highly-evacuated glass tube. This tube was hence named after another British investigator known as William Crookes as Crookes tube.

To Röntgen surprise and uncertainties, he figured out that any object across the room started to glow as his cardboard-covered tube was charged. It turned to be a barium platinocyanide-coated screen, an object that was involved in the coincidental discovery. As he continues to experiment by placing various materials between the tube source and the screen by testing the new generated rays, he also viewed the bones of his own hands well exposed in an outline of flesh.

Röntgen presented his introductory report to a medical society which was followed by radiographs including the image of his wife's right hand with a ring on it. Also, on the new year day of 1896, Röntgen sent the printed reports across the entire Europe to other physicists to have a glimpse of his new coincidental discovery.

On January 1896, the world was never the same as his discovery solves certain hidden problems of the medical age. Röntgen was then crowned the discoverer of a medical miracle in which he was awarded the first Nobel prize winner in physics in 1901. He then donated the money obtained from the Nobel prize to his university. He also refused to seek patents on his discovery of the new age, and he also shunned eponymous descriptions of the numerous applications embedded in his discovery. Another two great men known as Goodspeed and Jennings had an accidental radiography of coins on 22nd February 1890 before Röntgen. Moreover, the plates in their work laid unnoticed and unremarked until Röntgen’s declaration encouraged them to review their findings, hence neither laid claims to the discovery [4].

Figure 1.1a - Wilhelm Conrad Röntgen [March 27, 1845 - February 10,1923] Inventor of the x-ray and the first Nobel prize winner in physics (1901) [5]

Hence, his discovery gave birth to the science called radiology. It involved the use of medical imaging to diagnose in order to treat diseases which can be seen inside the body. Advancement in recent era has improve upon obtaining images of the interior of the body known as tomography. This is an imaging technique where three-dimensional view of the interior part of the body is obtained using many two-dimensional slices. Many of the two-dimensional modalities such as ultrasound, x-radiology, magnetic resonance imaging, and nuclear medicine can bring data into existence in three-dimensional view. The focus of this work is based on x-ray tomography which had improved many areas of life, including medicine, geoscience and as a non-destructive testing method for both interior and external inspection of engineering components of industrial materials.

After the x-ray radiography, came another breakthrough in that same field known as x-ray computed tomography by an English electrical engineer Sir Godfrey Newbold Hounsfield in 1972. He was the Nobel price award winner in 1979 for his numerous contributions in the field of physiology and medicine. He also contributed to the model of the very first computed tomography (CT) scanner and hence regarded the father of computed tomography. His role was highly accepted and applied in 1971 with a scan of a patient's cystic frontal lobe tumor at the Atkinson Morley Hospital in the United Kingdom. This great contribution made CT accepted immediately into the medical community, making his invention being the most important in radiology diagnosis after the discovery of x-rays. [6]

Figure 1.1b - Sir Godfrey Newbold Hounsfield [28th Aug. 1919 – 12th Aug. 2004]. Right is the first prototype CT scanner designed by Hounsfield [7]

In 1980's, the first application of the computed tomography in an industrial setting was revealed in the fields of non-destructive testing. This involves the gathering of small pieces of slices taking from different angles of object used in inspection routine. Moreover, in the 1990's, computed tomography 3D quantitative applications came out in a simple volume but takes a long time to analyze. [8]

Technological improvement in both hardware systems and software had made the computed tomography a potent and most wide spread non-destructive technique (NDT) tool which can inspect both internal and external part of complex industrial structures without leaving a trace of destruction. Furthermore, advancement in x-ray sources and improved detectors made the CT system design more complex which gives higher accuracy by providing accurate and precise geometrical information on the structures under inspection in recent times.

Determination of material composition, geometrical characteristics of test objects, density variation inspection and many others greatly employed CT techniques. Moreover, the CT technique can produce an accomplished three-dimensional framework of the scanned structural parts verified.

1.2 Interactions of x-rays with matter

X-rays are produced by accelerating electrons of high voltage and directing them towards a target metal. X-rays have an inbuilt energy that is capable of influencing matter during collision. These x-rays are generated when high speed electrons suddenly undergone deceleration by colliding with a target metal. When this occurs, x-rays are produced. This kind of x-rays are known as *bremsstrahlung x-rays* or in other word as ‘braking radiation’. Sufficient energy of bombarding electrons can easily knock out some electrons from the atom in the inner shell of the targeted metal. As this happens, electrons can change their states from higher energy level to occupy the vacancy created in the inner shell. During the transition process, x-ray photons with exact energies are emitted which can be determined by the energy levels of the electrons and are therefore known as *characteristic x-rays*.

There are five x-ray attenuation processes. These includes, coherent or elastic scattering, Compton scattering, Photoelectric effect, pair production and photodisintegration, hence, these are classified under two major groups of interactions known as scattering and absorption.

1.2.1 Coherent scattering

Coherent scattering, also known as elastic, classical, or Rayleigh scattering is a phenomenon which is mainly encountered by radiation with low energies. This process is among the photon interaction when x-rays or gamma photon's energy is smaller comparable to ionization energy of the atom. After interaction with an attenuation medium, the photon is unable to remove the electron from its state. Since the photon energy is far less than the binding energies of the electrons involved, the photon may encounter deflection from the its path which may have no loss of energy of the photon. Moreover, the energy of the electron may be raised, but would not be enough to move to an excited state or even become ionized. This makes the electron to quickly return to its original energy level which is then accompanied with emitting photons with same energy as that of the incident photon. Finally, the photon can undergo scattering and never absorbed. This is because, energy has not been completely transferred to the material. [9]

1.2.2 Photoelectric effect

Photoelectric effect also known as photoelectric absorption is a kind of interaction between gamma and x-ray photons with matter. It involves the emission of electrons from the surface of a metal as photon or light is shone on the metal surface as shown in the figure below.

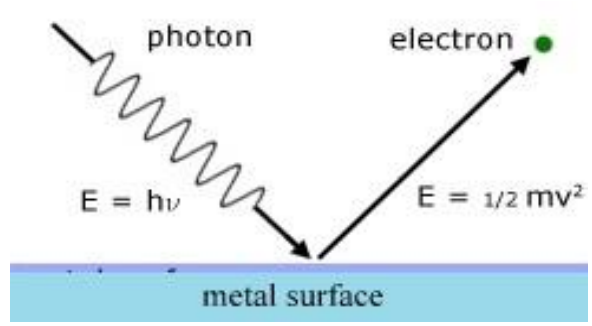

Figure 1.2.2a - Diagram showing the photoelectric emission.

The equation (1) represents the energy of the photon, where *h* represents Planck's constant, and *f* represents frequency of photon. Also, equation (2) represents the energy of the emit electron, where *m* and *v* are the mass and velocity of the emitted electron respectively.

$$E = hf \tag{1}$$

$$E = \frac{1}{2} m v^2 \tag{2}$$

During this interaction, an electron of an atom is easily removed from its shell by a low energy photon. This effect is highly probable when the electron is strongly bound such as the electrons in the K-shell. Also, the incident photon's energy must be either equal or almost greater than the electron's binding energy. Therefore, vacancies left in the K-shell would be occupied immediately by electrons in the closest shell, thus the L-shell. Since energy cannot be destroyed, the quantum jump then produces *characteristic radiation*. Therefore, the difference in energy levels where the transition occurred equals the energy carried by the x-rays in order to satisfy the principle of conservation of energy. Photoelectric effect can cause both absorption and attenuation, but not scattering. [10]

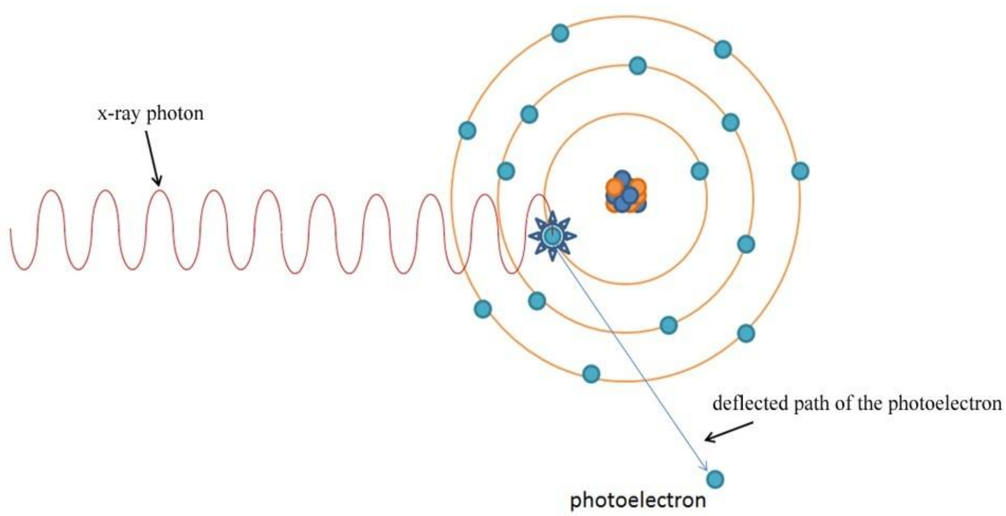

Figure 1.2.2b - Diagram showing how an x-ray photon knocks out electrons from the inner shell of the atomic nuclei during photoelectric emission phenomenon

1.2.3 Compton scattering

This is the process in which an incident x-ray photon undergoes deflections from its original path due to interaction with an electron. This is then followed by ejection of electron from its orbital, and a loss of energy of the x-ray due to the interaction yet continues to move in an altered path through the material. When a photon energy seems to be much higher than that of the electron's binding energy, this electron can be termed as free-electrons. However, interactions that exist between a photon and a free electron is regarded Compton scattering. During the process, both energy and momentum are being conserved. Also, the x -ray's photon energy becomes less and that resulted in longer wavelength with less penetrating ability of the incident photon.

The Compton effect was discovered by an American physicist, Arthur Holly Compton in 1923, and was awarded in 1927 a Noble prize in physics. This prominent discovery proves that light can never be well explained solely as just a wave phenomenon. This great work persuaded the entire scientific community based on Compton's view that, light behaves as a bundle of particles called photons, and this photon is proportional to the frequency. The equation (3) below depicts the change in wavelength of the scattered photon.

$$\lambda' - \lambda = \frac{h}{mc}\left(1 - \cos\theta\right) \tag{3}$$

Where λ' is the wavelength of the incident x-ray photon, λ being the scattered x-ray photon's wavelength, h represents Planck's constant, m is the electron rest mass, c represents the speed of light, and θ as the angle of the scattered photon. [11]

1.2.4 Pair production

This is a phenomenon involving high energy form of gamma interaction. The process involves the creation of a pair of charged particles out of a single high energy photon. Also, a kind of photon matter interaction that can only occur when photon's energy exceeds 1.02 MeV. During pair production, photon energy is converted into matter as the photon interacts with the nucleus, and this gives a pair of particles, namely, electron or negatron and its antiparticle known as positron as shown in the figure 1.2.4 below.

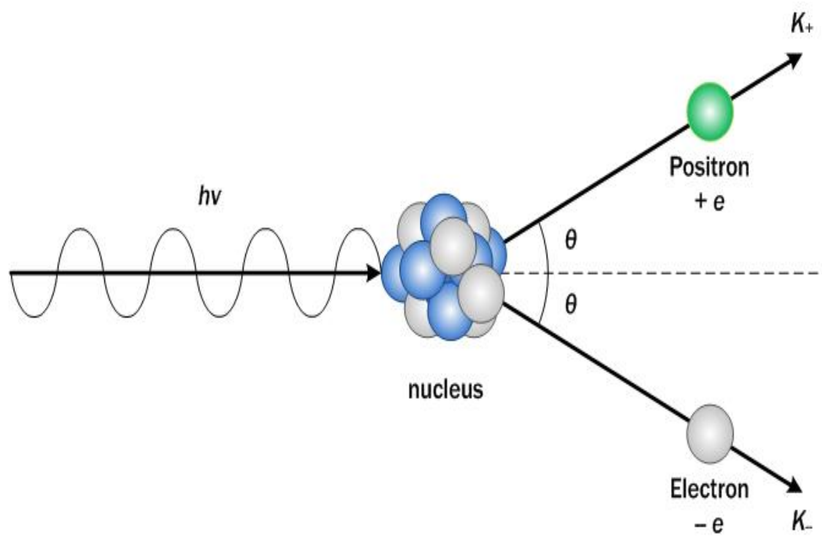

Figure 1.2.4 - Diagram showing pair production process

The remaining energy is being transferred to the pair particles as kinetic energy. However, the kinetic energies of the pair particles are absorbed by the medium involved, and the absorbed energy is always lesser than the original photon's energy. Moreover, electrons tend to lose all its energy whiles the positron eventually crashes with the electron, and this phenomenon is called positron-electron annihilation. This produces an equal rest mass of energy of 0.51 MeV each. [8] The equation (4) below explains the properties of the photon's energy during pair production.

$$E = (m_0 c^2 + T_1) + (m_0 c^2 + T_2) \tag{4}$$

Where E – is the energy of the photon, m_0 – is the particles rest mass, c – is the speed of light, T_1 and T_2 represents the kinetic energies of the electron and positron respectively.

1.2.5 Photodisintegration

For photodisintegration process to occur, an x-ray photon of energy greater than 10 MeV is required, and this is capable of escaping interactions with nuclear electric field and electrons. Since it involves collision of a very high energy photon with an atomic nucleus, and the photon may completely absorb the energy and projects it to enter the excited state. The nucleus splits, and then followed by emitting sub-atomic particles, such as neutrons, protons, and alpha particles.

1.3 The X-ray Tube

The x-ray tube is a vacuum cylindrical glass having positively charge electrode (Anode) where electrons leaves an electrical device, and a negatively charged electrode as an electron source for entering the device. In the internals of the tube lies an electrical contact connecting the terminals to a power source and a heating filament. To achieve an excellent heat conduction towards a target area of either tungsten or rhodium, copper is used in building the anode. The tungsten has a higher melting point than copper. X-rays tube degree of efficiency is very poor, because only very small number of kinetic energy of the electron beams is really emitted as x-ray. The equation below describes the efficiency of the x-ray.

$$\eta = k \cdot U \cdot Z \tag{5}$$

k – proportionality constant $\approx 1.1 \cdot 10^{-9}$, U – the voltage of the anode, Z - atomic number of the anode material. Typical, only about 1% of the total energy is emitted as x-rays whiles the remaining 99% is lost as heat in the tube.

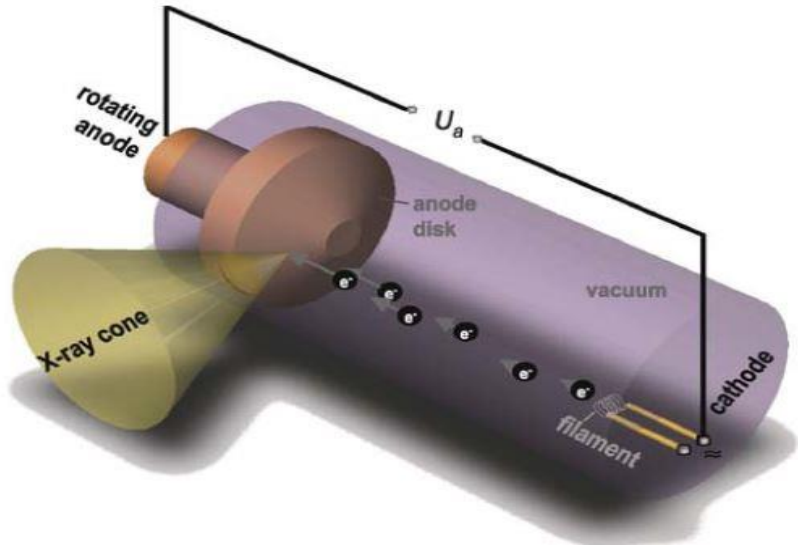

Figure 1.3 Schematic representation of an X-ray tube. [12]

The cathode is heated by the tungsten filament to approximately 2400K. This is then followed by a thermionic emission, where electrons are discharged into the vacuum. These electrons are then accelerated due to the electrostatic field existing between the two terminals. When these electrons knock the target anode material, x-rays radiation are then emitted due to deceleration taking place during the collision. Moreover, heat is then generated and transported outside the tube due to the huge size of the anode metal. To keep efficiency at an optimum level, rotating anodes are used for x-rays purposely designed for continuous operations instead of fixed ones. This is done by rotating the large disc of the anode with an electric motor and lowers the local heating of the tube than a fixed one. [13]

1.4 Types of contrast

Visible light in modern science serves as a powerful and most wide spread tool with several applications in all aspects of life. Contrast is a term used to distinguished between objects appearance or to differentiate an object from its background. This is based on the relative intensities of light on the objects and background under discussion. The effects of light on objects on a microscopic scale does not absorb much light, and they required ways to improve the contrast to achieve accurate details of the images. In this paper, three main types of contrast effects enacted by x-rays on objects would be discussed, namely absorption, phase, and dark field contrast.

1.4.1 Dark field contrast

Dark field imaging occurs in both electron and light microscopy in which the unscattered beam from the image is excluded, and this results in creating field around the specimen which is generally dark. This is also because, there exists no specimen at that field to scatter the beam. Even with many works done on x-ray imaging by early pioneers, such as the x-ray interferometry in the 1960s by Hart and Bonse [14], the main work on both phase and dark field imaging techniques were introduced in the late 1990s. [15] Moreover, these development of advanced imaging techniques are difficult to respond to hard x-rays within the energy range of several kilo-electronvolts (keV), due to lack of effective x-ray optics. The main limitations associated with dark field microscopy is the low level of light even in the final image, meaning the sample had to be well brightened, but this can also lead to damages to the final result of the image under study. Therefore, dark field imaging ought to be worked on with absolute care during processing and interpretation stages to avoid damaging bright field images as well.

1.4.2 Phase-contrast x-ray imaging

The term *phase contrast x-ray* imaging is used to describe the technical methods that involves changes in the phase of an x-ray photon that penetrates an object and results in creating its images. X-ray imaging techniques such as radiography and CT occurs when the intensity of the x-ray beams decreases as they attenuate or travels through a sample. This can be measured with the aid of an x-ray detector. [16]

Also, three-dimensional projection images can be achieved with phase-contrast x-ray imaging when it is combined with tomographic techniques. An improved soft tissue contrast images are obtained when this technique is applied to samples that are of low atomic number, Z, since the phase contrast imaging becomes more sensitive towards density variations in the sample than a conventional x-ray imaging. [17]

In the past two decades, various techniques of the x-ray imaging have been upgraded to exploit the phase contrast of the x-ray, and these are based on the interference patterns observed between diffracted and undiffracted waves. [18] these phase contrast methods can be grouped into five main categories. These includes, crystal interferometry, analyzer-based imaging (ABI), propagation-based imaging (PBI), grating interferometry method (GI), and edge-illumination imaging.

Brief description of PBI, GI, and ABI Phase-contrast techniques.

1.4.3 Propagation based imaging (PBI)

This is the simplest method due to the simplicity in the setup. In this method, the sample is irradiated with highly spatial consistent radiation when the detector is carefully placed at a distance from the sample under investigation. It does need any sophisticated optical elements in between the sample and the detector. According to Kirchhoff Fresnel's on near field diffractions, differences in phase shifts as introduced by the beam onto the object will lead modulation of measurable intensities on the detector. [19] The figure 1.4.3 below describes the propagation-based imaging as explained above.

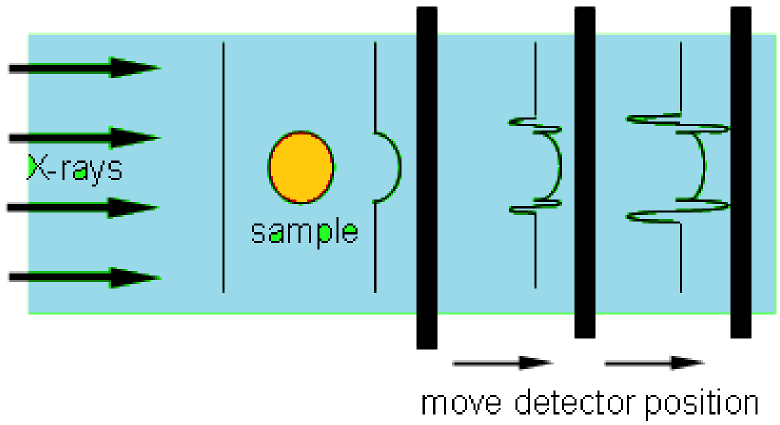

Figure 1.4.3 Diagram of the propagation-based imaging

1.4.4 Grating based imaging

This method is also known as the grating interferometry. It irradiates the image sample with highly coherent x-rays. This radiation through the object are analyzed using a pair of gratings. Hence, the phase grating introduces a periodic phase shift, but of negligible absorption on the beam. However, the second absorption grating is placed at a fractional Talbot distance away from the source, accompanied by a self-imaging effect from interference fringes created by the first grating. [20]

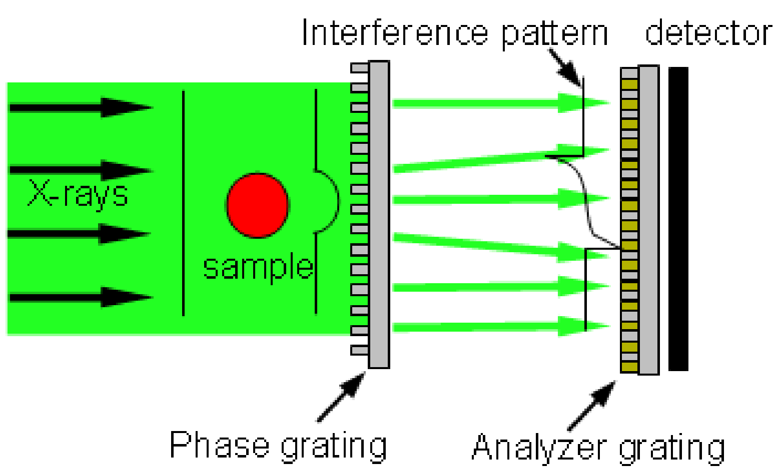

Figure 1.4.4 Diagram of the Grating based imaging (GI)

1.4.5 Analyzer based imaging

This technique setup consists of a monochromator in the front of the sample and the analyzer crystal positioned in between the sample and the detector according to Bragg's geometry as show in the figure 1.4.5 below.

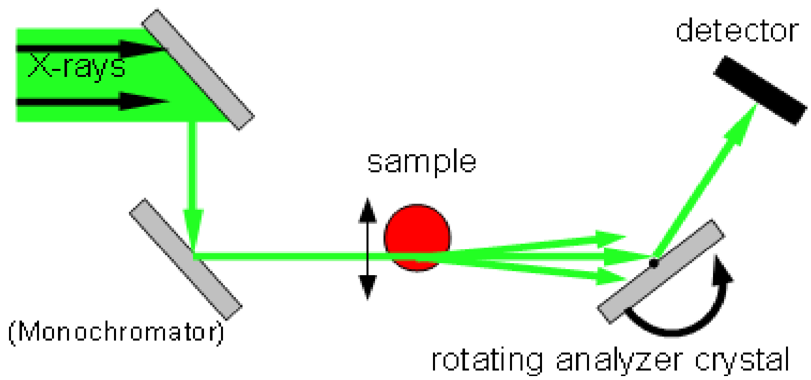

Figure 1.4.5 Diagram of the Analyzer-based imaging

X-rays hits the analyzer crystal which acts as an angular filter for the incoming radiation from the sample. The conditions of Bragg's diffraction become satisfied only for very narrow range of incident angles. Therefore, the unscattered or refracted x-rays whose incident angles lies out of the range won't undergo reflection, and they don't also contribute to the signal formed. [21]

1.4.6 Absorption contrast imaging

Absorption contrast imaging is one of the commonest and wide spread technique used in hospital x-ray imaging systems. This technique gives a shadowgraph which is being generated per various attenuating strengths of materials in the sample. The high intensity of synchrotron x-rays with tiny spot dimension makes scanning samples possible and also gives a complex image in a high-quality detail compared to that of the conventional sources.

Moreover, working with both x-ray techniques and absorption contrast imaging techniques yields a fine image with detailed information. Absorption contrast imaging is widely applicable in the fields of material science, environmental science, engineering, nanotechnology, bio-medicine and many more. [22]

1.5 Principles of modern radiography / tomography

Computed tomography also known as computed aided or axial tomography is a technique that involves the utilization of computed procedures in addition to several x-ray measurements obtained from different angles of the part of the material under investigation, and then producing cross-sectional images or slices of the scanned areas. This then grants the user the ability to view the internals of the object without cutting through. The introduction of computed tomography into the industrial environment was about four decays ago, and since then, there has been several upgrades on the technology involved, more importantly in the fields of non-destructive testing. This has a great advantage over the traditional destructive techniques. Moreover, the advancement in the production of more stable x-ray sources combined with better detecting technology boost the interest in engineering and scientific studies. As a non-destructive testing technique, it gathers several methods which makes it unique during inspection without leaving a trace of destruction of the part under investigation. Modern tomography has gain several applications in the industrial, medical, scientific environment and many more [23]. The figure 1.5.1 below represents the basic setup for the conventional tomography.

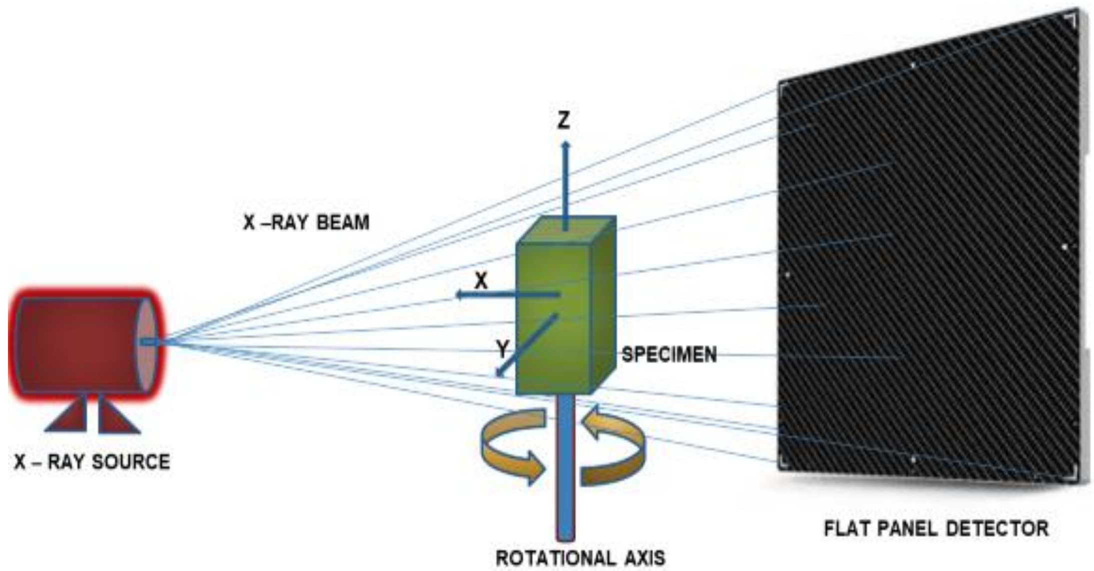

Figure 1.5.1 - Sketch of the conventional tomography setup.

The setup in figure 1.5.1 represents the basic scheme of conventional x-ray computed tomography data acquisition setup, also known as the rotational technique. It involves an x-ray source, the specimen under investigation, a flat panel detector where the data acquisition system coupled with reconstruction complex system.

In the x-ray tube, x-rays are generated inside the evacuated glass tube. From a high voltage source, the positive terminal is connected to the anode and is made of a refractive metal to enhance heat conduction. The negative pole is connected to the thermionic cathode as shown in the figure 1.5.2 below

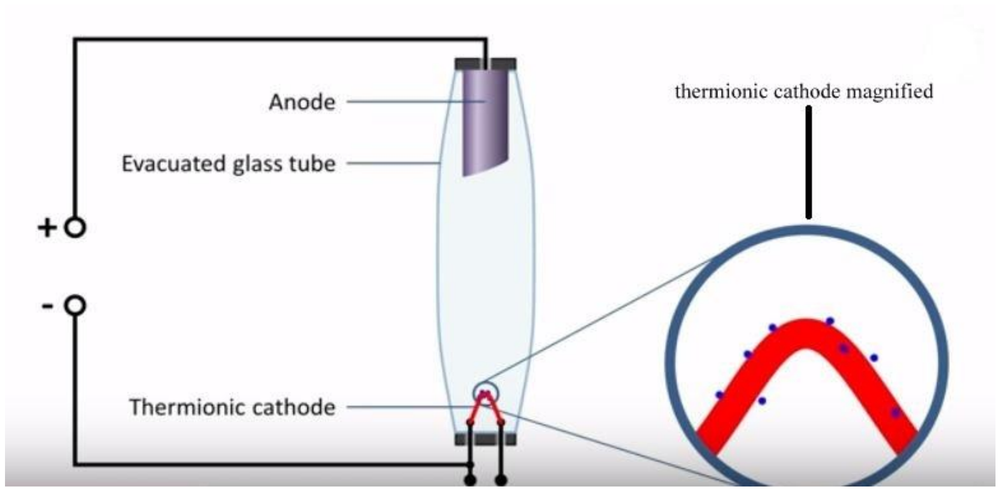

Figure 1.5.2 - Schematic view of the x-ray tube.

This thermionic cathode is then heated by electric current, where the thermal movement enable some electrons inside the wire to leave the metal surface. This phenomenon is known as thermionic emission. Therefore, by switching the high voltage source, strong electric field between the thermionic cathode and the anode is created. This strong electric field accelerates the emitted electrons towards the anode to form an electron beam. The electron beam collides with the anode at high velocity which is then slowed within a short distance as shown in the figure 1.5.3 below.

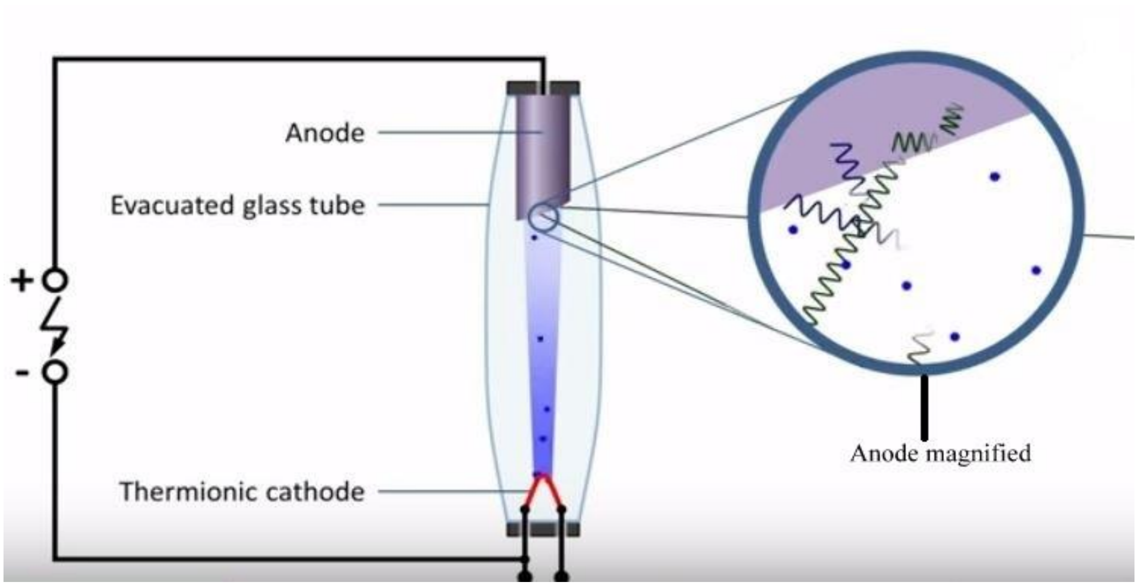

Figure 1.5.3 - Schematic view of the x-ray tube.

These generates the desire x-rays and large amount of heat. Therefore, the x-ray source casing is responsible for directing the x-rays to a specified direction. A transparent window created close to the anode at a suitable angle where the x-rays are generated is responsible for directing the x-rays out of the tube as shown in the figure 1.5.4 below. To enhance the quality of x-ray as well as the contrast of the image, an electromagnetic lens inside the tube is installed to focus the electrons on a small spot of the anode surface as shown in the figure 1.5.4 below.

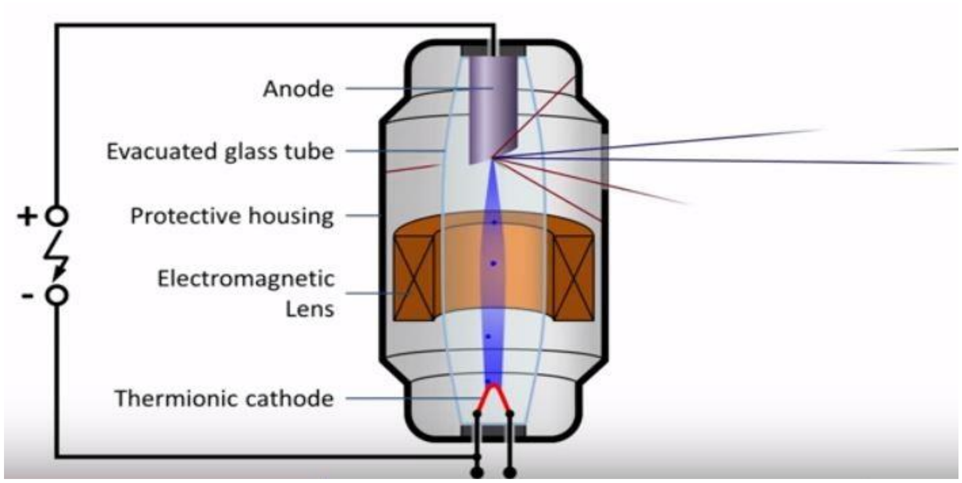

Figure 1.5.4 - Schematic view of the x-ray tube

This then focus the x-ray beam to give a sharper, and higher contrast of the x-ray image. In the production of x-ray imaging, the usable x-rays are directed through the transparent window of the source onto the test specimen. To obtain an image, an x-ray film or digital detector of suitable capturing power is used. The x-ray films give darker images because of higher intensity. The digital detector field measures the intensity of the radiation and converts to electrical signals. As the radiation intensity is plotted as a function of the position, a uniform distribution is attained as shown in the figure 1.5.5 below.

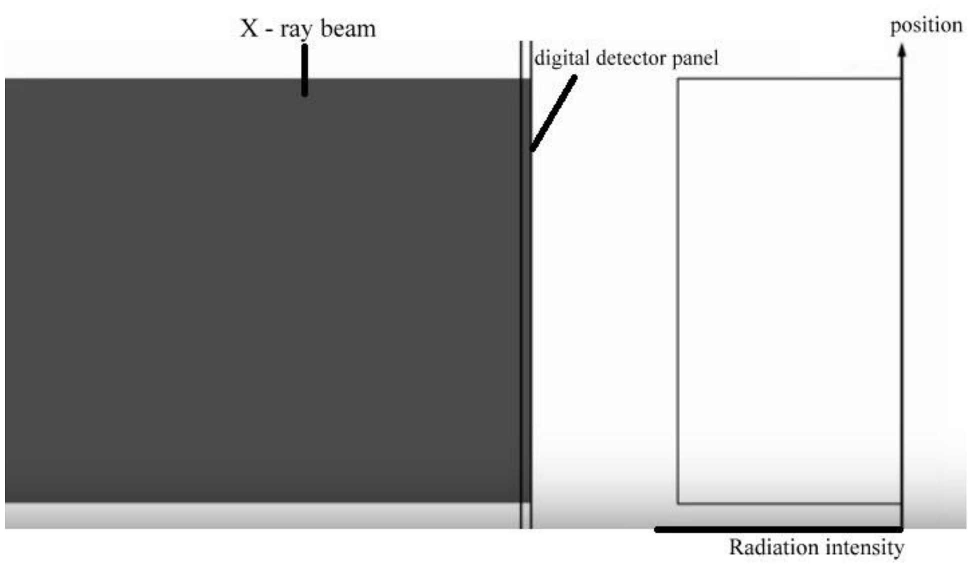

Figure 1.5.5 - Schematic view of the usable parallel x-ray beam and its effect.

When an object is placed between the x-ray source and the detector, the object absorbs some part of the x-ray radiation. The principle of this phenomenon is that, the thicker the object in the direction of the x-ray beam propagation, and the higher the density, the less radiation reaches the image capture unit as indicated in the figure 1.5.6 below.

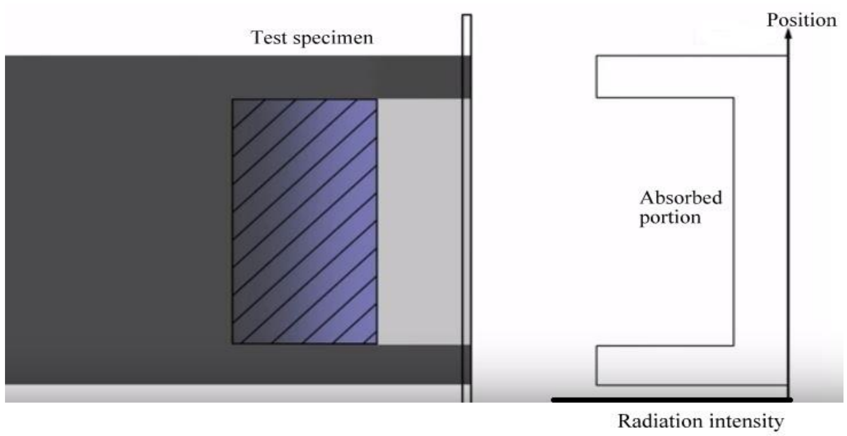

Figure 1.5.6 - Diagram showing radiation absorbed by the test specimen.

Defects such as cracks and pores absorb very little radiation and then lead to higher propagation intensity on the image capture unit. Cracks or faults in the direction of propagated beam can be seen very clear that those that are not in the same direction. For instance, the crack (c) in the figure 1.5.7 below cannot be seen at all. Places with more defects looks darker. This is because, more x-ray radiation reaches the image detector unit.

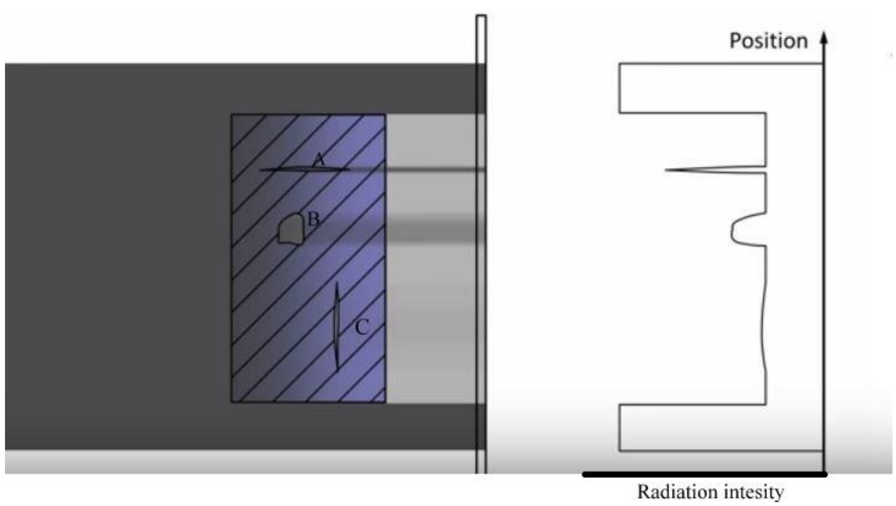

Figure 1.5.7 - Schematic view of defect records on the image detector unit.

The figure 1.5.7 explains why the defect position as well as the defects which are not in the direction of the x-ray propagation cannot be exactly identified with just a single x-ray imaging. To detect the depth of the location of the defect, whether left or right, it requires an additional source of x-ray image taking from a different direction. Therefore, computed tomography uses this approach to arrive at a 3D view with much details on the depth and position of the defects. This is then achieved through using the rotational or translational techniques. The rotational technique has to do with rotating the test specimen as the beam strikes it and the results and images saved. The translational technique considers the variations of magnification. For instance, changing the x-ray focal length distance and that of the detector panel will yield different ray paths and the beam angles with respect to the test specimen under inspection.

1.6 Industrial tomographic set-up

Computed tomography is highly applicable in inspecting and detecting defects in engineering materials in many industries. The figure 1.6 below is the exact set-up employed in creating tomographic images of test specimen.

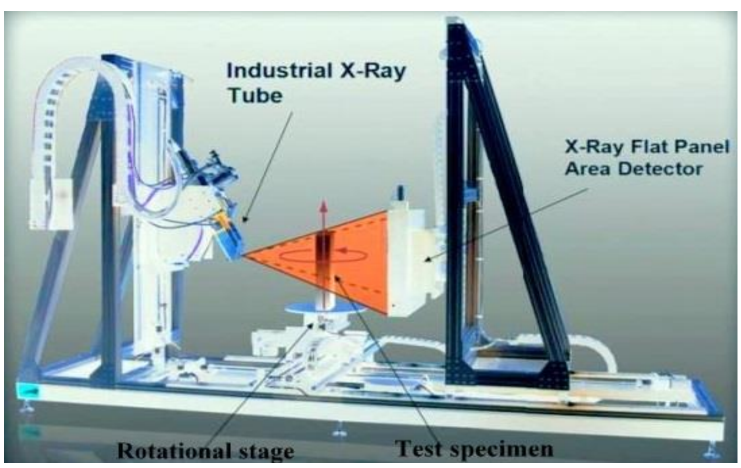

Figure 1.6 - Industrial x-ray rotational imaging set-up. [24]

The x-ray tube is placed at the left side and the x-ray detector unit place at the right side, while the test specimen placed in between them fixed on a rotation stage. In this set-up, the x-rays from the source are projected to strike the test specimen or object under inspection, where some of these radiations are absorbed and the resulting image recorded and saved on a computer system. After each recording, the object is rotated at a given angle by the rotational stage results recorded and saved. These rotational processes continue until 360-degree turn is obtained. The thicker areas or parts free from defects of the object under inspection shows darker whiles parts with thinner or with defects appears light, and in the case of any holes in the test specimen, the resulting image appears clearly visible.

1.7 Medical tomography set-up

The word tomography evolved from the Greek words "tome" meaning cut and "graphein" meaning to write. Tomography can simply be described as imaging by sectioning. [25] Cutting into objects for inspections can be possible sometimes but cannot be applicable in the case of humans. Tomographic technique uses software programme to obtain several slices to model into a three-dimensional view to have access to the interior of the object. Hence, in x-ray tomography used for medical purposes involves a complete system of rotating x-ray tube, detector, data acquisition system, electron gun, target ring and many more known as CT scanner as shown in the figure 1.7.1 below.

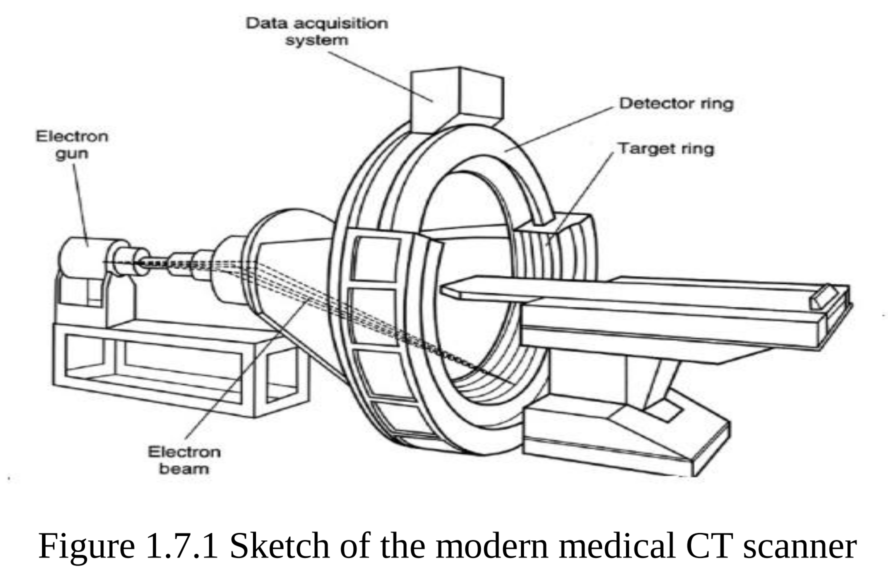

Figure 1.7.1 Sketch of the modern medical CT scanner

It comprises a narrow x-ray tube in which a beam of narrow x-ray is projected from the electron gun through the patient and rotated speedily around the patient. This process generates signals which are quickly processed by the system's computer to give cross-sectional images known as slices of the patient's body.

The conventional x-ray uses a fixed x-ray tube whiles a CT scanner uses a motorized x-ray system. This system turns around the circular opening known as gantry. During a CT scan section, the patient lies on the bed and he or she is moved gently through the gantry as the x-ray turns around the patient. This is followed by projecting the narrow x-ray beams through the body. Unlike the film used to receive the images in the conventional x-ray, the CT scanner has a special x-ray detector system located just opposite the x-ray source. Immediately x-rays penetrate and leaves the patient, the detector records the signal received and then transmits to a computer.

Each complete rotation of the x-ray source generates enough data of the patient, where the data is processed by the CT computer using sophisticated mathematical techniques to build a 2D image slice of the patient. Moreover, the tissues in each slice varies and is dependent on the type of CT machine, and these tissue dimensions' ranges between 1-10 mm. After a complete slice is achieved and stored, the motorized bed is moved into the gantry. This scanning process is repeated to obtain another image slice until the expected number of slices are obtained.

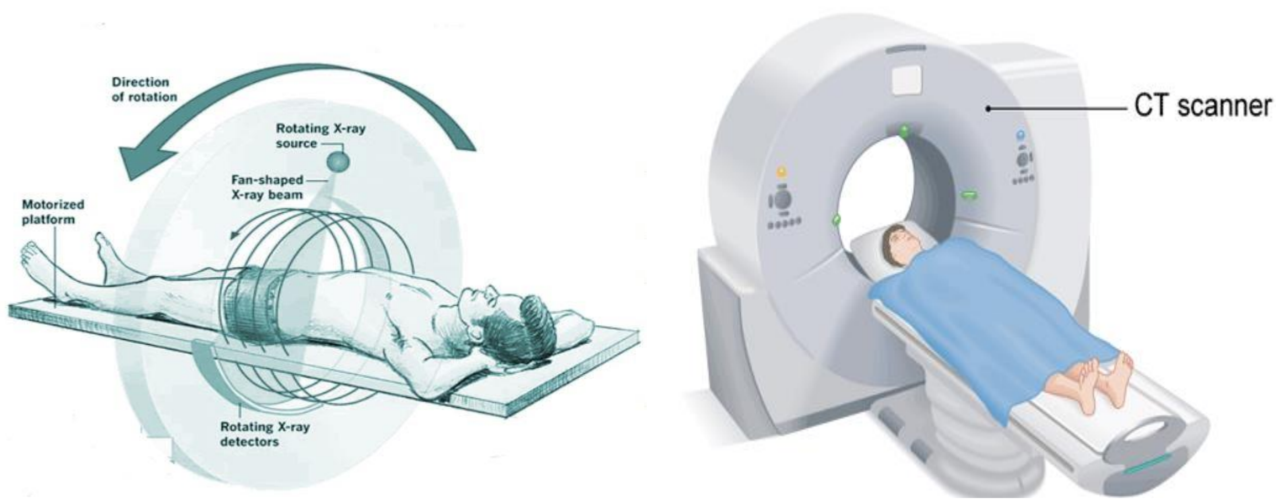

Figure 1.7.2 Diagram of a patient undergoing a CT scan. [26]

However, the slices can be displayed separately or stacked by the computer to yield a 3D image showing the tissues, organs, skeletons and possible abnormalities the physician might be struggling to identify. One major distinguished advantage of the method is the tendency to rotate the 3D image in a space or even view slice by slice in series to easily locate the exact position of the problem.

1.8 Limitations of the conventional data acquisition technique.

Despite all the effort and improvement in the conventional rotational data acquisition technique such as increasing the scan speed, most systems depend on a fan-beam type or cone beam geometry [27]. These developments enhance the acquisition of more than a slice in a single rotational scan through the test specimen. Hence, this is achieved by using multi-row or flat-panel detectors. However, there are several objects in situations which demands inspections for safety and for many reasons yet cannot be rotated due to the inaccessible positions they are located, size and many more. For instance, rotating a large scale industrial object using the conventional technique seems impossible. This is because, it requires complex technologies to design a rotational stage which can carry very large objects and to be able to rotate them precisely and accurately at very small rotational angle as small as 0.1 degree.

Figure 1.8.1 – Partially complete reactor pressure vessel [Atomenergomash]

Assuming, we want to inspect for defects in the reactor pressure vessel in the figure 1.8.1 above, it will be difficult to build the stage to accommodate it, it will also be difficult to fixed it firmly on the rotational stage and even to think of rotating it mechanically. However, it will be highly expensive to be able to achieve the aim of bringing all these ideas to reality. In addition, it will be very expensive to order for the design of a large panel detector for this kind of inspection.

1.9 Translational based data acquisition scheme

This data acquisition technique can overcome the main limitation posed by the conventional technique. In the translational data acquisition scheme, a rotational stage is not needed, since it involves the variation and changing of the focal distances and directions between the source x-ray and the detector only, hence the object under investigation is maintained in a stationary position. These are done for the purpose to obtained different ray paths and beam angles to acquire enough data for the image processing stage and to give a detailed and brighter image at the end. For instance, the figure below illustrates a translational based data acquisition scheme involving the linear translation of just the source x-ray.

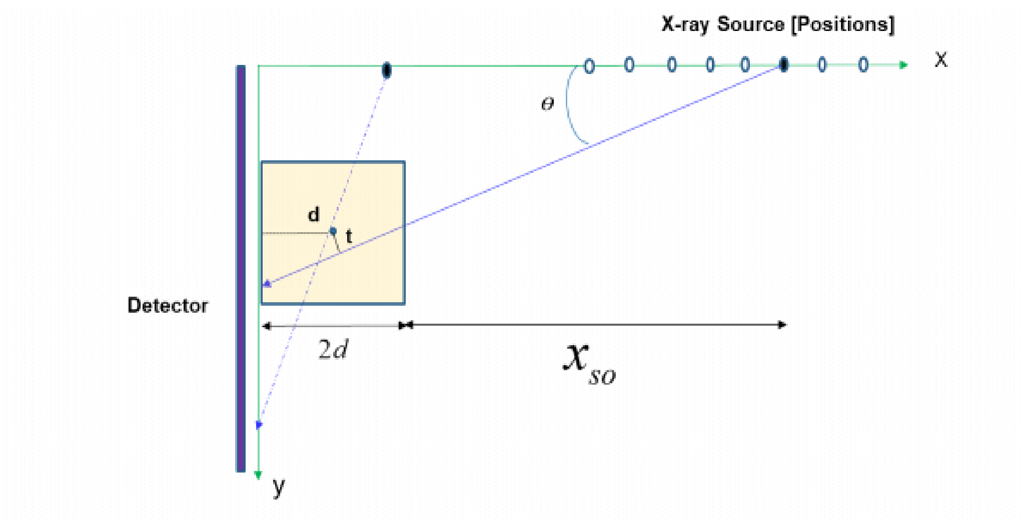

Figure 1.9 Scheme for translational based data acquisition

From the scheme, scans were taken from different focal distances as well as directions as the source x-ray position was varied. This technique can be used to acquire data of larger and complicated objects compared to the classical method. The thick blue vertical line represents the detector and is positioned behind the object. The distance *d* of the object indicates the dimension of the cross-section that encompasses the measured field. Also, χ_{so} represents the distance between the x-ray source and the object at a point of arrangement. However, the beam angles directed through the object varies as the source position is translated [28].

Chapter 2 – Theoretical aspect of the reconstruction process

2.1 Reconstruction algorithms.

Image processing and reconstruction depends greatly on mathematical modeling procedures that aids to generate tomographic images from the x-ray projection data as obtained from different angles around the specimen as explained above. In this stage, several useful reconstruction methods coupled with tomography software to reconstruct a multidimensional image view of the interior of the specimen under inspection exist. These reconstruction algorithmic techniques include the filtered back-projection algorithm technique (FBP), algebraic reconstruction technique (ART) and Iterative Reconstruction Algorithm, but this work will consider the FBP and ART algorithm reconstruction techniques only.

Radiation is the emission or the transfer of energy in form of either particles or waves through a material medium or through space. [29] Radiation can interact with a material to cause atomic or molecular excitation, ionization or activation of the nucleus. Due to the properties of x-rays and gamma radiation being an ionizing electromagnetic radiation with no charge, and high penetrating ability; they are suitable for use in tomography. However, these radiations suffer an exponential decay in the intensity of radiation projection as illustrated in the figure 2.1 and mathematically in the equation 2.1 known as the Beer-Lambert law. This equation describes the overall attenuation coefficient when radiation beams interact with matter.

The most important objective of x-ray computed tomography is being able to reconstruct two-dimensional and the three-dimensional view of the internal structures from signals gathered through directing radiation, mostly gamma and x-rays through an object. A reconstructed image depicts the distribution of a radiation beam linearly through a material. As represented in the figure below, x-rays intensities values, I as the beam penetrates an object are the acquisition data recorded in an array format from a detector.

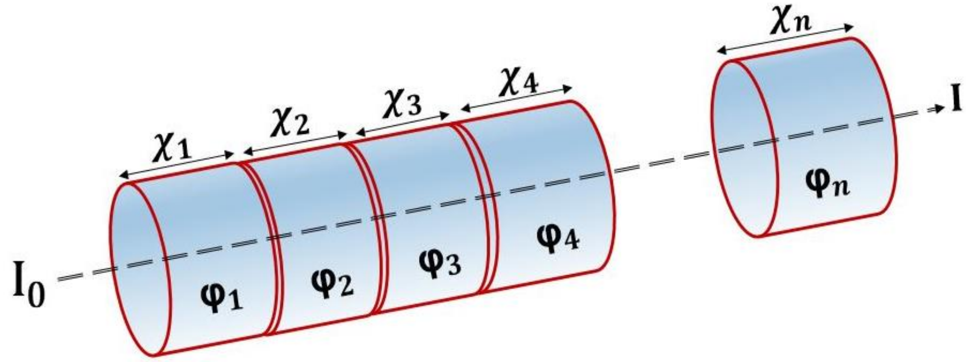

Figure 1-Diagram illustrating different attenuation coefficient of radiation through materials

$$I = I_0 e^{-(\varphi_1 \chi_1 + \varphi_2 \chi_2 + \varphi_3 \chi_3 + \varphi_4 \chi_4 \cdots \varphi_n \chi_n)} \tag{2.1}$$

$$\ln \frac{I_0}{I} = \sum_{n-1}^{N} \varphi_n \chi_n \tag{2.2}$$

Where I_0 and I represents the initial and the final radiation intensities as transferred through the materials of interest. In the equation 2.2, the $\ln\left(\frac{I_0}{I}\right)$ is the one-dimensional projection in the path travelled by the ray. In computed tomography, series of projections are recorded as the radiation source detector moves round the axis of the object undergoing a scan. The φ represents weakening in intensity or the linear attenuation as the radiation passes through the material and χ represents the ray distance through the material. Hence, the portion of the object that has undergone the transfer of radiation is processed as a function φ (x, y) followed by establishment with some reconstruction techniques to reveal the true view of the scanned portion. [30]

2.2 The Radon transform

The history and discovery of reconstruction of images in computed tomography cannot be completely tackled without acknowledging great men such as Johann Radon, Allan M. Cormack and many more. In the early 1917, the Austrian mathematician Johann Radon came up with a mathematical solution on which the analytical reconstruction is founded. The Radon transform also known as the forward projection or transform states that, if one integrates a 2D function, $f(x, y)$ in a plane, that can satisfy an appropriate regularity conditions along an arbitrary straight-line L, then the values of the projection path defines the function of the line. [31]

Figure 2.2 Johann Karl August Radon [16 December 1887 – 25 May 1956]

2.3 The relationship between projections and line integrals

There exists a direct proportionality between the projection paths and the line integral theorem. A line integral is a complete representation of certain parameters of the object along in a line. For instance, the attenuation of x-rays as they penetrate through a material. Considering an object with a two dimensional function, $f(x,y)$ which is projected at an angle θ, with projection line integral parameters of each projection $P_n(\theta,t)$, where n represents the number of rays propagated through the object, and the paths of each ray in the projected x-ray beam represented by t, $t_1 \ldots t_n$ in that sequence as illustrated in the figure 2.3 below.

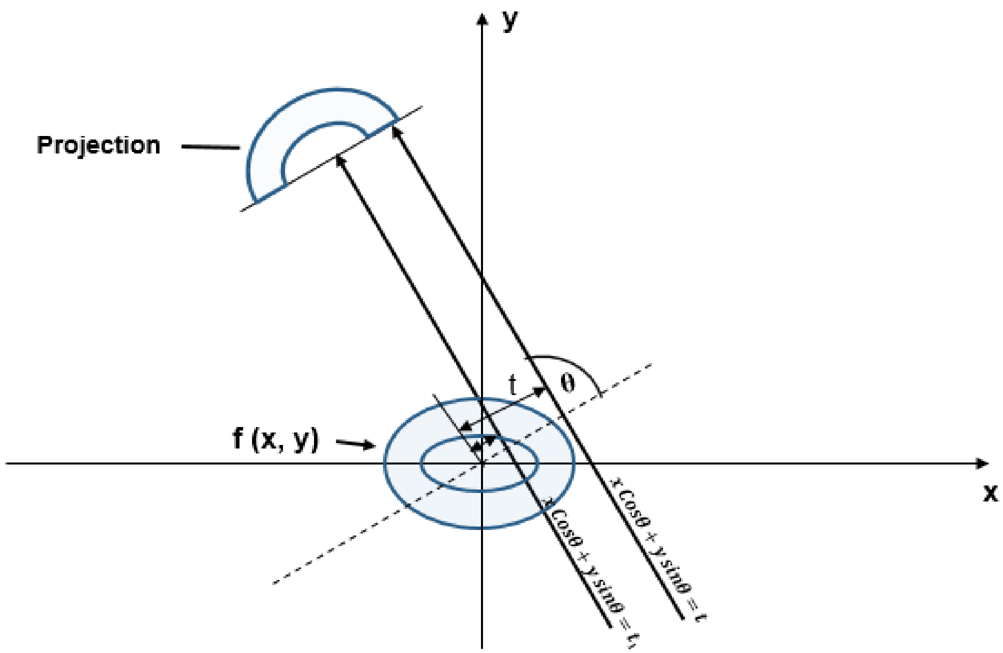

Figure 2.3 – An object $f(x,y)$ showing some of its projection details

However, each line and line integral are defined by the equation 8 and 9 respectively.

$$t = x\cos\theta + y\sin\theta \tag{2.3}$$

$$P_\theta(t) = \int_{L(\theta,t)} f(x,y)ds \tag{2.4}$$

$$P_\theta(t) = \int_{-\infty}^{\infty}\int_{-\infty}^{\infty} f(x,y)\delta(x\cos\theta + y\sin\theta - t)dxdy \tag{2.5}$$

Therefore, the projection function $P_\theta(t)$ in equation 2.4 represents the Radon transform of the function $f(x, y)$. The projection can be rewritten in detail form using the Dirac delta-function as in the equation 2.3 above.

2.4 Parallel projection

There are different methods of gathering projections depending on the type of equipment and setups involved, such as parallel, fan-beam and cone beam techniques. Combining sets of line integrals of each rays gives a projection. A parallel projection is the simplest and the basic form of analyzing projections and it involves collecting parallel ray integrals as presented in the equation 9 for a constant angle θ. The parallel projections are well illustrated and explained in the figure 2.4 below. During the process of projection, the x-ray source and the detector positions are adjusted oppositely along parallel lines of the object under investigation [32].

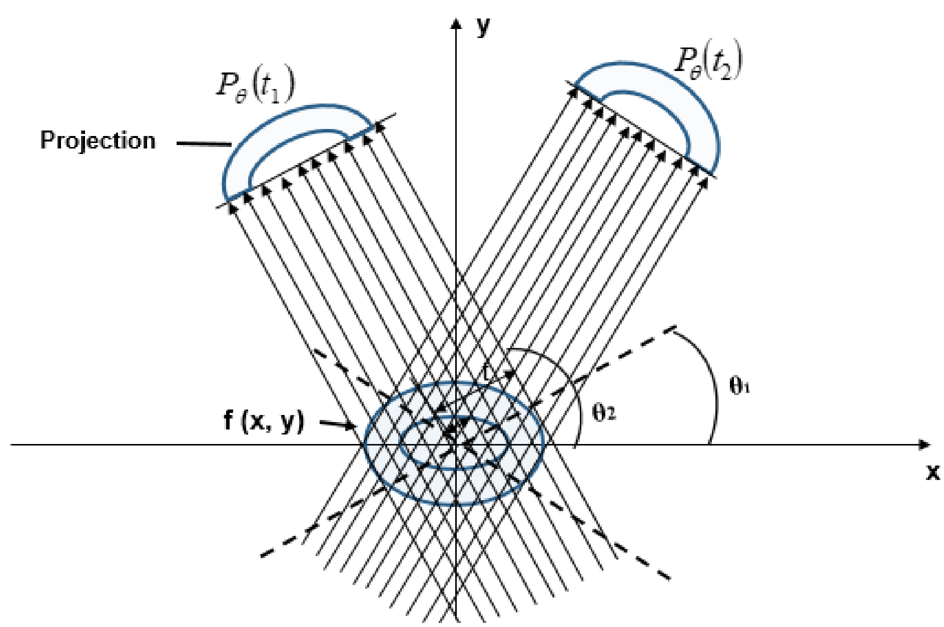

Figure 2.4 – Parallel beam projection showing the individual rays, angle of projection θ and projection view function $P_\theta(t)$ involved.

2.5 Numerical interpretation of the Radon forward transform

The projection numerical process involves the summation of assigned pixel values in columns and rows in which the results obtained are converted into a sinogram as described below. Data acquired during x-ray propagation are represented with numbers in an array as collected from the detector. These numbers range from 0 to 255 according to the specific colours they represent. However, the colour codes involved in the grayscale images used in this work after flattening ranges between 0 to 1 only, hence each pixel is occupied by the range of values as numerically presented for the sake of explanations below, whiles the simulation outcome can be found in the next chapter.

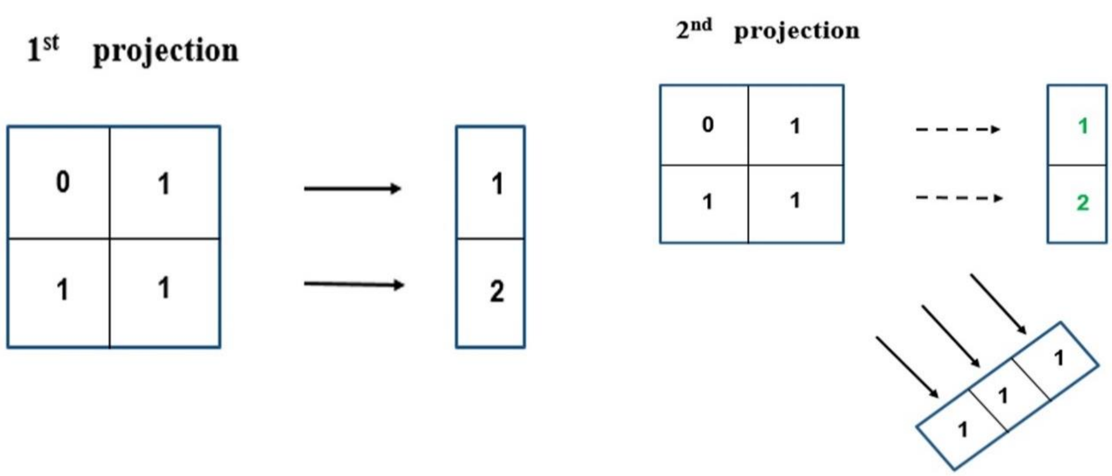

Figure 2.5 – Numerical illustration on how projections are computed from 2-dimensional array to 1-dimensional array to form a sinogram

2.6 The Inverse Radon Transform and the back-projection

The analytical approach to the inverse Radon transform can be established using the Fourier slice theorem. According to this theorem, a one-dimensional Fourier transform of the Radon transform relates to a two-dimensional Fourier transform of the function. In tomography, a 2D object function, $f(x, y)$ can be transformed into a 2D

Fourier domain using the projection slice theorem. This theorem is suitable for computed tomography image reconstruction involving parallel beams. Image reconstruction method is a classic inverse problem, when applied produces the image from its projection data. When we obtain a sinogram, the next step aims at retrieving our true image, because the sinogram doesn't make any sense in terms visibility of what we expecting to get at the end.

In 1963, an American physician, neurologist, and the founding member of the American society for neuroimaging William H. Oldendorf announced the direct back-projection method.

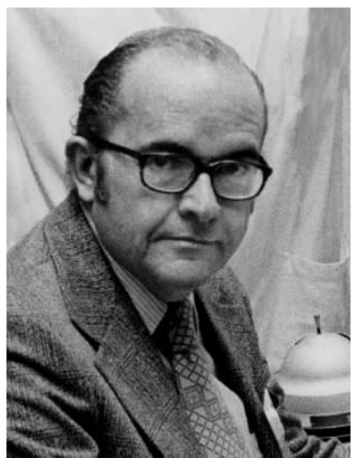

Figure 2.6a – William Henry Oldendoff [March 1925 – Dec 1992]

Back-projection is simply the process of smearing back all the projection data along the same path followed during the forward projection. Hence, by doing this, an image is reconstructed. According to the Fourier slice theorem, a one-dimensional Fourier transform of the detector function at an angle is an exact replica as a line through the 2D Fourier representation of the entire object. Therefore, it represents the line through the origin at the exact angle of projection. Hence, by taking measurement of a single projection of an object, a single line can be filled in the Fourier domain as in illustrated in the figure 2.6b below.

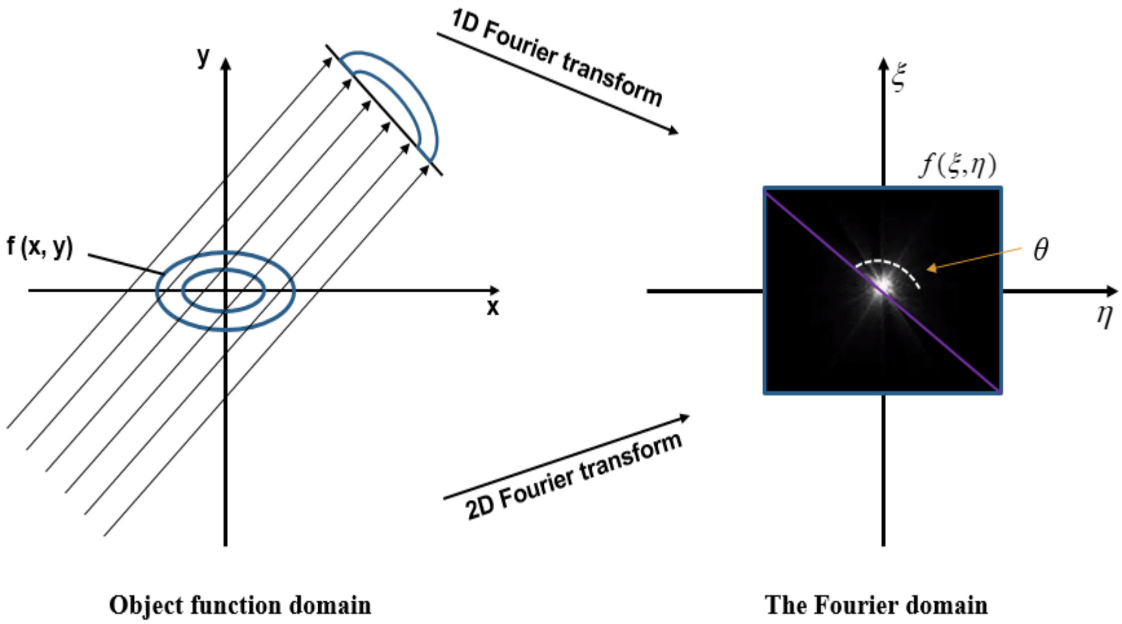

Figure 2.6b – Scheme of Fourier representation of a single projection

Apparently, as the projection is collected from multiple angles and transforming it into the Fourier domain will result in obtaining a full Fourier representation as shown by the figure 2.6c below.

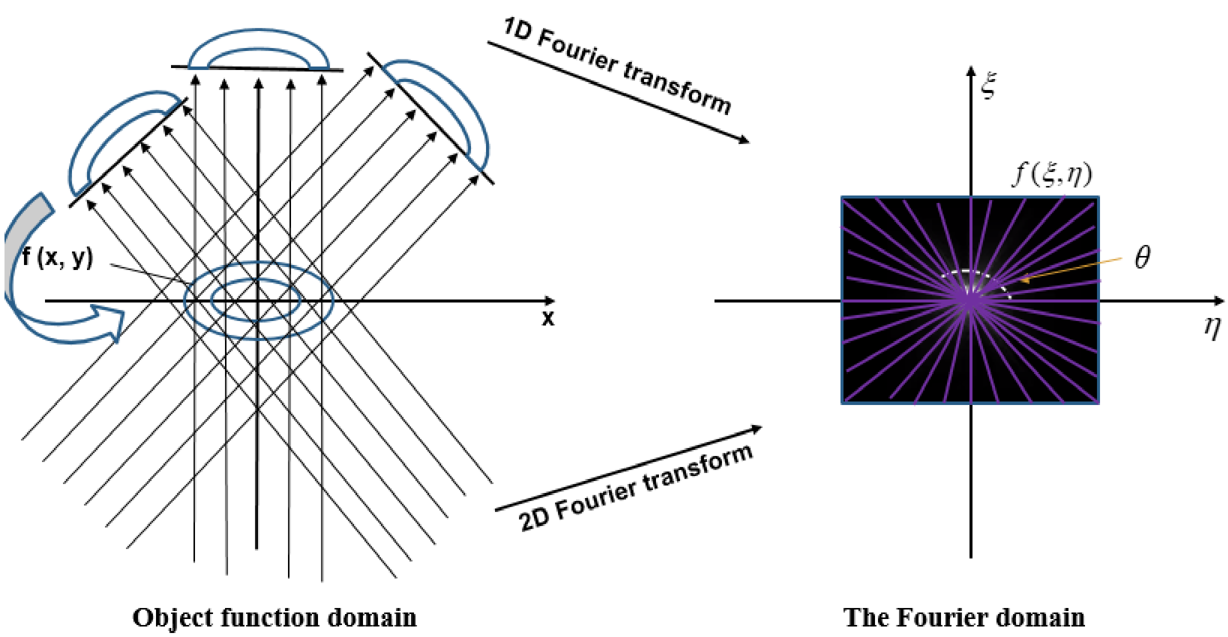

Figure 2.6c – Full Fourier scheme of projections taking from multiple angles

Therefore, as the Fourier domain is completely built, a 2-dimensional Fourier transform can be assigned to the obtained data to successfully reconstruct the original object function. Unfortunately, there are two main problems with the back-projection approach. These limitations all trickle down to the fact that the amount in real practice is finite which leads to a sampled domain which is difficult to work with. The first limitation is that the Fourier sample lies in circles than in square grits which needs to be interpolated from the pixel data into square grits. This is achieved by interpolating from the Fourier domain into the frequency domain as illustrated in the figure 2.6d below.

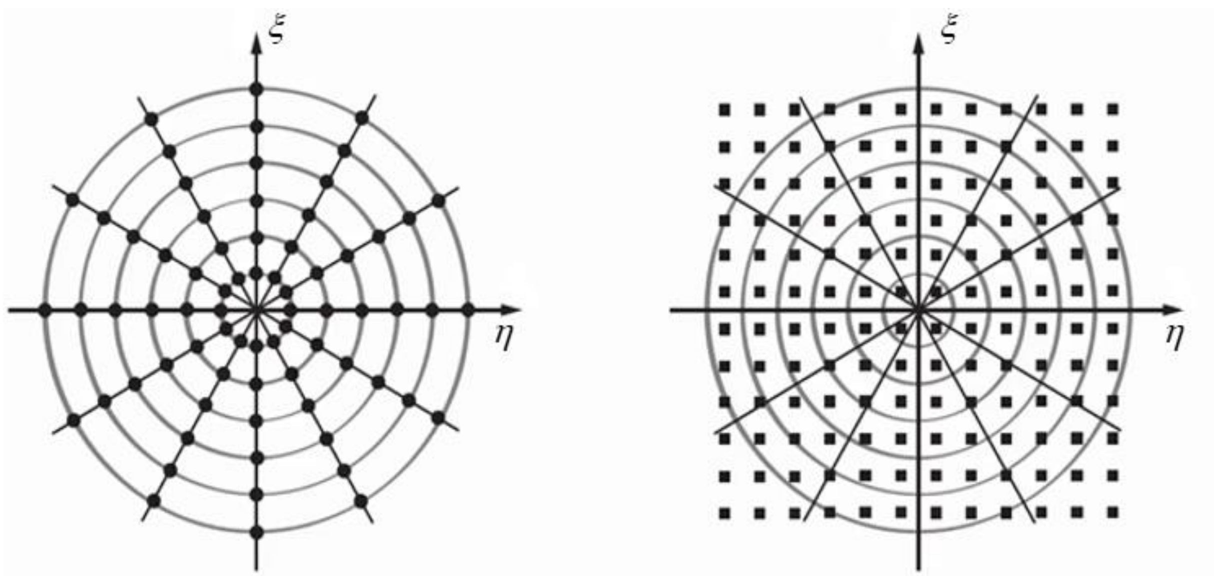

Figure 2.6d – Scheme showing the circular representation in the Fourier domain [left] and the square grids in the frequency domain [right]

Also, it is noted that the sample distribution of the Fourier domain is much denser in the origin or the central portion than the outer region as shown in the figure 2.6e below. This is thus that the area with the lowest frequency is loaded with excess data than the area of higher frequency. Hence, the lower frequency region would be accurately reconstructed than the higher frequency region.

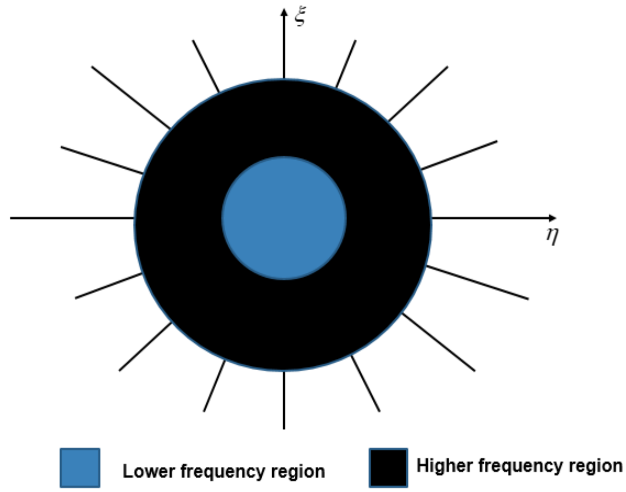

Figure 2.6e– Sketch of the frequency regions in the Fourier sampling domain

The higher frequency region is where the final details of the object are located, but it is not well sampled and cannot be accurately reconstructed after the implementation of the inverse Fourier transform, hence the reason why very blurred images are always obtained after back-projecting, and this is the main limitation of the back-projection approach.

2.7 Numerical understanding of the back-projection approach

During back-projection, the array is being emptied which is then proceeded by step by step smearing back all the projection data from same angle and path into the empty array. After summing up all the back-projection data, the process is then followed by subtracting total sum in the array. Finally, each entry in the array is then divided by the number of projection minus one. By reference from the figure 2.4 above, the back-projection numerical explanation is established as explained in the figure 2.7a below.

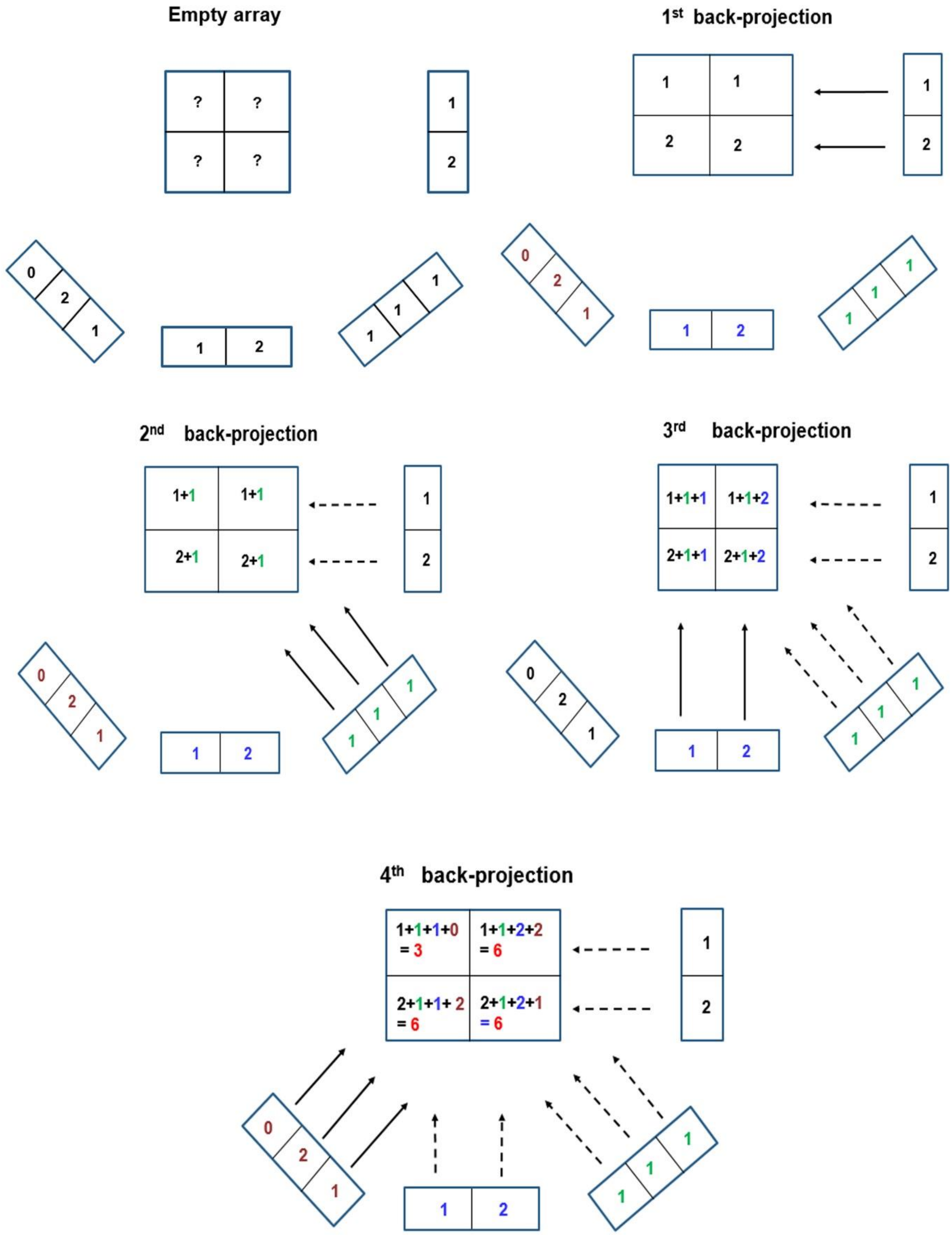

Figure 2.7a – Numerical representation of the back-projection from the creation of an empty array to the 4th back-projection.

However, the total sum of the original array is computed [0 + 1 + 1 + 1 = 3] and subtracted from the 4th back-projection results. Hence the result is obtained by dividing each entry by the number of times the projection is conducted minus one, i.e. 4 – 1=3 as shown in the figure 2.7b below.

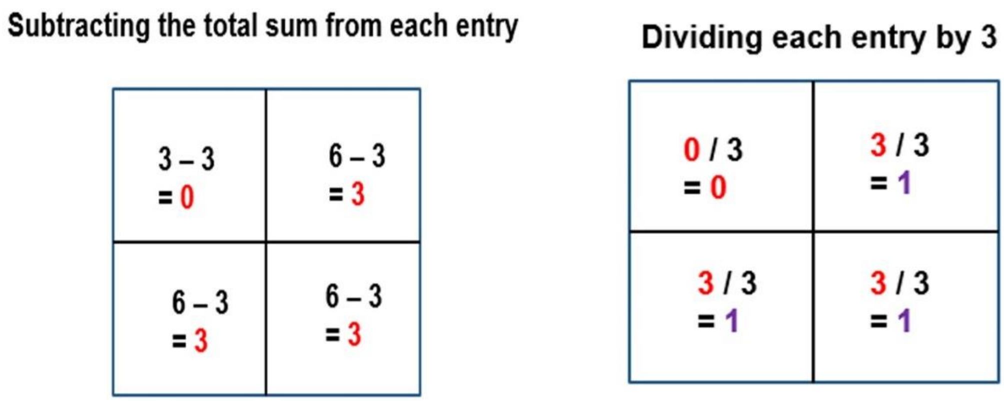

Figure 2.7b – Scheme showing the subtraction done by taking out the sum of each entry and dividing by the number of projections minus one.

2.8 Filtered back-projection (FBP)

The filtered back-projection reconstruction technique clearly manages to overcome the limitations presented by the back-projection method described above. This technique introduces an additional filtering phase and then replaces the inverse Fourier transform with a different operation system to yield an image with a better resolution. This idea of the filtered back-projection was first proposed in 1967 by Bracewell and Riddle, and probably forms one of the most outstanding development in the field of reconstruction. The technique is derived from the Fourier slice theorem and it is extensively used in reconstruction due to its level of exactitude and efficiency. Hence, applying the Fourier transform to the projections, the space frequency distribution of densities is revealed [30, 33]. The filtered back-projection is summarized below as follows:

1) Compute the Fourier transform 1D projections for reaching the frequency domain.
2) These projections transformed are then filtered with a low pass filter of any of the following; the Ramp filter, Shepp – Logan filter, Hamming filter etc.
3) Place the filtered projections in a polar grid where each single projection remains exactly in its conforming angle.
4) Resample the outcome in step 3 by interpolating into a Cartesian grid.
5) Compute the 2D inverse Fourier transform which finally yields the reconstructed image, hence, the filtered projection is finally back projected.

2.9 The fan beam computed tomography (FBCT)

It's a kind of beam projection technique that gives a geometric pattern produced by collimating a spatially extended x-ray beam with a long narrow slit. In the earlier reconstruction algorithms and beam projections, the beam propagation was centered on the parallel beam projecting techniques as described basically in the section 3.3. However, recent computed tomography scanners direct an x-ray beam through a point source to produce a divergent beam which either can give a two-dimensional beam system known as the fan beam or a three-dimensional type which is popularly referred to as the cone beam due to several inbuilt merits.

The fan beam CT has several advantages such as; low artifact presence, low noise level, greater signal to noise ratio, and the ability to discriminate low contrast objects compared to cone beam computed tomography. However, the Fourier slice theorem as discussed in the section above has a lot of complications in dealing with the geometry associated with the divergent beam system, hence difficult to be applied in the development of the reconstruction algorithms. In view of this, an alternate approach is employed to redesign the fan beam reconstruction with a parallel beam algorithm concept using a suitable coordinate transformation system.

There exist two known types of the fan beam geometric setup namely; the equispatial and the equiangular fan beam setups. These setups depend mostly on the way the beams are projected from the source and the type of detector used to collect the data as shown in the figure 2.9a and 2.9b below.

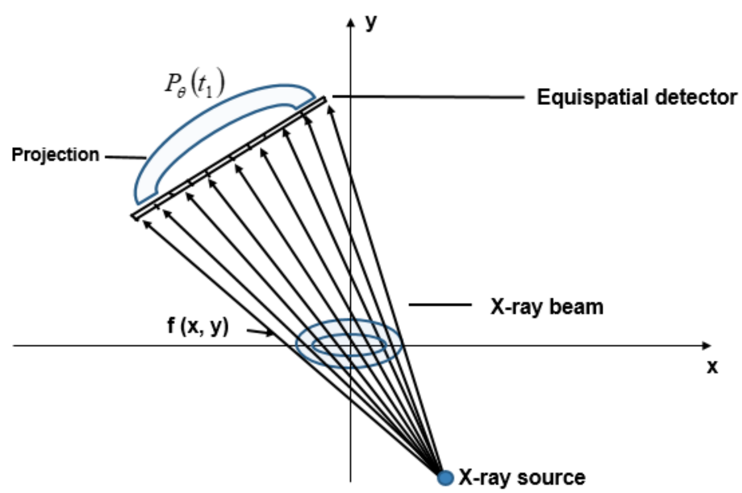

Figure 2.9a – Equispatial sampling fan beam geometry.

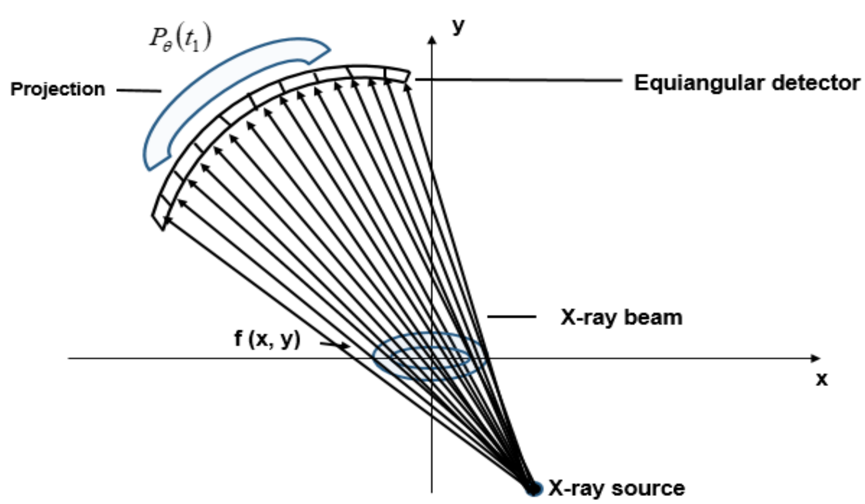

Figure 2.9b Equiangular sampling fan beam geometry.

2.10 Rebinning algorithm

This is a reformatting process in which the fan beam reconstruction can be strategically reformed into parallel beam projections. In the process of rebinning, an x-ray fan beam point data is put into a new order to a parallel beam data. Hence, after the data has undergone rebinning, the next stage is to initiate the reconstruction using a parallel filtered back-projection approach involving the necessary algorithm. However, this rebinning algorithm does not involve just rearranging the projection data but required an interpolation stage as well. Sometimes, a bilinear interpolation approach is applied by considering the angle of projection and the position the detector is placed during a specific projection. One main advantage associated with the rebinning approach is the ability to extend it to other paths. However, to avoid the complications involved with the rebinning process, a fan beam reconstruction algorithm which can be applied directly to the data obtained from the fan beam projection approach is used. This then increases the computational expenses compared to parallel beam reconstruction.

2.11 Cone beam computed tomography (CBCT)

The cone beam CT is a further modern improvement in computed tomography data acquisition setup. In this setup, an X-ray beam is emitted in a conical pattern which is projected through the object of interest and detected by a two-dimensional detector instead of a fan-shaped x-ray beam and one-dimensional detectors. As discussed earlier, in cone beam CT, a divergent cone shaped source of X-ray radiation is directed through the object of interest and the attenuated X-rays are then detected on the detector opposite the source. This detector screen is made up of multiples of dexels in two dimensions x and y-axis whiles a fan beam CT detector has dexels only in the x-axis. These dexels basically describes the picture elements in the detector than visible pictures. These dexels are to be processed, joined, resampled or even mangled to form a picture. [33]

However, the invention of this technique has brought some merits over its fan beam counterpart, but also has some inherent drawbacks. For instance, the cone beam CT system provides a shorter time for examination which helps to improve the sharpness in the image by translating the object and improves the x-ray tube efficiency. One major disadvantage is in handling larger field of views which can limit the quality of the image due to noise and contrast resolution which is because of the detection of larger quantity of scattered radiation.

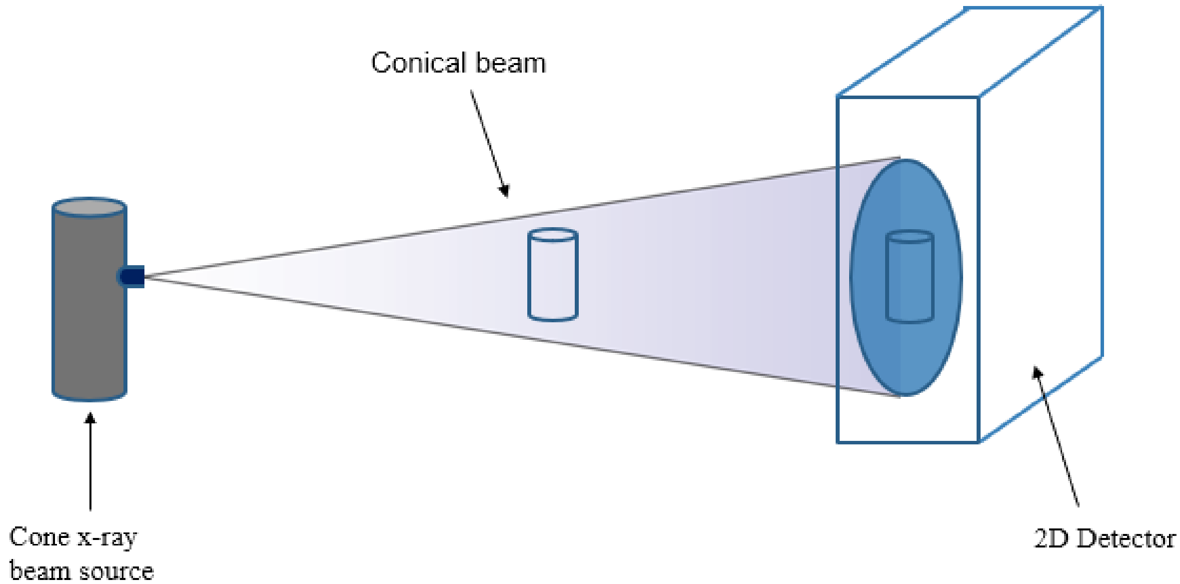

Figure 2.11 – Scheme of the Cone beam geometric setup.

The conventional approach to take scan of a 3D object is by illuminating the object with a narrow beam x-rays and process the data by applying a 2D reconstruction algorithm. A 3-dimensional object can be reconstructed from the cone beam by illuminating successive planes within the object and stacking these 2D resulting reconstruction to obtain a 3-dimensional view of the object. [34]

Chapter 3 – The experimental aspect of the reconstruction

3.1 Forward projection simulations using the parallel projection algorithms

The simulation on the forward projection was done using python coding packages. Below is the summary to generate the sinogram;

- Import all necessary python libraries.
- Define the input and output paths.
- Read and import the sample from its path.
- Define the angular range and step involved.
- Create an empty 2D array for the proposed sinogram.
- Develop a loop function to rotate and create 2D empty array and interpolate the array with pixel values to form the sinogram.
- Sum up the rows pixel values from the 2D array and convert into 1D array
- Build a sinogram for all the 1D arrays.
- Specify the save path and details.

From the simulation, the following figures below gives the phantoms and their corresponding sinograms. The exact codes for the simulation can be seen in the appendix A Task 5[Sinogram 1] and Task 6[Sinogram 2] respectively.

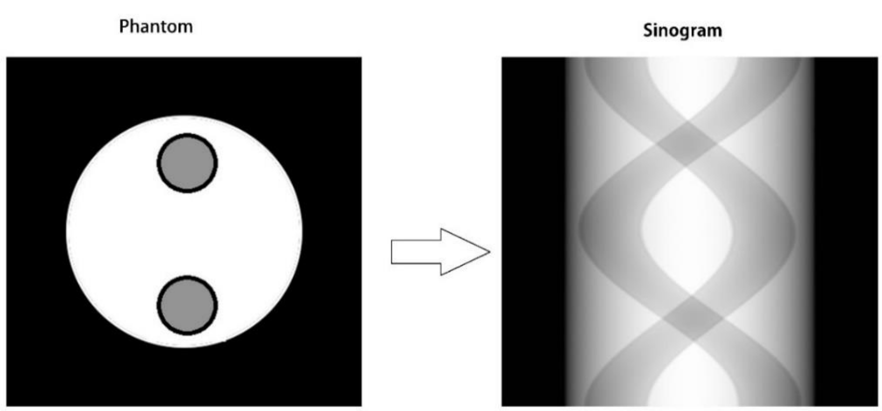

Figure 3.1a – Phantom 1 [left] and its corresponding sinogram[right]

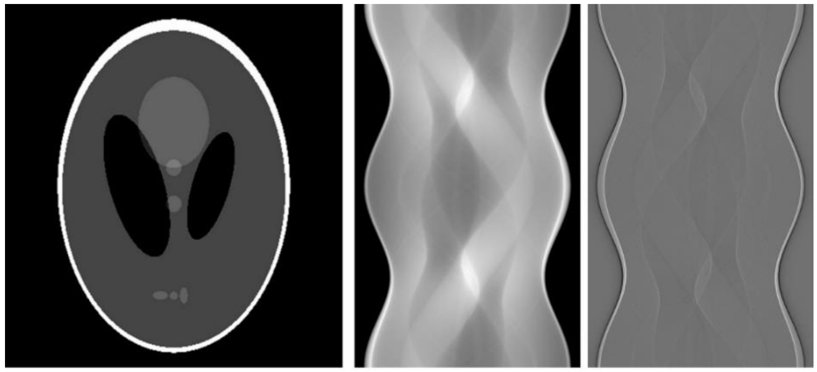

Figure 3.1b – The Shepp-Logan Phantom[left] and its unfiltered corresponding sinogram[middle] and filtered sinogram [right]

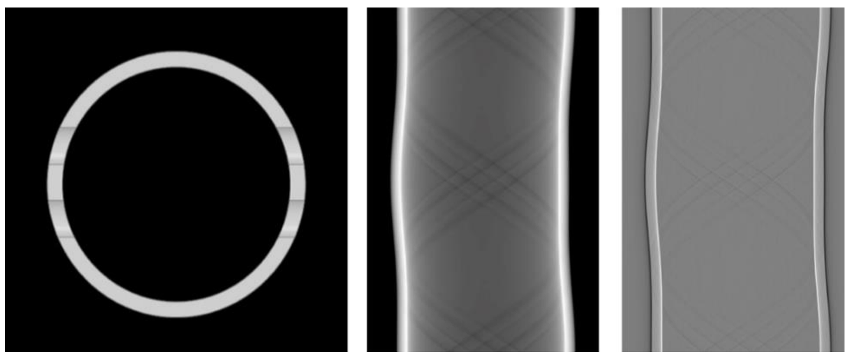

Figure 3.1c – Phantom 2 [left], its unfiltered corresponding sinogram[middle] and filtered sinogram [right]

3.2 Simulation of the back-projection with parallel projection algorithm

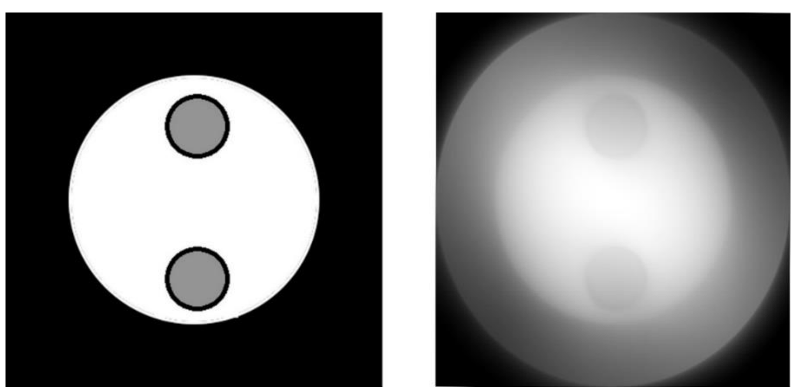

Figure 3.2a - Phantom 1 [left] and its unfiltered back-projection reconstructed image[right]

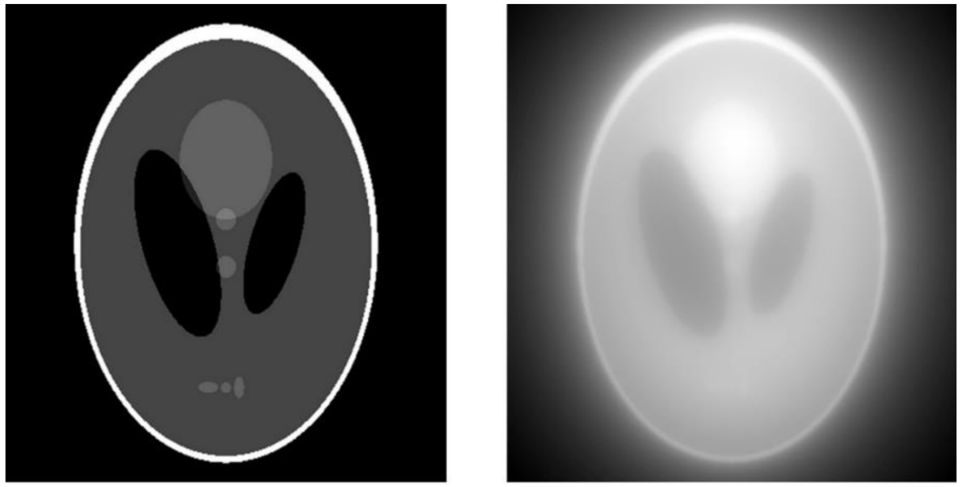

Figure 3.2b – The Shepp-Logan Phantom [left] and its unfiltered back-projection reconstructed image[right]

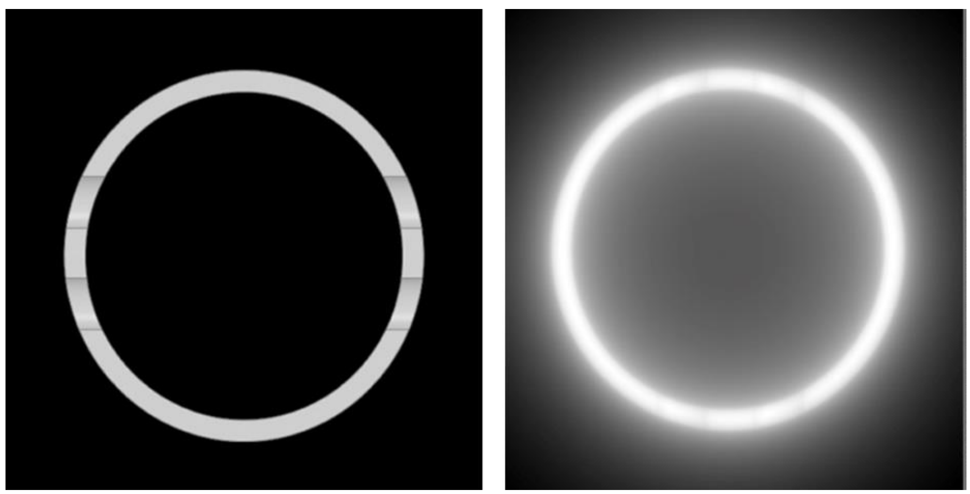

Figure 3.2c - Phantom 2 [left] and its unfiltered back-projection reconstructed image[right]

The codes for the simulation is obtained in the appendix A task 7[Simple back-projection].

However, the blur effects from the simple back-projection does not makes the reconstruction technique involving the Inverse Fourier transform ineffective or inferior, but it rather forms the basis for another reconstruction approach known as the filtered back-projection.

3.3 Simulation of the FBP reconstruction with parallel projection algorithm

From the codes in task 8 known as [Filtered back-projection] in the appendix A, the reconstruction image in the figure 3.10 below is obtained.

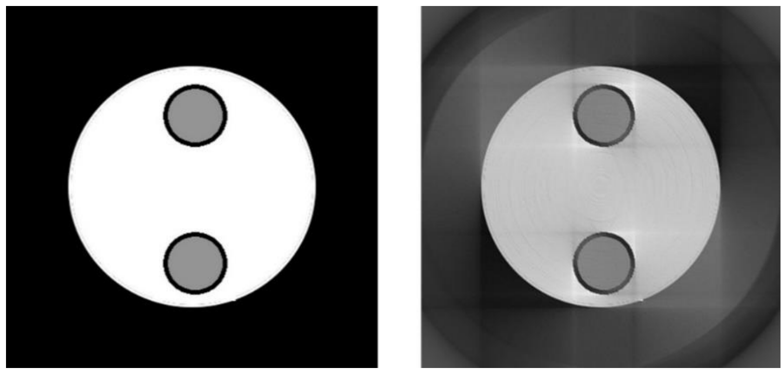

Figure 3.3a – Phantom 1 [left] and its FBP reconstructed image[right]

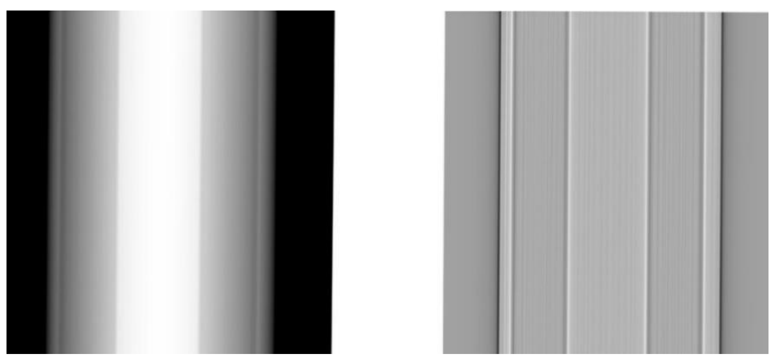

Figure 3.3b – Projection view of the unfiltered back-projection[left] and filtered back-projection [right] of phantom1.

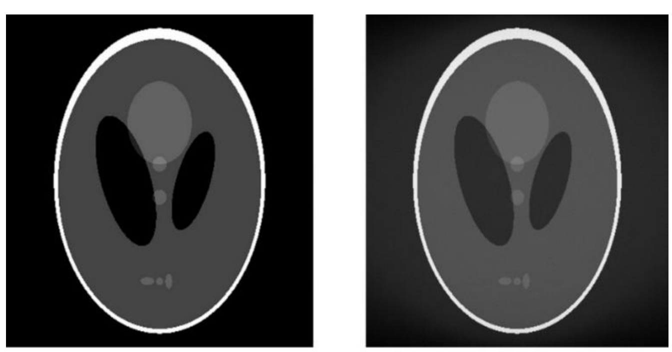

Figure 3.3c – The Shepp-Logan phantom [left] and its FBP reconstructed image[right]

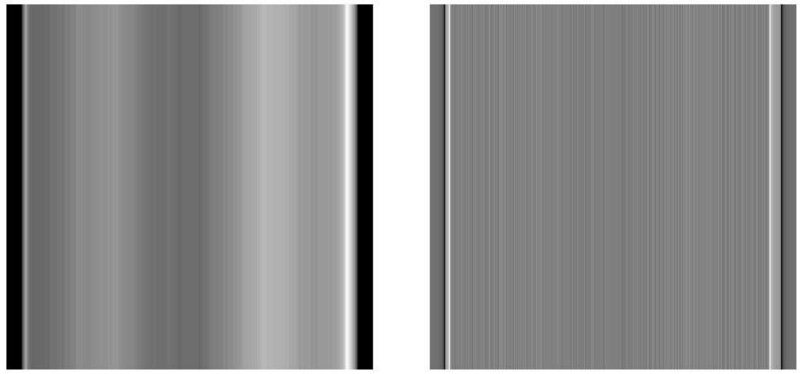

Figure 3.3d – Projection view of the unfiltered back-projection[left] and filtered back-projection [right] of the Shepp-Logan phantom.

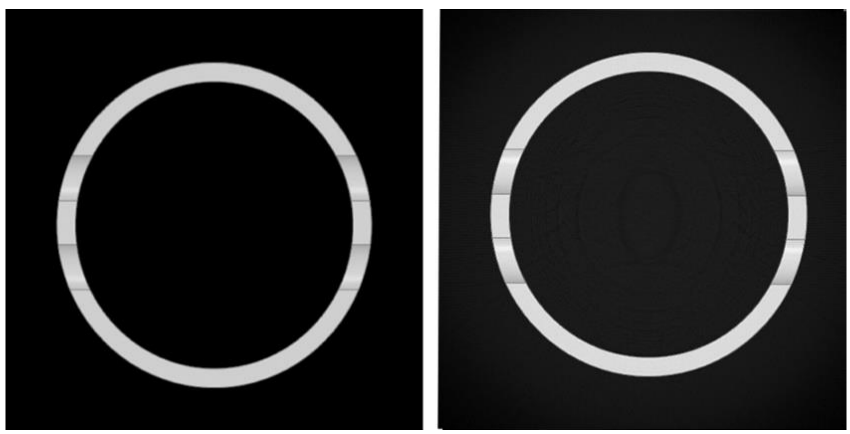

Figure 3.3e – Phantom 2 [left] and its FBP reconstructed image[right]

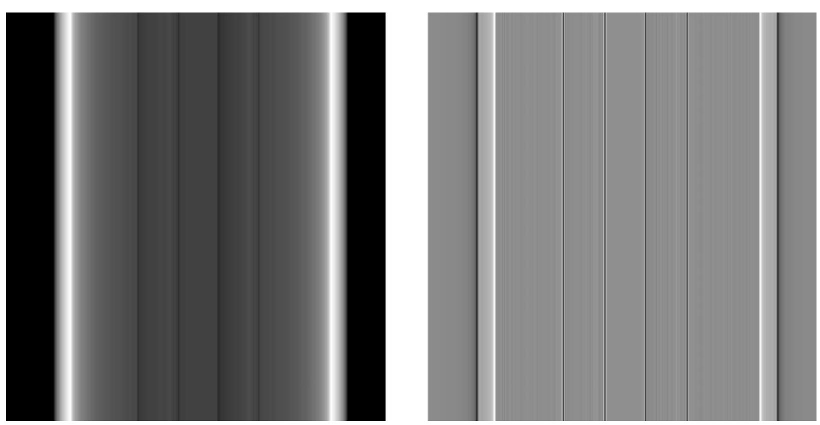

Figure 3.3f – Projection view of the unfiltered back-projection[left] and filtered back-projection [right] of the phantom 2.

The filtered back-projection technique involves two main processes, the Ramp filtering process and the back-projection process. During the filtering process, the Ramp filter can be applied as either convolution in the spatial domain or multiplication in the Fourier domain. The figure 3.3b, 3.3d and 3.3f are the exact projection of a single slice of the unfiltered back-projection and the filtered back-projection when the Ramp filter is implemented. From the figure, the unfiltered back-projection looks very blur due to the presence of unnecessary frequencies from negative infinity to positive infinity whiles the filtered back-projection looks smoother, sharper and detailed due to filtering away of frequencies of noise and distortions during the Ramp filtering process.

3.4 Forward projection simulations using the cone beam algorithms

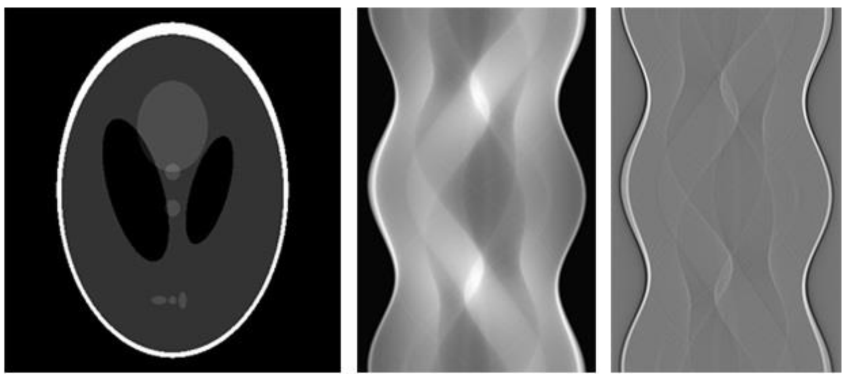

Figure 3.4a – The Shepp-Logan Phantom[left] with its corresponding unfiltered sinogram[middle] and filtered sinogram[right]

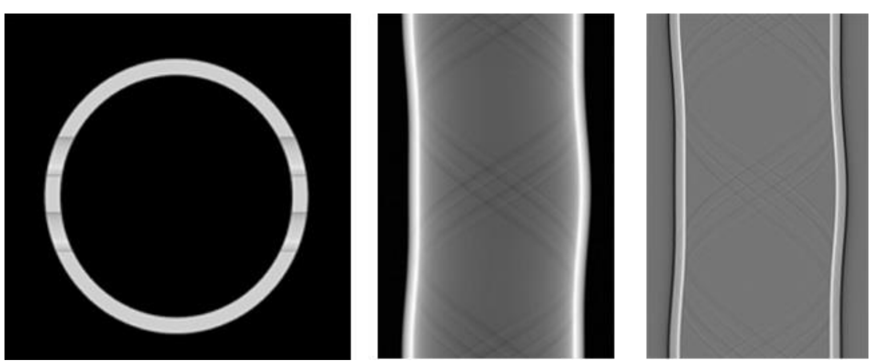

Figure 3.4b – Phantom 1 [left] with its corresponding unfiltered sinogram[middle] and filtered sinogram[right]

3.5 Simulation of the back-projection with the cone beam algorithm

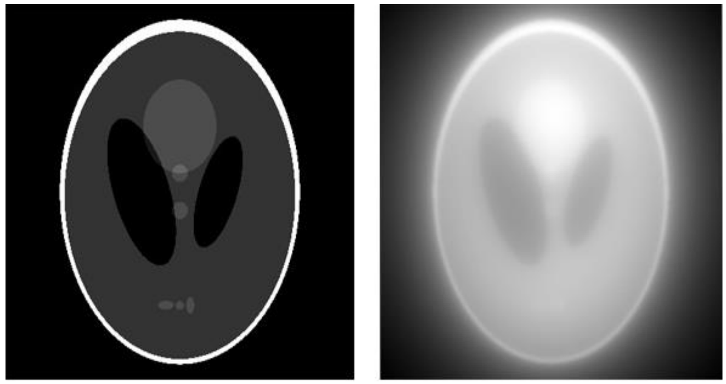

Figure 3.5a – The Shepp-Logan Phantom [left] and its unfiltered back-projection reconstructed image[right]

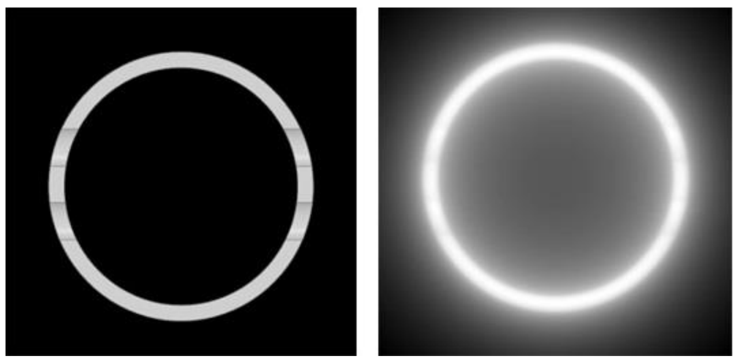

Figure 3.5b - Phantom [left] and its unfiltered back-projection reconstructed image[right]

3.6 Simulation of the FBP reconstruction with the cone beam algorithm

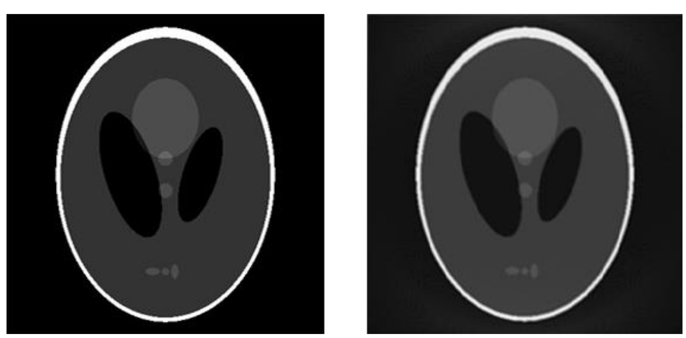

Figure 3.6a – The Shepp-Logan phantom [left] and its FBP reconstructed image[right]

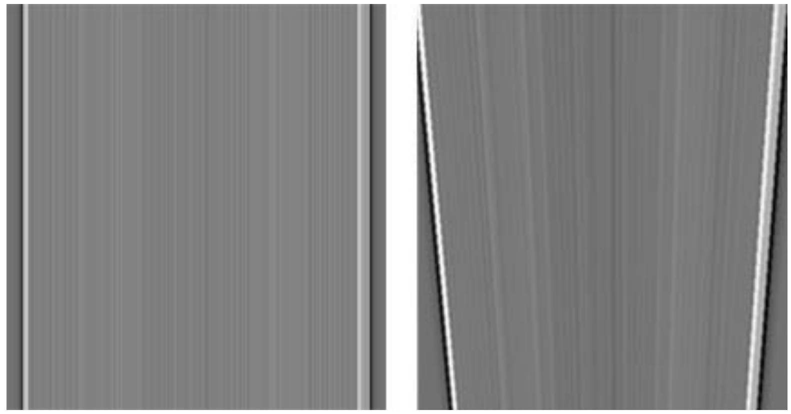

Figure 3.6b – Projection view of a sample of the filtered Shepp-Logan phantom with the parallel beam projection [left] and cone beam projection[right].

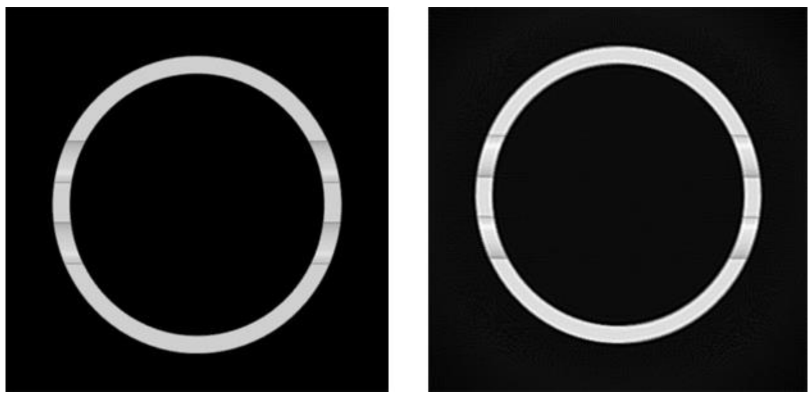

Figure 3.6c – Phantom [left] and its FBP reconstructed image[right]

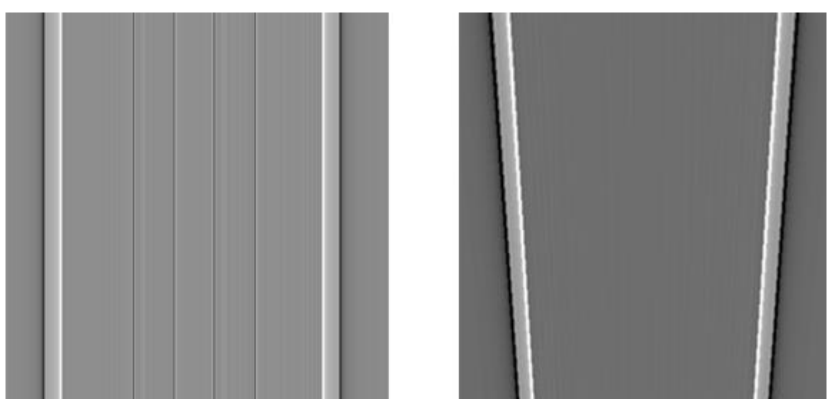

Figure 3.6d – Projection view of a sample of the filtered phantom with the parallel beam projection [left] and cone beam projection[right].

3.7 Discussions

In recent times, high energy particle accelerators are designed to be able to deliver higher penetrating energy x-rays through thick and large industrial objects such as the betatrons during defect inspections. However, these x-ray beams generated in the betatrons are directed in a conical pattern through the object under investigation and the attenuated radiation that reaches the two-dimensional detector is received and recorded onto a computer system for further processing of the acquired data. However, the conical pattern of the beam is taking into several fan beam planes in order to be able to simplify the geometry as shown in the figure 3.7a and 3.7b below.

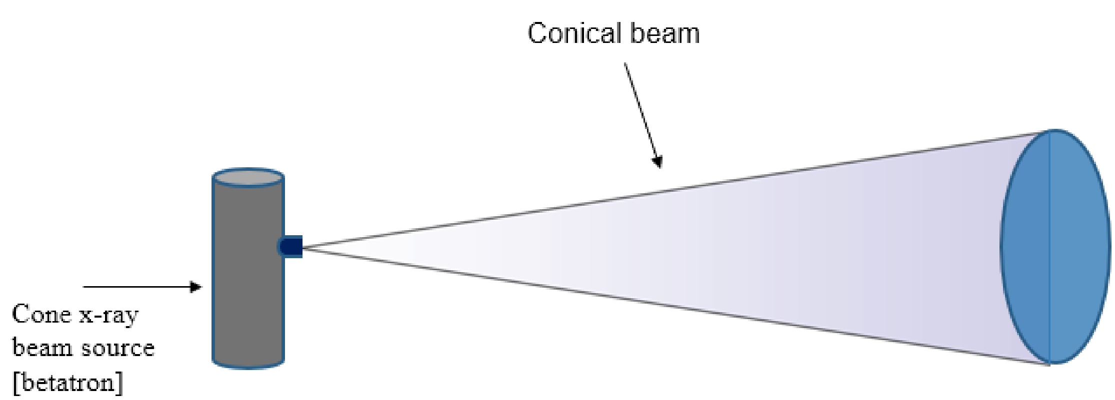

Figure 3.7a – Simplify scheme of the cone beam x-rays

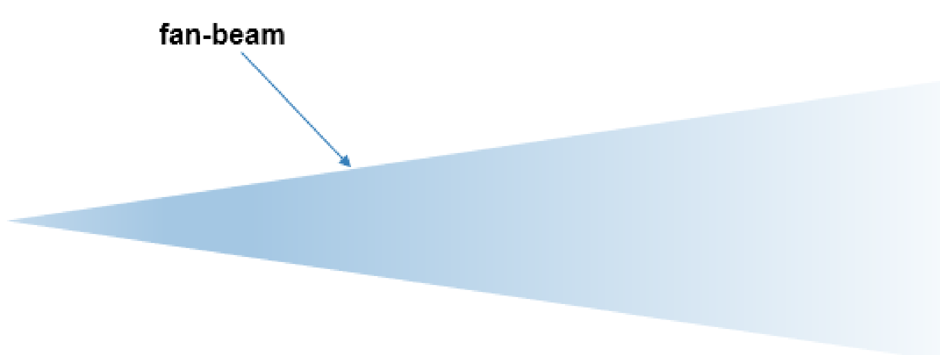

Figure 3.7b – Scheme of Fan shape beam x-ray

Therefore, the developed algorithm was based on the fact that, several fan shape planes of x-rays built up a cone beam. This algorithm is responsible for sampling the data in the trajectories from the fan beams as a subset of the cone beam. Meanwhile, during rebinning algorithms, the fan beams are then formatted into parallel beams by applying a geometrical and mathematical approach. This then result in a long conversion process as well time during the reconstruction of the image. It also has a limitation of losing the quality of data involved in all these conversions. Therefore, the algorithm developed in this research work has helped to minimize the time involved during cone beam projection data reconstruction compared to using the rebinning technique as can be envisaged in the figure 3.7c and 3.7d below.

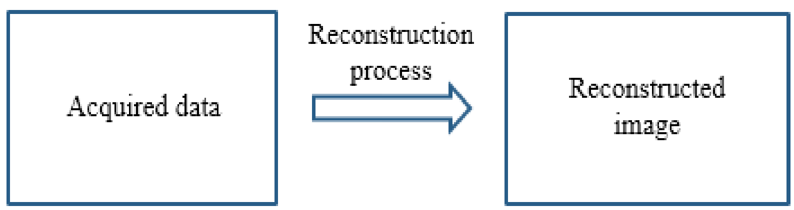

Figure 3.7c – Scheme relating the major processes involved in the developed algorithm

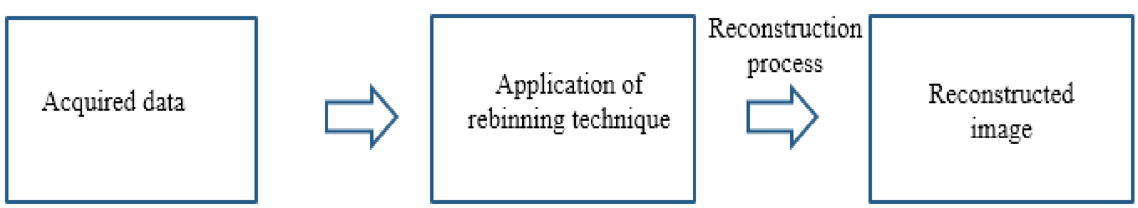

Figure 3.7d – Scheme relating the major processes involved in rebinning algorithm reconstruction technique.

Hence, from the figure 3.7c and 3.7d, it is clear that a major step in the 3.7d is completely skipped during reconstruction using the algorithm developed from the research.

During reconstruction, there are stages that are involved in the process to arrive at the final result. The first and foremost of all is the building of the sinogram from the acquired data. Assuming, a reactor vessel as shown in the figure 3.7e is under inspection at the mechanical building site, it will be required to scan through using the betatron in order to propagate high energy x-rays through the vessel due to its size and thickness.

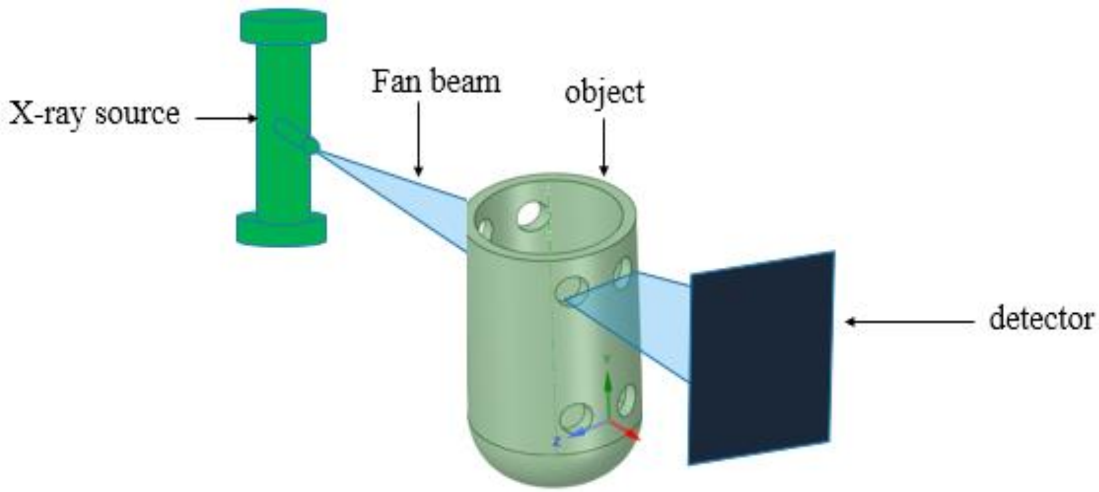

Figure 3.7e – Sketch of a reactor vessel under inspection

From the figure 3.7e, it is assumed that the x-ray beam propagated through the vessel is a fan beam since the developed algorithm is responsible for sampling the data on each fan beam plane as a subset of the cone beam. Therefore, when the data recorded on the detector is saved on the computer system and the sinogram algorithm for both parallel and the cone beam are implemented, the result in the figure 3.7f are obtained below.

Figure 3.7f – Unfiltered sinograms obtained from the acquired data, parallel [left], and the cone beam sinogram algorithm [right]

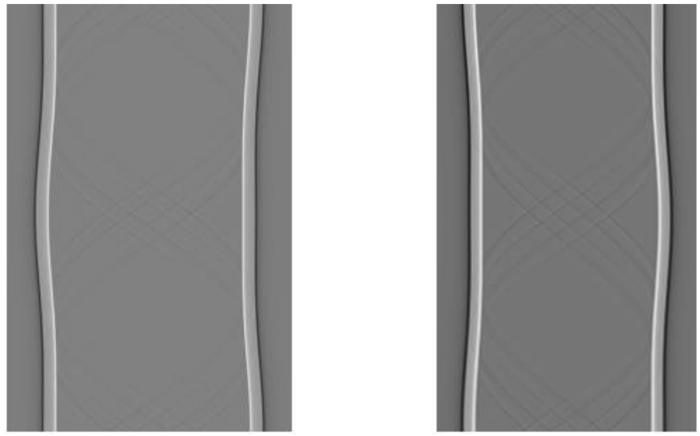

Figure 3.7f – filtered sinograms obtained from the acquired data, parallel [left], and the cone beam sinogram algorithm [right]

During reconstruction, the filtering of the data can be done during the forward projection algorithm by building the sinogram through the implementation of the Ramp filter to the algorithm responsible for generating the sinogram or filtering during back-projection.

After building the sinogram, the next step is to recover the real image through back-projection algorithm. In case the filtering is done during the back-projection, it is called filtered back-projection while the otherwise is known as simple back-projection.

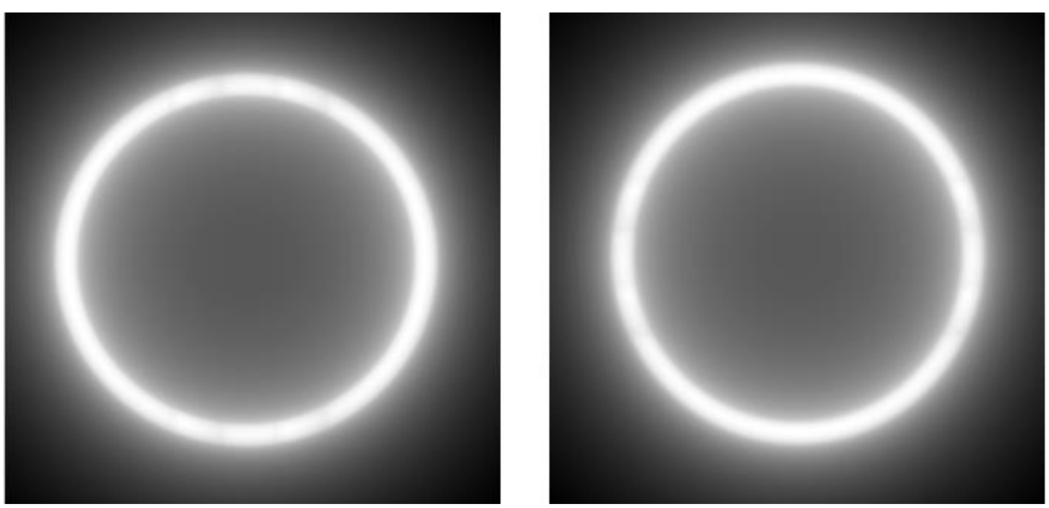

Figure 3.7g – Simple back-projection images from parallel projection algorithm [left] and that of the cone beam projection algorithm [right].

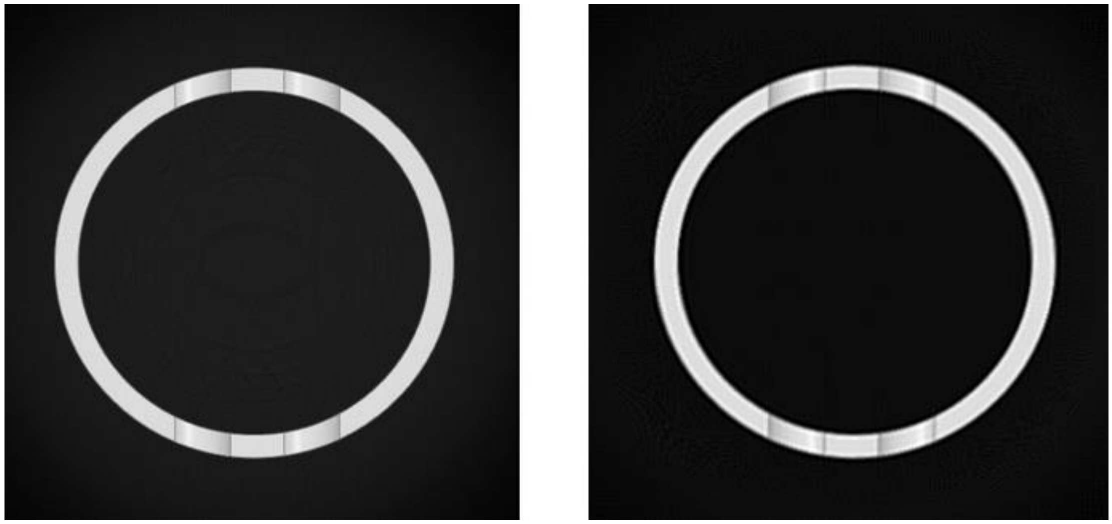

Figure 3.7h – Simple back-projection images from parallel projection algorithm [left] and that of the cone beam projection algorithm [right].

Hence, from the above figures, there is not much difference between the results from the parallel projection and the cone beam projection algorithm outcomes, except from the shape of the samples during back-projection or the filtered back-projection as shown in the figure 3.7i below.

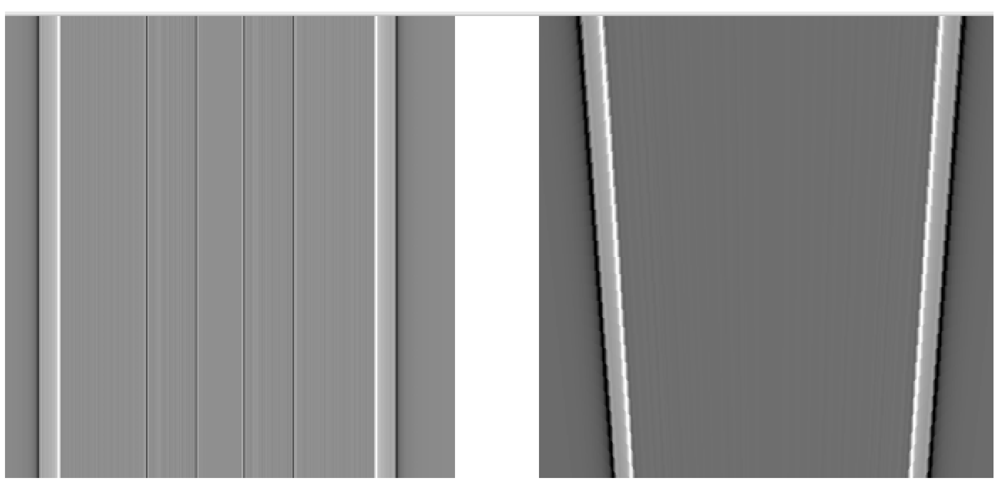

Figure 3.7i – Projection sample during the filtered back-projection with parallel reconstruction algorithm [left] and that of the cone beam algorithm [right].

From the figure 3.7i, the sampling techniques of parallel projection algorithm and that of the cone beam projection reconstruction algorithm outcomes have clear distinct view on how the data is being sampled. In the parallel projection image left, it can be seen clearly that all details of the image have been sampled in a parallel pattern. However, in the right image, it can be noted clearly that, all available details in the image have been sampled along the trajectories of the conical beam, hence takes the shape of a fan beam. This then proves the accuracy of the developed algorithm for direct reconstruction from cone beam to reconstructed image without conversions done during rebinning. Therefore, when the reconstructed image is placed in between the scanned reactor vessel, the figure 3.7j is obtained.

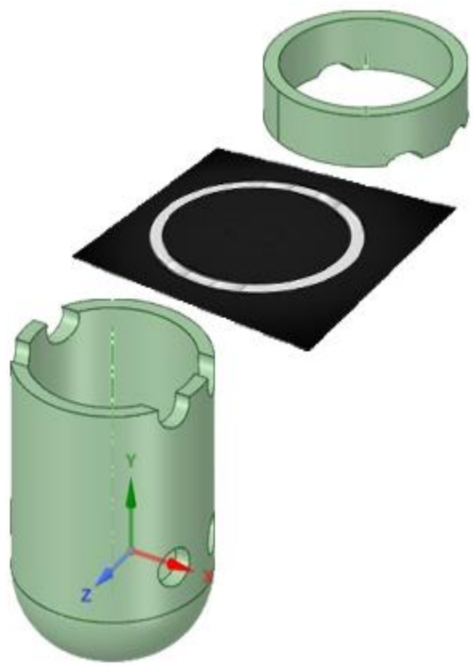

Figure 3.7j – Scheme showing a single slice of the scanned vessel

Hence, from the discussions and comparisons with the parallel projection algorithm, the developed algorithm is proven accurate and can be applied in any context of reconstruction involving the cone beam x-ray projection.

3.8 Summary

X -ray computed tomography has been on the edge of undergoing further research and development, both in hardware and software in recent times. Modern industrial tomography mainly uses the betatrons which delivers high energy x-rays in a conical pattern, hence required a suitable reconstruction algorithm to perform the necessary simulations of the reconstructed images of investigated objects. Though, there exist some few methods towards obtaining the goal, but these techniques have their own shortcomings such as the lost in quality of data coupled with the complexities in evaluating the rebinning algorithm to suit the fan beam and the cone beam projections.

To successfully achieve the objective of the research, certain analytical tactics in the fields of mathematics must be understood vividly to make the research work easier. These includes the detailed understanding of the famous Radon transform, the Fourier transform and slice theorem in relations to parallel, fan beam and the cone beam projections in order to breakdown any geometry and paths followed by the projected beams. Moreover, the implementation of the analytical knowledge into algorithmic understanding of building of the sinogram, back-projection, and the filtered back-projection of the parallel which can be obtained easily from MATLAB and other coding packages paves the way for understanding and success in achieving the main goal of the research. Even though, there are codes for handling the fan and cone beam projection issues, but they remain scarce, expensive and protected by copyrights till date. Therefore, this forms the basis of the research to generate codes to handle the simulations of the reconstruction of the cone beam data directly in order to skip certain steps and limitations posed in rebinning.

In this research, python coding packages were used to run the codes generated in ATOM IDE editor as python development environment. With the implementation of the analytical and mathematical knowledge into the development of the algorithms based on the fan and cone beam geometries, the cone beam reconstruction codes were successfully generated, and its accuracy investigated with same phantom which were used in the parallel projection outcomes.

From observations of the reconstruction algorithm developed, it reduces simulation time compared to the rebinning algorithm approach. It also gives a good resolution on the part of the reconstructed images when compared with the phantoms under investigation, hence overcoming some limitations posed by the rebinning algorithm tactics. Therefore, these codes developed for the cone beam projection reconstruction can be functional in the nuclear industry, mechanical and machine building industries that are into the inspection of possible defects in huge components that are scanned using high energy particle accelerators such as the betatrons to reconstruct directly without undergoing rebinning.

4.0 Social responsibility

The social responsibility concerning the workplace is very paramount to the safety and well-being of the workers and the people around. The human life is so important that nothing can replace it when damaged or death. This is the reason why there should be radical improvement in safety techniques in the working environment to reduce accident rates.

The working environment involved in this research is mainly based on processing the acquisition data with sophisticated software and computer-based programs. Hence, the workplace involved an enclosed room stocked with high speed computers and other gadgets to aid in the processing of data and necessary simulations.

Safety in the workplace is a system of legislative, socio-economic, technological, organizational, therapeutic and prophylactic actions and tools that is taken to ensure the safety, protection of the human health and the optimum performance of the human during working hours [35]. However, there should be laid down rules for labor protection and safety tactics that should be enacted in the working environment in order to prevent accidents and to guarantee safe and reliable working atmosphere on the part of the workers as obligatory. These should cover all workers from the highest hierarchy to the lowest rank in exception to none.

In the industries, there are dangerous factors whose impact under certain circumstances might led to trauma, sudden shock and severe worsening of the health of the worker. Therefore, a harmful factor or an industrial health hazard is a factor whose effect on a worker under certain conditions may result to a decrease in the working capacity which has a direct negative influence on productivity of the workplace.

4.1 Analysis of the hazardous and harmful factors

The workplace is characterized by circumstances involving hazardous and harmful factors. These factors are grouped into distinct categories namely; biological, physical, chemical, and psychophysiological. The main elements of the production process that form dangerous and harmful factors are presented in table 1 below.

Table 1 - The key elements of the production process, forming hazardous and harmful factors

FACTORS GOST 12.0.003-74 Occupational safety standards system		Documents
Harmful	Dangerous	
	Chemical Toxic	GOST 12.1.007-76 Occupational safety standards system of Harmful substances.
	Electricity	GOST 12.1.038-82 Occupational safety standards system of electrical safety.
The impact of radiation (HF, UHF, SHF, etc.)		SanPiN 2.2.2 / 2.4.1340-03 Sanitary-epidemiological rules and regulations. "Hygienic requirements for personal computers and organization of work"
Increased level of ionizing radiation in the work area		Radiation Safety Standards (NRB-99/2009). SP 2.6.1. 2523 -0 9.
	Fire	Fire and explosion safety of industrial installations GOST R12.1.004-85 SSBT

In a working environment such as the one involves in the reconstruction processes as discussed in this research has to with working entirely with the computers. There are several factors that have great influence on the person working on the computers and these factors are classified based on physical and psychophysiological effects as displayed in the table 2 below.

Table 2 – Physical and psychophysiological factors and its effects in a computer based working environment.

Physical factors	Temperature and humidity: Sometimes, humans in general feels so tired and disturbed due to the hotness, coldness and the moisture content in an enclosed environment. Hence, these conditions may sometimes reduce the productivity and affects the physical well-being of the worker.
	Noise: Continual background noise from the computer systems sometimes has a physical damage on the hearing organ of the worker. This damage may continue to affect the person each day, weeks, months and years.
	Static electricity: this an inequity of electrical charges on the surface or within a material which exist around a field until its able dissipate through an electric current or an electrical discharge. One main physical effect of static electricity to the worker is having an airborne particulate influence on him. For instance, if a worker is positively charged, it has the possibility of attracting negatively

	charged particles from the air around him, hence setting up static electric field which is unhygienic and causes other problems. Many scientific findings have established that electric fields around a person intensely increase the plate-out rate of airborne particulates. Hence, from speculations, it's been point out that incase such particulates has an allergic effect, the plate-out might cause an incidence of skin irritation or disease, though has not proved. [36]
	Electromagnetic field of low purity
	Illumination: Lightening from the monitor screen of the computer has a direct effect on the eye of the worker involved. Spending many hours working with the computer has a blurry effect on the eye and as a sign of digital strain on the eye. The most damaging of all is too much exposure of the eyes to blue light.
Psychophysiological	Physical overload (static, dynamic)
	Mental stress: Sitting at one place for a long time with the computer by straining the eye, involving the brain with much work may result in mental overstrain, monotony of work, emotional overload and many more that have psychophysiological effects on the worker.

4.2 Justification and development of measures to reduce the levels of hazardous and harmful effects and eliminate their influence.

4.2.1 Organizational arrangements

All workers are required to know and strictly observe the safety rules. The training of personnel in occupational safety and industrial sanitation consists of introductory briefing and briefing at the workplace by the responsible person.

The qualification commission or staffs responsible for checking safety issues concerning the workplace are responsible for imparting knowledge on safety rules and training workers in the workplace. After that, commission assign the safety qualification group corresponding to the employee's knowledge and experience of work and issue a special certificate.

Persons serving electrical installations must not have injuries and illnesses that interfere with manufacturing activity. The state of health is established by medical examination before being employed.

4.2.2 Technical Activities

The rational plan of the workplace offers for a clear order and perpetual placement of objects, means of labor and documentation. Object, what is required to perform the work more often, should be located in the easy reach of the workspace, as shown in Fig. 1

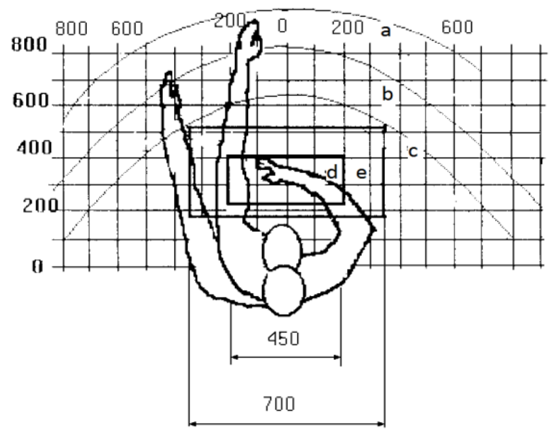

Figure 1 - Hand reach zones in the horizontal plane

Where, a - Zone of maximum reach of hands, b - reach zone of fingers with outstretched arm, c - easy reach zone of the palm d. Optimum space for fine handmade work, e. the optimum space for rough manual work;

Top placement of objects of labor and documentation in the reach of hands:

- the display is located in zone a (in the center);
- keyboard - in the area of e / d;
- the system unit is located in zone b (on the left);
- the printer is in zone a (right);

The documentation is placed in the easy reach of the palm - in (left) - literature and documentation necessary for work; In the drawers of the table - literature that is not used constantly.

When designing a desk, the following requirements must be taken into account.

The height of the working surface of the table should be within 680-800 mm. The height of the working surface with the keyboard should be 650 mm. The working table must be at least 700 mm wide and at least 1400 mm long. There should be a legroom of not less than 600 mm in height, a width of at least 500 mm, a depth at the knee level of at least 450 mm and at the level of elongated legs - not less than 650 mm.

The work chair must be liftable and adjustable in height and angle of inclination of the seat and backrest, as well as the distance of the backrest to the front edge of the seat. It is recommended that the height of the seat be above the floor level of 420 to 550 mm. The design of the working chair should ensure: the width and depth of the seat surface is not less than 400 mm; Seat surface with recessed front edge.

The monitor should be located at the eye level of the operator at a distance of 500 to 600 mm. According to the norms, the viewing angle in the horizontal plane should be no more than 45º to the normal of the screen. It is better if the viewing angle is 30 °. In addition, it should be possible to select the level of contrast and brightness of the image on the screen.

It should be possible to adjust the screen:

- height +3 cm to 5cm;
- slant from 10 to 20 degrees with respect to the vertical;
- in the left and right directions.

The keyboard should be placed on the surface of the table at a distance of 100 - 300 mm from the edge. The normal position of the keyboard is at the elbow level of the operator with an angle of inclination to the horizontal plane of 15º. It is more convenient to work with keys that have a concave surface, a quadrangular shape with rounded corners. The key design should provide the operator with a click sensation. The color of the keys should contrast with the color of the panel.

It is recommended to choose soft, low-contrast floral shades that do not disperse attention (low-saturated shades of cold green or blue colors) in the case of monotonous mental work requiring considerable nervous tension and great concentration. Shades of warm tones are recommended at work, which requires intense mental or physical tension, due to excitation of human activity.

4.3 Safe work conditions

The main parameters characterizing the working conditions are microclimate, noise, vibration, electromagnetic field, radiation, illumination.

The air of the working area (microclimate) is determined by the following parameters: temperature, relative humidity, air speed. The optimum and permissible values of the microclimate characteristics are established in accordance with [36] and are given in Table 2.

Table 2 - Optimal and permissible parameters of the microclimate

Period of the year	Temperature, ^oC	Relative humidity, %	Speed of air movement, m / s
Cold and changing of seasons	23-25	40-60	0.1
Warm	23-25	40	0.1

The measures for improving the air environment in the production room include: the correct organization of ventilation and air conditioning, heating of room. Ventilation can be realized naturally and mechanically. In the room, the following volumes of outside air must be delivered:

- at least 30 m^3 per hour per person for the volume of the room up to 20 m^3 per person;
- natural ventilation is allowed for the volume of the room more than 40 m^3 per person and if there is no emission of harmful substances.

The heating system must provide sufficient, constant and uniform heating of the air. Water heating should be used in rooms with increased requirements for clean air.

The parameters of the microclimate in the laboratory regulated by the central heating system, have the following values: humidity 40%, air speed 0.1 m / s, summer temperature 20-25 ° C, in winter 13-15 ° C. Natural ventilation is provided in the laboratory. Air enters and leaves through the cracks, windows, doors. The main disadvantage of such ventilation is that the fresh air enters the room without preliminary cleaning and heating.

Noise and vibration worsen working conditions, have a harmful effect on the human body, namely, the organs of hearing and the whole body through the central nervous system. It results in weakened attention, deteriorated memory, decreased response, and increased number of errors in work. Noise can be generated by operating equipment, air conditioning units, daylight illuminating devices, as well as spread from the outside. When working on a PC, the noise level in the workplace should not exceed 50 dB.

The screen and system blocks produce electromagnetic radiation. Its main part comes from the system unit and the video cable. According to [37], the intensity of the electromagnetic field at a distance of 50 cm around the screen along the electrical component should be no more than:

- in the frequency range 5 Hz - 2 kHz - 25 V / m;
- in the frequency range 2 kHz - 400 kHz - 2.5 V / m.

The magnetic flux density should be no more than:

- in the frequency range 5 Hz - 2 kHz - 250 nT;
- in the frequency range 2 kHz - 400 kHz - 25 nT.

There are the following ways to protect against EMF:

- increase the distance from the source (the screen should be at least 50 cm from the user);
- the use of pre-screen filters, special screens and other personal protective equipment.

When working with a computer, the ionizing radiation source is a display. Under the influence of ionizing radiation in the body, there may be a violation of normal blood coagulability, an increase in the fragility of blood vessels, a decrease in immunity, etc. The dose of irradiation at a distance of 20 cm to the display is 50 μrem / hr. According to the norms [37], the design of the computer should provide the power of the exposure dose of x-rays at any point at a distance of 0.05 m from the screen no more than 100 μR / h.

Fatigue of the organs of vision can be associated with both insufficient illumination and excessive illumination, as well as with the wrong direction of light.

4.3.1 Electrical safety

Depending on the conditions in the room, the risk of electric shock to a person increases or decreases. Do not operate the electronic device in conditions of high humidity (relative air humidity exceeds 75% for a long time), high temperature (more than 35 ° C), the presence of conductive dust, conductive floors and the possibility of simultaneous contact with metal components connected to the ground and the metal casing of electrical equipment. The operator works with electrical devices: a computer (display, system unit, etc.) and peripheral devices. There is a risk of electric shock in the following cases:

- with direct contact with current-carrying parts during computer repair;
- when touched by non-live parts that are under voltage (in case of violation of insulation of current-carrying parts of the computer);
- when touched with the floor, walls that are under voltage;
- short-circuited in high-voltage units: power supply and display unit.

Measures to ensure the electrical safety of electrical installations:

- disconnection of voltage from live parts, on which or near to which work will be carried out, and taking measures to ensure the impossibility of applying voltage to the workplace;
- posting of posters indicating the place of work;
- electrical grounding of the housings of all installations through a neutral wire;
- coating of metal surfaces of tools with reliable insulation;
- inaccessibility of current-carrying parts of equipment (the conclusion in the case of electroporating elements, the conclusion in the body of current-carrying parts) [38].

4.3.2 Fire and explosive safety

According to [39], depending on the characteristics of the substances used in the production and their quantity, for fire and explosion hazard, the premises are divided into categories A, B, C, D, E.

The room belongs to category B according to the degree of fire and explosion hazard. It is necessary to provide a number of preventive measures.

Possible causes of fire:

- malfunction of current-carrying parts of installations;
- work with open electrical equipment;
- short circuits in the power supply;
- non-compliance with fire safety regulations;
- presence of combustible components: documents, doors, tables, cable insulation, etc.

Activities on fire prevention are divided into: organizational, technical, operational and regime.

Organizational measures provide for correct operation of equipment, proper maintenance of buildings and territories, fire instruction for workers and employees, training of production personnel for fire safety rules, issuing instructions, posters, the existence of an evacuation plan.

The technical measures include: compliance with fire regulations, norms for the design of buildings, the installation of electrical wires and equipment, heating, ventilation, lighting, the correct placement of equipment.

The regime measures include the establishment of rules for the organization of work, and compliance with fire-fighting measures. To prevent fire from short circuits, overloads, etc., the following fire safety rules must be observed:

- elimination of the formation of a flammable environment (sealing equipment, control of the air, working and emergency ventilation);
- use in the construction and decoration of buildings of non-combustible or difficultly combustible materials;
- the correct operation of the equipment (proper inclusion of equipment in the electrical supply network, monitoring of heating equipment);
- correct maintenance of buildings and territories (exclusion of the source of ignition - prevention of spontaneous combustion of substances, restriction of fireworks);
- training of production personnel in fire safety rules;
- the publication of instructions, posters, the existence of an evacuation plan;
- compliance with fire regulations, norms in the design of buildings, in the organization of electrical wires and equipment, heating, ventilation, lighting;
- the correct placement of equipment;
- well-time preventive inspection, repair and testing of equipment.

In the case of an emergency, it is necessary to:

- inform the management (duty officer);
- call the Emergency Service or the Ministry of Emergency Situations - tel. 112;
- take measures to eliminate the accident in accordance with the instructions.

5.0 Financial Management, resource efficiency and conservation

5.1 Introduction to the Research

The simulation of translational based data acquisition scheme and the reconstruction algorithms of X-ray tomography in Non-destructive testing applications in the nuclear industry is a very important aspect which requires detail research and technology. In the nuclear industry, there exist several components that needs to be inspected before commissioning. Also, during the reactor campaign, inspections are conducted from time to time. This is a very important routine to check for any possible defects in order to prevent any unpleasant eventualities. The nuclear power plant is one of the most important power generation facility and the most dangerous site to live in case of accident conditions such as reactor core meltdowns, fire outbreaks and radiation leakage in such facilities. This is since nuclear accidents and its effects takes a longer time to even generations to bring the effects to an end.

However, there are several non-destructive testing techniques which are used in monitoring possible defects in industrial materials, such as the ultrasonic testing, magnetic particle testing, visual testing, leakage testing, radiation testing and many more. Despite all these non-destructive testing techniques has their own advantages and disadvantages, but the radiation testing still possesses some merits over some others as being one of the best surface, subsurface and internal defects testing methods. Moreover, it is able to give much information of the defects in the object of interest as well as repeatability of test results in many folds.

Radiography as a 2D defect viewing technique has been used some decades back since the discovery of the X-ray. However, it faces limitations of not completely giving enough details on the defect in any field of applicability. The discovery of tomography which involves the building of 3D volume of the scanned object using several 2D slices came to overcome those limitations posed by the traditional radiography technique, though still being used today. In modern times, a 3D reconstructed image of inspected region makes inspection and monitoring carrier more detailed and real.

To detect defects in industrial materials, there are two major steps to arrive at the result. Firstly, the data acquisition stage which involves the setting up of equipment for projecting the radiation through the object of interest and registering the radiation absorbed data from the detector onto a computer unit. Secondly, the data collected are processed using codes with specific reconstruction algorithms to generate the image out of the data and this procedure is known as the reconstruction stage.

In the nuclear industry, there exist thousands of equipment of varied sizes which are liable to any kind of defects. Small and medium sizes of nuclear reactor components, spare parts and many others can be tested with the conventional x-ray tomography technique which can handle those sizes. However, large scale industrial objects such as the reactor vessels, steam generator vessels, pressurizers, condensers, turbines, emergency core cooling systems and many others of such sizes cannot be tested using the conventional set-up, since these sizes and weight cannot be rotated with the current rotational stage available. The figure 1 and figure 2 below is an example of such reactor components.

Figure 1 – Reactor vessel under construction in Atomenergomash

Figure 2 – Partially designed Reactor vessel in Atomenergomash

Hence, it requires the use of particle accelerators such as the modern betatrons that are designed to generate high energy x-ray beam to scan through such large industrial components. With the use of different data acquisition approach such as the translational based data acquisition technique, it is possible to acquire the necessary data required to process and reconstruct the image expected. However, x-rays projected from betatrons area not in the usual parallel beam pattern but in a conical beam shape. Therefore, this requires that the conical beam pattern undergoes rebinning to arrive at the fan beam or the parallel beam pattern which would simplify the reconstruction algorithm to be implemented. Rebinning is a process where by a conical beam is taking into fan beam shape and reformatted into parallel beam projections. This mathematical and algorithmic conversion sometimes alters the final reconstructed image by losing some qualities in the data.

Therefore, many industries that employs the rebinning approach prefer to use an algorithm that can process the cone beam data directly to obtain the image in order to avoid data loss and the other complications associated with the rebinning algorithm processes.

The main objective of this research work would be focused on building a reconstruction algorithm which is capable of direct image reconstruction from the cone beam data acquired to obtain the final image to avoid the limitations that would be incurred during rebinning. Moreover, there are other algorithms of this kind already in existence but are very rare and expensive. Hence, success achieved in this research would help the nuclear industries, machine building industries, hospitals and many other industries that uses the cone beam x-ray computed tomography set-ups and data generated from betatrons to have access to these codes to enhance productivity and to reduce the time involved in the acquisition and processing of data. Therefore, the theme "Simulation of Cone Beam X-ray Computed Tomography and the Development of Reconstruction Algorithm for NDT Applications in the Nuclear Industry".

Therefore, the main objective of this work is to reconstruct an algorithm which can sample the data acquired from the cone beam x-ray projection straight to obtain the reconstruction image without passing through a conversion process known as the rebinning process. Hence, the algorithm developed can be used to simulate the reconstruction images of inspected large industrial objects in the nuclear and other industries as discussed earlier.

5.1 Introduction to Financial Management

In modern times, the expectations with regards to scientific and engineering research are ascertain not on just the level of it discovery, which is even more complicated in terms of estimation to real life application, but rather considered on a commercial scale in the development of the sector involved. Moreover, being able to draw a commercial plan for a discovery or invention helps to search for sources of funding for the research and the commercializing the results. The aspect of commercialization seems to be more important since the commercial attractiveness of the scientific research should not be based on just exceeding technical parameters over the already existing ones, but also on how efficient the developer will be appreciated for his or her work as demanded by the market. Taking into considerations the price, customer satisfaction, project budget and many more helps to measure the worth of the research and can promote future ongoing research in the field as well. Hence, the aim of the section “Financial Management, Resource Efficiency and Resource savings” is to measure the prospects and success of a research project in order to design a mechanism for managing and acquiring special supports during the implementation stage of the project to enhance productivity. [40]

5.2 Definitions of Financial Management by some scholars

"Financial management is that activity of management which is concerned with the planning, procuring and controlling of the firm's financial resources. " By Deepika &Maya Rani. “Financial Management is an area of financial decision making, harmonizing individual motives and enterprise goals." -By Weston and Brigham

“Financial management may be defined as that area or set of administrative function in an organization which relate with arrangement of cash and credit so that organization may have the means to carry out its objective as satisfactorily as possible." - by Howard & Opton. Financial management deals with procuring funds and their effective use in the business “by S.C. Kuchal”. Hence, considering the above definitions of the scholars, it can be concluded that:

Financial management is the sector responsible for effective and efficient channeling of monetary funds into a project in order to achieve an optimum goal in the chosen area.

5.3 Potential consumers of research results

The research outcome is very sensitive to the development of tomography in various industries such as the medical, scientific, and engineering fields where there is a possibility of x-rays applications. However, this project tends to focus more on the nuclear industry and all related industries that build the various reactor component such as Atomenergomash and many others. In these industries, larger reactor components are tested of any possible defect before their campaign and also in the course of their campaign. Therefore, this research was embarked to reduce the time of examination and to reduce the cost involved in the purchase of these software from any external source. This ultimately leads to a reduction in the economic costs of acquiring the software and the complications involved in handling it in times possible failures of the software which will request the attention of the software designer with related copyright issues and finances.

5.4 SWOT Analysis

SWOT analysis has four elements in a 2x2 matrix. Own strengths illustrate to the company where they are good and should pay attention on its development. By that companies can compensate for their own weaknesses and strengths of the head to obtain information about threats on the background of the future impact of the elimination purposes. Weaknesses can be eliminated by emphasizing the strengths. External opportunities can be obtained from the company's use of research and development activities, teaming with trusted partners and outsourcing some activities.

External threats can be barred by finding the real threats backgrounds. Also changing company´s own attitudes from the threats to opportunities (Lipiäinen 2001, 46-49).

The table below is the SWOT Analysis of the research work.

Table 1 – SWOT Analysis of the research work

	Positive Factors	Negative Factors
Internal Factors	STRENGTHS 1. Able to work with acquired data from cone x-ray beam. 2. Can reconstruct data using betatrons for cone beam projection for large industrial objects. 3. Does not require higher electrical energy to operate. 4. Simple to use. 5. Reduction in time for the reconstruction.	WEAKNESSES 1. Need technical know-how on python and ATOM coding packages to operate at the workplace. 2. It effectiveness depends on the data acquisition stage taking by an expect in that field.

	Positive Factors	Negative Factors
External Factors	OPPORTUNITIES . Making the software to be easily obtained by companies involved in NDT of large industrial materials. . Would help to develop a 3-D reconstruction image of inspected objects to enhance efficiency in NDT. . It would be applicable in the medical field for tomographic imaging	THREATS 1. Strong competition of alternate package from other sources.

	involving cone beam projection techniques.	

The tables below show the Interactive matrix of the project

Table 2 – Interactive matrixes of the project

Project strength						
Project Opportunities		S1	S2	S3	S4	S5
	O1	+	+	-	+	+
	O2	+	+	-	0	+
	O3	+	+	-	+	+

Project weakness			
Project Opportunities		W1	W2
	O1	-	-
	O2	-	-
	O3	0	+

Project strengths						
Project Threats		S1	S2	S3	S4	S5
	T1	+	+	-	0	+

Project threats		
Project Weakness		T1
	W1	-
	W2	-

Table 3 – SWOT Analysis

	Strengths Strengths of the research project:	Weaknesses Weaknesses of the research project:
Opportunities	SO 1. Distribute these codes among all industries especially nuclear related ones to monitor defect presence in the facility to ensure safe use of the reactor components.	WO 1. The project should be published on international bases to advertise to all sectors applicable for large market size. 2. Should be copy right protected to prolong its existence in the industrial sphere.

	2. Can be applicable in medical imaging to enhance tomography.	
Threats	ST 1. The technical knowledge on how to use the software need to be clearly explained to whoever is going to use it for reconstruction. 2. The codes should be more simplified and compact for the user.	WT 1. Would require more research and development to keep the codes updated in order to avoid it being obsolete in the future.

5.5 Evaluation of the project ready for commercialization

Table 4 – Evaluation of the project ready for commercialization

Criteria	Degree of elaboration in the research project	Level of developers existing knowledge
Scientific and technical potential is determined	4	4
Promising areas of commercialization of scientific and technological potential are identified	5	3
Industries and technologies (products and services) to offers on the market are identified	3	4

Commodity form (product form) of the scientific and technical basis for the presentation to the market is determined	1	2
Author is identified, and protection of their rights is secured	5	4
Assessment of the value of Intellectual Property is done	4	5
Marketing research of potential markets is carried out	3	5
Business plan for commercialization of scientific development is developed	2	2
The ways of promoting scientific development to the market are defined	3	5
The strategy (form) the implementation of scientific development is developed	4	5
International cooperation potential and access to foreign markets are studied	1	2
Use of infrastructure support services to receive benefits is studied	3	2
Funding issues commercialization of scientific development are worked out	2	3
Team for the commercialization of scientific development is formed	2	3
Arrangements for the implementation of a research project are made	2	3
TOTAL POINTS	44	52

Method for the commercialization of scientific and technological research

5.5.1 Trade Patent Licenses

Research commercialization permits technology created during research activities to be further developed into merchantable products for the use of the public. This is attained through technology transfer, which is a method by which technology, skills, or knowledge developed during research activities at the research institution are applied and used in another place. Technology transfer usually refers to transferring a technology between a research laboratory and a commercial partner, plus industry, academia, and state and local governments.

Patents include a legal monopoly granted to the discoverer, inventor, licensee or assignee of the finding and comprises a limited legal right to exclude others from making, using or selling that which has been patented for the duration of a patent.

Transfer to third parties the rights of intellectual property on a license basis. In the patent law distinguishing types of licenses: exclusive (simple), the exclusive, full license, sub-license, options.

The technology transfer process characteristically will include:

1. Recognizing new technologies stemming from the research activities;
2. Protecting the intellectual property of technologies through patents and copyrights;
3. Forming marketing strategies to further develop and commercialize the technology to existing private sector companies or newly created startup companies.

This method of commercialization of the research will enable for engineering and implementation of technologies since this technology needs a lot of money to be implemented. This strategy will also formulate strategies to develop and commercialize to existing nuclear facilities and radiochemical facilities so as to realize the goal of the research.

5.5.2 Initiation of the Project

To reduce fatigue involved in the reconstruction process with it related limitations using the rebinning algorithm techniques, it is required to develop a technology to guarantee improvement on the already existing one. The developed algorithm is intended to be used at nuclear industries, machine building industries and many others to enhance in cone beam projection application for non-destructive testing. To achieve these purposes, this research seeks to develop an algorithm which is able to reconstruct inspected objects directly using the acquired data without passing through several stages to arrive at the result.

5.7 Objectives and Outcomes of the Project

The table below shows the project goals and results

Table 5 – The goals and expected results for the research work

Project Objectives:	Development of reconstruction algorithm to directly simulate data acquired from cone beam x-ray Tomography set-up.
Expected results:	Develop algorithm to handle the cone beam projection x-rays.
Requirements for project results:	Requirement:
	Python programming software
	ATOM IDE [Python working environment]
	Laptop Computer
	ImageJ software
	ANSYS Spaceclaim
	Mathematical model and Algorithm

5.8 The organizational structure of the project

The table shows the organizational structure and functions of the various participants.

Table 6 – Organizational structure and functions

#	Participant (Name, job position)	Role in the project	Functions	Labor costs per hour (Ruble)
1	Supervisor 1	Project Head and Supervisor	Responsible for the implementation of the project within the given resource constraints and coordinates the activities of the project participants.	300 Ruble 4hours in a month for 7 months 300*4*6 = **7200 Rubles**
2	Supervisor 2	Co-supervisor	Financial and Resource efficiency management under the project	300 Rubles 4hours in a month for 2 months 4*2*300 = **2400 Rubles**
3	Supervisor 3	Co-supervisor	In charge of formulating the work	300 Rubles 12 hours a month for 7 months 12*6*300 = **21,600 Rubles**
4	Supervisor 4	Co - Supervisor	Social responsibility aspect	300 Rubles 2 hours a month for 2 months

				2 *2 * 300 = **1200 Rubles**
TOTALS				**32,400 Rubles**

5.8.1 Morphological matrix for research implementation alternatives

Characteristics	Variant			
	1	2	3	4
Base	University	Research Institute	Business Company	
Executives	Supervisor	Head of Lab	Research Director	Student
Materials	Free	Bought		
Equipment	Free	Bought	Rented	
Software	Free	Bought		
Facilities (office)	Free	Bought	Rented	

5.8.2 Limitations and Assumptions of the Project

Project constraints - are all factors that can serve as a limited degree of freedom of members of the project team, as well as the "project boundary" - parameters of the project or product that will not be realized within the framework of this project.

Table 8 – Constraints and budget for the project

Factor	Limitations/ Assumptions
Project Budget	70,000 Rubles
Source of funding	Internal
Duration of the project:	Seven (7) months

Date of approval of the project management plan	11^{th} October, 2017
Date of completion of the project	15 May, 2018
Other limitations and assumptions *	Time limitations, time allocated for the research work was not enough due to lectures and industrial attachment issues.

5.9 Planning and Management of Scientific and Technical Project

5.9.1 Hierarchical structure of the project works

This research demands that a working calendar graph is drawn to represent activities undertaken during the course of the project. This was used to monitor and guide the progress of work.

The Gantt chart was used to map the distribution of the work carried out. Gantt chart is a type of bar charts which is used to illustrate the planned schedule of project, in which the works can be shown the extensive length of time, characterized by the dates of beginning and end of the implementation of these works.

Calendar schedule of R&D on the topic:

Work Code (WBS)	Type of works	Executive	$T_k$cal days	Nov		Dec			Jan		Apr			May			Jun		
				2	3	1	2	3	1	2	1	2	3	1	2	3	1	2	3
1	Compilation of technical specifications	Supervisor 1	5	■															
2	Developing of Research Structure	Engineer (graduate student)	3		■														

3	Study of the literature	Engineer (graduate student)	5																
4	Selecting the direction of research	Supervisor 1 and engineers	1																
5	Writing of Literature Review	Engineer / Student	14																
6	Developing of Research Method	Engineer / Student	8																
7	Review by Supervisor	Supervisor 1	4																
8	Corrections	Engineer	4																
9	Results and Discussions	Engineer	10																
10	Writing of Financial and Resource Efficiency	Engineer	5																
11	Social Responsibility	Engineer	4																
12	Conclusion	Engineer	5																
13	Pre – Defence	Engineer	1																
14	Final defence	Engineer	1																

Calculation of material costs STR:

Material cost calculation is carried out according to the following formula:

$$C_m = (1 + k_{tr}) * \sum_{i}^{m} P_i * N_i \qquad (5.1)$$

Where

m – number of types of material resources consumed in carrying out scientific research;

N_i – the number of physical resources i-th species, planned to be used in carrying out scientific research (pieces, kg, m, mon.)

P_i – acquisition unit price i-th species consumable material resources (rubles / pc, rub / kg, rub / m, rub)

k_{tr} – coefficient taking into account transportation and procurement costs.

Name	Quantity			Price per unit., Ruble.			Costs of materials**(Wm)**,rub.		
	Alt.1	Alt.2	Alt 3	Alt.1	Alt.2	Alt.3	Alt.1	Alt.2	Alt.3
Computer	1	1	1	20000	25000	34000	20000	25000	34000
Software	1	1	1	-	10000	10000	-	10000	10000
Electricity cost (kWh)		300	250	-	6	6	-	1800	1500
Pens	15	11	10	10	10	10	150	110	100
Note books	8	3	5	30	30	30	240	90	150
Printing	23	25	15	10	6	20	230	150	300
Transpor-tation							5000	5400	6000
Total							25620	42550	52050

The basic salary performers:

$$S_b = S_h * 8 \tag{5.2}$$

where S_h - basic salary of one employee per hour, rub/hour;

Hourly labor rate may vary depending on the type of executive in the research project.

$$S_b = 300 * 8 = 2400$$

Calculation of basic salary

#	Executives			Work, person-days.			Salaries per one person-hours, ths. Rub.			Total salaries at the rate (salary), ths. Rub.		
	Alt.1	Alt.2	Alt.3	Alt.1	Alt.2	Alt.3	Alt.1	Alt.2	Alt.3	Alt.1	Alt.2	Alt.3
	Sup	L.T	R.D	70	65	60	20000	25000	30000	237 30	2938 0	3390 0
Total:												

Additional salary:

$$S_{ad} = k_{ad} * S_b \tag{5.3}$$

where k_{ad} - factor of additional salary (taken at the design stage at 0.12 - 0.15)

$$S_{ad.1} = 0{,}13 * 20000 = 2600$$

$$S_{ad.2} = 0{,}13 * 25000 = 3250$$

$$S_{ad.3} = 0{,}13 * 30000 = 3900$$

Contributions to these funds determined based on the following formula:

$$S_f = k_f * (S_b + S_{ad}) \tag{5.4}$$

where k_f - coefficient for payments to funds (SIF, PF, MIF).

Artist	Basic salary, rubles.			Additional salary, rubles.		
	Alt.1	Alt.2	Alt.3	Alt.1	Alt.2	Alt.3
Project Manager	20000	25000	30000	2600	3250	3900
Student	-	-	-	-	-	-
ratio of contributions to social funds	25.2%	25.5%	30%	25.2%	25.5%	30%

Total amount of social fund payments, rubles	
Alternative 1	5695
Alternative 2	7204
Alternative 3	10170

Overheads cost is calculated as follows:

Their value is determined by the following formula:

$$C_{ovh} = C_{total} * k_{ovh} \tag{5.5}$$

where

C_{total} – Total costs of the above cost items

k_{ovh} – Overhead coefficient, which can be taken at a rate of 16%.

$C_{ovh.1}$ = (25620 + 20000 + 2600 + 5695) * 0,16 = 8626 rubles

$C_{ovh.2} = (42550 + 25000 + 3250 + 7204) * 0{,}16 = 12481$ rubles

$C_{ovh.3} = (52050 + 30000 + 3900 + 10170) * 0{,}16 = 15379$ rubles

5.10 Budget of Scientific Research

Calculation of the budget cost of STI

Item	Amount, rub.		
	Alt.1	Alt.2	Alt.3
1. Material costs STR	25620	42550	52050
2. Costs of basic salary	20000	25000	30000
3. Costs of additional salaries	2600	3250	3900
4. Contributions to the social funds	5695	7204	10170

5. Costs of research and production trips	-	-	-
6. Outsourcing	-	-	-
7. Overhead costs	8626	12481	15379
8. Budget expenditures STI	**62540**	**90485**	**111499**

5.11 Effectiveness and efficiency

Effectiveness is measured based on the calculation of the integral index of the effectiveness of scientific research. It is done through weighted average of financial efficiency and resource efficiency.

Comparative evaluation of characteristics of the project alternatives

Integral financial efficiency indicator:

$$E_{fin}^{alt.i} = \frac{TC_i}{TC_{max}} \tag{5.6}$$

Where:

$E_{fin}^{alt.i}$- an integral index of financial efficiency,

TC_i- total cost of the $i-th$ alternative,

TC_{max}-the maximum total cost of research project.

Total cost of research at the university in ruble – 62540

Total cost of research at research institute in ruble– 90485

Total cost of research at business company in ruble – 111499

$$E_{fin}^{alt.U} = \frac{62540}{111499} = 0{,}56$$

$$E_{fin}^{alt.R} = \frac{90485}{111499} = 0{,}812$$

$$E_{fin}^{alt.B} = \frac{111499}{111499} = 1$$

Comparative evaluation of characteristics of the project alternatives:

Table 11 – Comparative evaluation of the project alternatives

Criteria	a_i Weight	b_i Score		
		Alt 1	Alt 2	Alt 3
1. Promotes growth user productivity	0,1	3	5	5
2. Ease of operation (corresponding to the requirements of consumers)	0,15	4	4	5
3. Interferences	0,15	2	4	4
4. Energy savings	0,20	4	2	3
5. Reliability	0,25	4	3	5
6. Material	0,15	3	5	4
TOTAL	1	20	23	26

Integral resource-efficiency indicator:

$$E_{res}^{alt.i} = \sum a_i * b_i \tag{5.7}$$

$$E_{res}^{alt.1} = 3 * 0{,}1 + 4 * 0{,}15 + 2 * 0.15 + 4 * 0{,}20 + 4 * 0{,}25 + 3 * 0{,}15 = 3{,}45$$

$$E_{res}^{alt.2} = 5 * 0{,}1 + 4 * 0{,}15 + 4 * 0{,}15 + 2 * 0{,}20 + 3 * 0{,}25 + 5 * 0{,}15 = 3{,}60$$

$$E_{res}^{alt.3} = 5 * 0{,}1 + 5 * 0{,}15 + 4 * 0{,}15 + 3 * 0{,}20 + 5 * 0{,}25 + 4 * 0{,}15 = 4{,}30$$

Integral total efficiency indicator:

$$E_{total}^{alt.i} = \frac{E_{res}^{alt.i}}{E_{fin}^{alt.i}} \tag{5.8}$$

$$E_{total}^{alt.1} = \frac{3{,}45}{0{,}56} = 6{,}160$$

$$E_{total}^{alt.2} = \frac{3,6}{0,812} = 4,433$$

$$E_{total}^{alt.3} = \frac{4,30}{1} = 4,30$$

Comparative project efficiency indicator:

$$E_{comp}^{alt.i} = \frac{E_{total}^{alt.i}}{E_{total}^{min}}$$

$$E_{comp}^{alt.1} = \frac{6,160}{4,30} = 1,432$$

$$E_{comp}^{alt.2} = \frac{4,433}{4,30} = 1,030$$

$$E_{comp}^{alt.3} = \frac{4,30}{4,30} = 1$$

Comparative development efficiency

Table 12 – Comparative efficiencies

№ p/p	Indicators		Alt.1	Alt.2	Alt.3
1	Integral financial efficiency indicator	$E_{fin}^{alt.i}$	0,560	0,812	1,000
2	Integral resource-efficiency indicator	$E_{res}^{alt.i}$	3,450	3,600	4,300
3	Integral total efficiency indicator	$E_{total}^{alt.i}$	6,160	4,433	4,300
4	Comparative project efficiency indicator	$E_{comp}^{alt.i}$	1,432	1,030	1,000

Conclusion

Observations from the calculated results above, it can be concluded that the best place to conduct this research work is Alt. 1 which is the university, in order to attain resource and financial efficiency.

References

1. Fuchs T., Schon T., Hanke R., A Translation-based Data Acquisition Scheme for Industrial Computed Tomography, ECNDT, 2010
2. Cantatore A., & Müller P., “Introduction to computed tomography”, DTU, Department of Mechanical Engineering, Denmark, 2011.
3. Avinash K., Malcolm S., “Principles of Computerized Tomographic Imaging”, [Electronic copy 1999] IEEE Press, ISBN 0-87942-198-3
4. F. Van Gelderen, Understanding X-Rays © Springer-Verlag Berlin Heidelberg 2004
5. http://www.gettyimages.com/detail/news-photo/wilhelm-conrad-rontgen-portrait-7-picture-id588243710.
6. W. A. Kalender, X-ray computed tomography, Physics in Medicine & Biology 51 (2006) 29–43.
7. http://en.wikipedia.org/wiki/godfrey_hounsfield (read 18/09/2017).
8. C. Reinhart, C. Poliwoda, T. Guenther, W. Roemer, S. Maas, C. Gosch, Modern voxel-based data and geometry analysis software tools for industrial CT, Proceedings of the 16thWorld Conference on NDT, Montreal, Canada (2004) 8.
9. https://radiopaedia.org/articles/coherent-scattering
10. Serway R.A, et al, College Physics 8th Ed.pdf, Belmont, CA 94002-3098, USA, Cengage Learning, 2009, page 872.
11. Parks J.E., Compton Scattering and Gamma Ray Spectroscopy, Department of Physics, University of Tennessee, Knoxville Tennessee 37996-1200, January 2015.
12. Buzug, T. M, “Computed Tomography from photon statics to modern cone-beam CT”, [E-resource, e-ISBN 978-3-540-39408-2], Springer, Verlag Berlin Heidelberg, Germany, June 2008.
13. M. A. Haidekker, Medical Imaging Technology, SpringerBriefs in Physics, DOI: 10.1007/978-1-4614-7073-1, _ The Author(s) 2013.
14. U. Bonse and M. Hart, Appl. Phys. Lett. 6, 155 1965.

15. F. Pfeiffer et al., “X-ray dark field and phase contrast imaging using a grating interferometer”, [Electronic Resource], Published online 19th May 2009.
16. Keyriläinen, J.; Bravin, A.; Fernández, M.; Tenhunen, M.; Virkkunen, P.; Suortti, P. (2010). "Phase-contrast X-ray imaging of breast". *Acta Radiologica*. 51 (8): 866–884.
17. Diemoz, P, et al., "Theoretical comparison of three X-ray phase-contrast imaging techniques: Propagation-based imaging, analyzer-based imaging and grating interferometry", (2012) Optics Express. 20 (3): 2789–2805. Bibcode:2012OExpr.20.2789D. PMID 22330515. doi:10.1364/OE.20.002789.
18. Weon, B. M.; Je, J. H.; Margaritondo, G. (2006). "Phase contrast X-ray imaging". *International Journal of Nanotechnology*. 3 (2–3): 280–297. Bibcode:2006IJNT.... 3..280W.
19. M. Born and E. Wolf, Principles of Optics: Electromagnetic Theory of Propagation, Interference and Diffraction of Light (Cambridge University Press, Cambridge, 1999).
20. T. Weitkamp, A. Diaz, C. David, F. Pfeiffer, M. Stampanoni, P. Cloetens, and E. Ziegler, “X-ray phase imaging with a grating interferometer,” Opt. Express 13(16), 6296–6304 (2005).
21. P. Coan, E. Pagot, S. Fiedler, P. Cloetens, J. Baruchel, and A. Bravin, “Phase-contrast X-ray imaging combining free space propagation and Bragg diffraction,” J. Synchrotron Radiat. 12(2), 241–245 (2005).
22. http://www.diamond.ac.uk/Science/Research/Techniques/Imaging/ACI.html
23. Fuchs, T., et al., “Principles of Computed Tomography”, [E-Resource], Kalpakkam, India, April 2007.
24. Julien N, “Advantages of CT in 3D scanning of industrial parts”, North Star Imaging Inc, December 2008.
25. Zvolský M., “Tomographic Image Reconstruction”, [E- Resource], 28.11.2014.
26. http://www.cyberphysics.co.uk/topics/medical/CTScanner.htm

27. Avinash K., Malcolm S., “Principles of Computerized Tomographic Imaging”, [Electronic copy 1999] IEEE Press, ISBN 0-87942-198-3
28. Radon, J.; Parks, P.C. (translator) (1986), "On the determination of functions from their integral values along certain manifolds",(170-176, doi:10.1109/ TMI .1986.4307775, PMID 18244009.
29. Weinstein, Eric W. "Radiation". *Eric Weinstein’s World of Physics*. Wolfram Research. Retrieved 2018-02-20.
30. Eric F. Oliveria et al., “Comparison among tomography Reconstruction Algorithms with a limited data”,2011 international Nuclear Atlantic Conference, Belo Horizonte, MG Brazil, October 2011, ISBN: 978-85-99141-04-5.
31. Thorsten M. Buzug, “Computed Tomography from Photon Statics to Modern Cone Beam CT”, 2008 Springer Verlag Berlin Heidelberg. e - ISBN 978-3540-39408-2.
32. Avinash K., Malcolm S., “Principles of Computerized Tomographic Imaging”, [Electronic copy 1999] IEEE Press, ISBN 0-87942-198-3
33. William R., “Cone beam computed tomography”, CRC press, Taylor and Francis group (2014), Group6000 Broken Sound Parkway NW, Suite 300, Raton, FL 33487-2742.
34. William C. Scarfe et al., “What is Cone Beam CT and How Does It Work”, Elsevier Saunders 2008.
35. Federal Law "On the Fundamentals of Labor Protection in the Russian Federation" of 17.07.99 № 181 – FZ.
36. URL: https://incompliancemag.com/article/static-electricity-and-people/, [14/05/2018].
37. SanPiN 2.2.2 / 2.4.1340-03. Sanitary-epidemiological rules and standards "Hygienic requirements for PC and work organization".
38. GOST 12.1.038-82 Occupational safety standards system. Electrical safety.

39. Fire and explosion safety of industrial facilities. GOST R12.1.004-85 Occupational safety standards system. Fire safety

40. Timur R. Rahimov. Financial Management, Resource Efficiency and Resource Saving. Tomsk – 2014.

Appendix A – Python coding tasks and training

TASK 1

```
import numpy as np
import matplotlib.pyplot as plt
import scipy as sc

"""
1. Add numbers to a file and name it "A", and another "B"
and make both an array of 10
2. import and multiply the two arrays and save the result in
another parameter (c)
3. compute square root of each number of the resulting array
C.
4. save the result of the question 3 in txt files.
5. find and print the maximum value in resulting array from
question
"""

input path =
"C:/Users/User1/Desktop/python_scripts/input_data/"
output path =
"C:/Users/Users1/Desktop/python_scripts/output_data/"

a_filename = "A.txt"
b_filename = "B.txt"
```

```
a = np.loadtxt(input_path + a_filename)
b = np.loadtxt(input_path + b_filename)



def productmatters (a_val, b_val):
    product=a_val*b_val     {# multiplying array a and b}
    print product

productmatters (2,3)

def squareroot(c_val):
    pass sqrt1(c_value)
    d = np.sqrt(c)

MAXD = np.amax(d)
print "The maximum value in the array D is", MAXD

np.savetxt(output_path + "C.txt",c,fmt="%s")
np.savetxt(output_path + "C.txt", c,fmt="%s")

print "Done"
```

TASK 2

```
import numpy as np
import matplotlib.pyplot as plt
import scipy as sc
from PIL import Image
```

```
"""
1.Create a 100 x 100 empty 2D array.
2. Save the array as an image.
3. Put in each element of created array random values.
4. Save the array with random values.
5. Find the maximum, minimum and average values from the array.
6. Display the founded values in convenient way for reading.
7. Finally, cut the array into 4 separate arrays with dimensions of 50x50
8. And save them as the way you can recognize them.
"""

input_path = "C:/Users/user1/Desktop/python_scripts/Input_data/"
output_path = "C:/Users/user1/Desktop/python_scripts/Output_data/"

a_filename = "A.txt"
b_filename = "B.txt"

image1 = np.zeros((100, 100))      #creating an array in 2D
plt.imshow(image1, cmap="plasma”)  #saving array as image
plt.show()

import random
a = np.random.random((100,100))   #random values in the created array
```

```
np.savetxt(output_path + "A.txt", a, fmt="%s”) #saving the 2D arrays

maxval = np.amax(a)                    #finding the maximum value
print 'maximum value is', maxval

minval = np.amin(a)                    #finding the minimum value
print 'minimum value is', minval
meanval = np.mean(a)                   #finding the average value
print 'average value is', meanval

image2 = image1[0:50, 0:50]
plt.imshow(image2, cmap="pink")            # 1/4 portion of image1
plt.show()

image3 = image1[0:50, 50:100]
plt.imshow(image3, cmap="Greens")          # 2/4 portion of image1
plt.show()

image4 = image1[50:100, 0:50]
plt.imshow(image4, cmap="spring")          # 3/4 portion of image1
plt.show()
```

```
image5 = image1[50:100, 50:100]
plt.imshow(image5, cmap="Wistia")             # 4/4 portion
of image1
plt.show()

Im=Image.open("C:/Users/user1/Desktop/python_scripts/myimag
es/Rotate_ images/phat1_360.png")
im.show()
im.save('phat1-gs','jpg')

print "Done"
```

Results

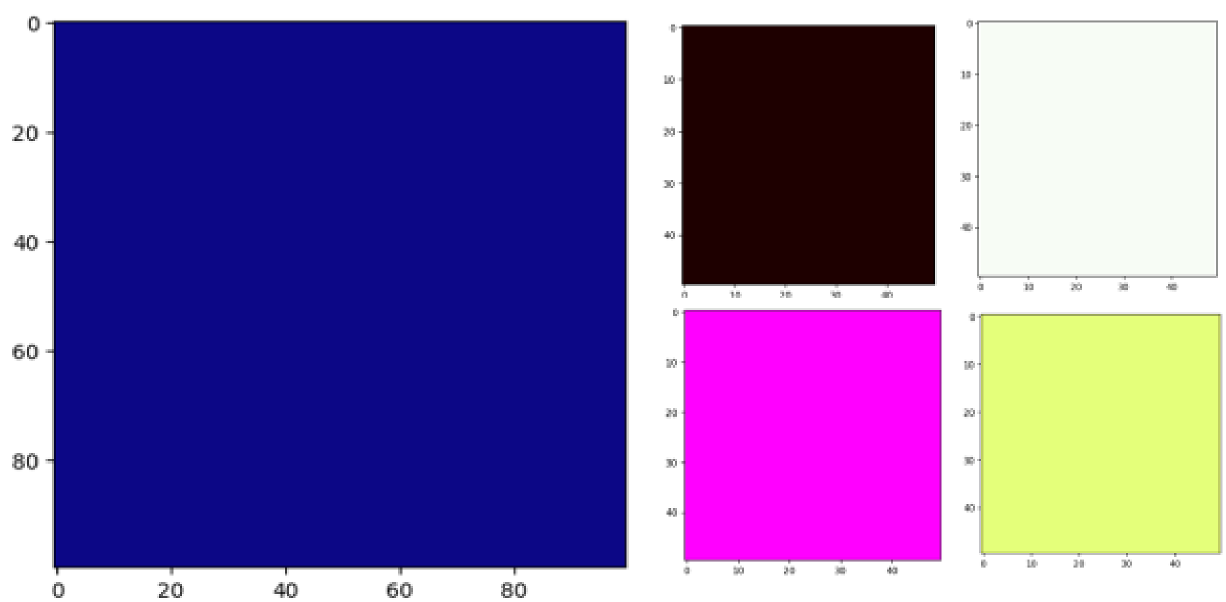

TASK 3

```
import numpy as np
```

```
import matplotlib.pyplot as plt
from scipy.ndimage.interpolation import rotate


"""
1. Download and install ImageJ
2. Create phantom image in Paint and change its type in ImageJ
3. Import image in your script
4. How to rotate image by 90, 180, 270, 360 degrees, and rotate created image.
5. Create and save 4 images which are the rotation of the phantom by proposed degrees.
6. Find the way how to rotate images by small degrees
"""
input_path = 'C:/Users/user1/Desktop/python_scripts/myimages/Rotate_images/'
save_path = "C:/Users/user1/Desktop/python_scripts/task3_save/"


test_image = plt.imread(input_path + 'phat1.png') #importing image.
  plt.imshow(test_image)
  plt.show()

  plt.imsave(save_path + '90deg_rotated.png', deg90rotated)
```

```
  deg180rotated = rotate(test_image, -180, reshape=False,
mode='nearest')
  plt.imsave(save_path + '180deg_rotated.png',
deg180rotated)

  deg270rotated = rotate (test_image, -270, reshape=False,
mode='nearest')
  plt.imsave(save_path + '270deg_rotated.png',
deg270rotated)

  deg360rotated = rotate(test_image, -360, reshape=False,
mode='nearest')
  plt.imsave(save_path + '360deg_rotated.png',
deg360rotated)

def angular_rotation(test_image, angular_range):
    for i in range(angular_range[0], angular_range[1],
angular_range [2]):
    angular_rotation = rotate (test_image, -i,
reshape=False, mode='nearest')
    plt.imsave(save_path + 'deg_rotation_'+str(i)+'.png',
angular_rotation)
    print i

angular_rotation (test_image, (1,361,60))
```

Results

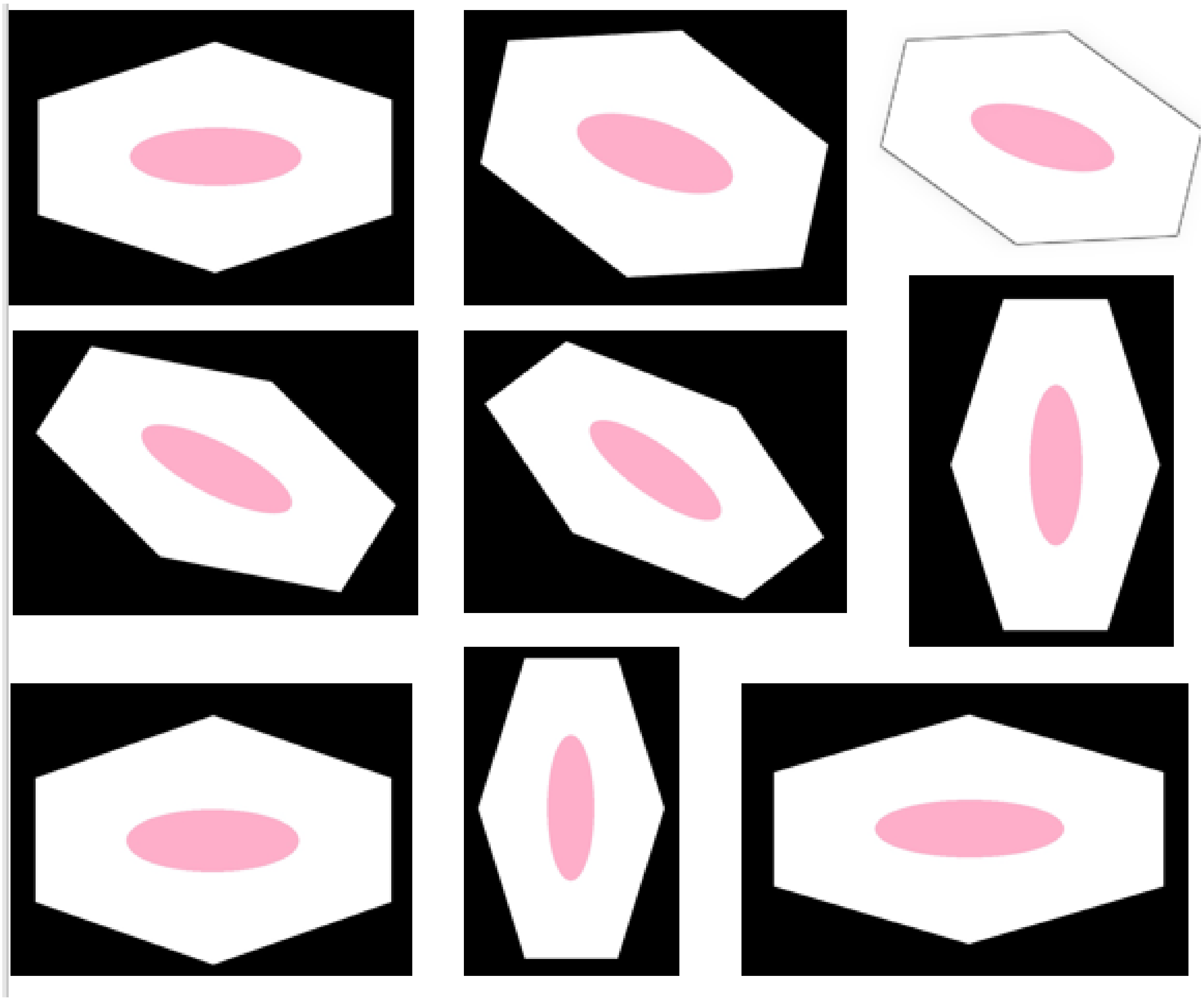

Task 4 [ROTATION OF SAMPLE IMAGE]

```
import numpy as np
import matplotlib.pyplot as plt
from scipy import ndimage

input_path = "C:/Users/User1/Desktop/python_scripts/"
```

```
output_path                                                        =
"C:/Users/User1/Desktop/python_scripts/Output_data/"

sample = plt.imread(input_path +'sample.png')
angular_range = 180
angular_step = 1

for i in range(angular_range):
rotated   image   =   ndimage.interpolation.rotate(sample,
angular_step,   reshape=False,   mode='constant')sample   =
rotated_imageplt.imsave(output_path                        +
'image_which_we_rotated_'+str(i)+'.png',     rotated_image,
cmap = "gray")
```

TASKS 5 [SINOGRAM OF IMAGE SAMPLE 1]

```
import numpy as np
import matplotlib.pyplot as plt
from scipy import ndimage

input_path = "C:/Users/User1/Desktop/python_scripts/"
output_path                                                        =
"C:/Users/User1/Desktop/python_scripts/output_data/Sinogram
_1/"

sample = plt.imread(input_path +'sample.png')
angular_range = 360
angular_step = 1
```

```
sinogram = np.zeros((360, 400))
for i in range(angular_range):
    rotated_image = ndimage.interpolation.rotate(sample, angular_step, reshape=False, mode='constant')
    sample = rotated_image
    #plt.imsave(output_path + 'image_which_we_rotated_'+str(i)+'.png', rotated_image, cmap = "gray")
    oneD_array = np.sum (rotated_image, axis=1)
    sinogram [i,:] = oneD_array

plt.imsave(output_path + 'sinogram.png', sinogram, cmap = "gray")
```

See figure 3.1a for the result of this simulation

TASK 6[SINOGRAM 2]

```
import numpy as np
import matplotlib.pyplot as plt
from scipy import ndimage

input_path = "C:/Users/User1/Desktop/python_scripts/Sample_data/"
output_path = "C:/Users/User1/Desktop/python_scripts/Output_data/"

sample = plt.imread(input_path +'sample3.png')
angular_range = 270
angular_step = 0.5
```

```
angles = np.arange(0, 270, angular_step)

sinogram=np.zeros((540, 400))
for index, i in enumerate(angles):

    rotated_image = ndimage.interpolation.rotate(sample, i,
   reshape=False, mode='constant')
    oneD_array=np.sum (rotated_image, axis=1)
    sinogram[index, :] = oneD_array

    if index == 540:
        break
    print index

plt.imsave(output_path + 'sino.png', sinogram, cmap = "gray"
```

Task 7 [Simple unfiltered back-projection]

```
input_path = "C:/Users/User1/Desktop/python_scripts/"
output_path                                                =
"C:/Users/User1/Desktop/python_scripts/output_data/"

angular_range = 270
angular_step = 0.5

angles = np.arange(0, 270, angular_step)
```

```
test_image = plt.imread(input_path + 'sinogram.png')

empty2D_array = np.empty([400, 400])

for index, angle in enumerate(angles):
    singleRow = test_image[index, :]
    backprojection = np.rot90(np.repeat(singleRow, 400).reshape(400, 400), -1)
    backprojection = ndimage.interpolation.rotate(backprojection, -angle, reshape=False, mode='constant')

    empty2D_array += backprojection
    plt.imsave(output_path + 'backprojection'+str(index)+'.png', backprojection, cmap='gray')
    print index

plt.imsave(output_path + 'empty2D_array.png', empty2D_array, cmap='gray')
```

Task 8 [Filtered Back-projection]

```
import numpy as np
import matplotlib.pyplot as plt
from scipy import ndimage
from scipy.fftpack import fft, ifft, fftfreq
```

```
def filt(sinogram):
    """
    Frequency domain Hamming filter
    Parameters:
    sinogram: array_like, dtype=float
     (Image containing radon transform. Each row of the image
    corresponds to a projection along a different angle.The
    rotation axis should lie at the pixel index)

    << radon_image.shape[1] // 2 >>

    Returns:
    radon_filtered : ndarray
        Filtered sinogram
    """
    width = int((2**np.ceil(np.log2(sinogram.shape[1])) -
    sinogram.shape[1])/2)
    img = np.pad (sinogram, width, 'reflect',
reflect_type='odd')
    # construct the Fourier filter
    # digital frequency
    f = fftfreq(sinogram.shape[1] + 2 * width). reshape (1,
-1)
    omega = 2 * np.pi * f                       # angular
frequency
    fourier_filter = np.abs(f)             # ramp filter
    # fourier_filter *= (1 + np.cos(omega / 2)) / 2
```

```
    # Hamming part of filter
    # fourier_filter *= (0.54 + 0.46 * np.cos(omega / 3))
    # applying the filter in frequency domain
    projection = fft(img, axis=1) * fourier_filter
    # inverse transform
    radon_filtered = np.real(ifft(projection, axis=1))
    # Resize filtered image back to original size
    radon_filtered                                          =
radon_filtered[width:width+sinogram.shape[0],

width:width+sinogram.shape[1]]

    return radon_filtered

input_path = "C:/Users/User1/Desktop/python_scripts/"
output_path                                             =
"C:/Users/User1/Desktop/python_scripts/output_data/"

angular_range = 270
angular_step = 0.5

angles = np.arange(0, 270, angular_step)

test_image = plt.imread(input_path + 'sinogram.png')
test_image = filt(test_image)


empty2D_array = np.empty([400, 400])
```

```
for index, angle in enumerate(angles):
    singleRow = test_image[index, :]
    backprojection = np.rot90(np.repeat(singleRow, 400).reshape(400, 400), -1)
    backprojection = ndimage.interpolation.rotate(backprojection, -angle, reshape=False, mode='constant')

    empty2D_array += backprojection
    plt.imsave(output_path + 'backprojection'+str(index)+'.png', backprojection, cmap='gray')
    print index

plt.imsave(output_path + 'empty2D_array.png', empty2D_array, cmap='gray')
```

Task 9 [Simulation codes for cone beam projection sinogram]

```
def radon (image, radius, pixelSize, fan_angle, angular_step, rotation_range, position):
        """
        Calculates the radon transform of an image at specified
        angular trajectory, rotation range, the beam divergency,
```

considering distance from source to rotation axis and detector pixel size.

```
        Parameters:

        image: array_like

        input image

        radius: dtype=float

The distance from source to sample or rotation axis in mm

        pixelSize: dtype=float

        Detector pixel size in mm

        fan_angle: dtype=float

The angle of the beam divergency in degrees

        angular_step: dtype=float

        The angular rotation step in degrees

        rotation_range: dtype=int

        General rotation range in degrees

        Returns:

        radon_image: ndarray

        Radon transform (sinogram)

        """

        print '\n'
```

```
if image. Shape [0] == image. Shape[1]:
    square = image
else:
lside = abs (image. shape [0] - image. shape [1])
if lside % 2! = 0:
lside += 1
if image. shape [0] > image. shape [1]:
square = matlib.pad (image, ((0, 0), (lside/2, lside/2)),
    mode='constant', constant_values=0)
    elif image. shape [0] < image. shape [1]:
square = matlib.pad (image, ((lside/2, lside/2), (0, 0)),
    mode='constant', constant_values=0)
    distance = radius/pixelSize
    number_of_porjections =
int(rotation_range/angular_step) width = int (np.
round(distance*np.tan(np. deg2rad(fan_angle/2))))
fan = np.flipud(np.linspace(0, fan_angle, 2*width)
- fan_angle/2)
dist = np.linspace(distance - square.shape[0]/2,
distance + square.shape[0]/2, square.shape[0])
height = np.zeros((2*width, square.shape[0]))
```

```
        for (i, angle) in enumerate(fan):

        for (j, distance) in enumerate(dist):

        height[i, j] = distance * np.tan(np.deg2rad(angle))
xaxis = np.arange(0, square.shape[0], 1) - square.shape[0]/2

 radon_image = np.zeros((number_of_porjections, 2*width))

         temp = np.zeros((square.shape[0], 2*width))

         height += position

         for number in range(int(number_of_porjections)):

         for column in range(square.shape[0]):

projected = griddata(xaxis, square[:, column], height[:,
column], method='linear', fill_value=0, rescale=False)

         temp[column, :] = projected

         radon_image[number, :] = np.sum(temp, axis=0)

square     =     scipy.ndimage.interpolation.rotate(square,
angular_step,
reshape=False, mode='constant')

progress_bar((number+1)*100/(number_of_porjections),

'SYNTHESIS')

          return radon_image
```

Task 10 [Simulation codes for the cone beam reconstruction]

```
def pixelbp(sinogram, pixelSize, source2center,
center2detector,

angular_range, step, position, outpuSize, shifts, method):

    """

Produces the 3D array containing all the backprojections in
the order they are acquired

    Parameters:

    sinogram : array_like, dtype=float

Image containing radon transform. Each row of

the image corresponds to a projection along a different
angle. The

rotation axis should lie at the pixel index

<< radon_image.shape[1] // 2 >>

pixelSize: dtype=float

Detector pixel size in mm

source2center:

The distance between the source of the beam the center of
rotation

    center2detector:

The distance between the center of rotation and the
detector plane
```

```
    angular_range : array_like

    Reconstruction angles (in degrees)

    step : dtype=float

    angular step size (in degrees)

    position : dtype=float

Transverse position of the beam source relatively to the
sample

    outpuSize : dtype=int

    Number of rows and columns in the reconstruction

    shifts : dtype=float

    The shift of the rotation axis

    Returns:

    tensor : ndarray

Tensor containing all the backprojections in the order they
are acquired

    """

    print '\n'

    save_path = 'C:/Users/ctMachine/Desktop/bright/output/'

    loops = int(180/step)

    limit = sinogram.shape[0] - loops

    angular_range = np.deg2rad(angular_range)
```

```
    step = np.deg2rad(step)
    source2center = source2center/pixelSize
    center2detector = center2detector/pixelSize
    y_dm = abs(position)
    dwidth = np.arange(outpuSize) - outpuSize/2
    r_dm = np.sqrt(center2detector**2 + y_dm**2)
    r_source = np.sqrt(source2center**2 + y_dm**2)
    alfa = np.arcsin(source2center/r_source) +
np.deg2rad(90)
    gamma = np.arctan(y_dm/center2detector)
    sigma = np.arctan(dwidth/center2detector)
    alfa_2 = alfa + np.deg2rad(180)
    gamma_2 = gamma + np.deg2rad(180)
    [xaxis, yaxis] = np.mgrid[0:outpuSize, 0:outpuSize]  #
the mesh
    xpr = np.rot90(xaxis - outpuSize / 2.)   # horizontal
coordinates
    ypr = np.rot90(yaxis - outpuSize / 2.)   # vertical
coordinates
    reconstructed = np.zeros((outpuSize, outpuSize))
    for number in range(loops):
        x_source = r_source * np.cos(alfa)
```

```
        y_source = r_source * np.sin(alfa)
        x_dm = r_dm * np.cos(gamma)
        y_dm = r_dm * np.sin(gamma)
        source2pixel = np.sqrt(((ypr + abs(position)) -

source2center*np.sin(angular_range[number]))**2.0 +(xpr -
source2center*np.cos(angular_range[number]))**2.0)
normal = (xpr*(y_dm-y_source) - ypr*(x_dm-x_source) -
x_source*y_dm + x_dm*y_source)/np.sqrt((y_dm-y_source)**2 +
(x_dm-x_source)**2)
source2normal = np.sqrt(source2pixel**2.0 - normal**2.0)
cfactor = source2normal / source2center
sample = normal / cfactor
mid_index = (sinogram.shape[1] - shifts[number])/2
xaxis = np.arange(sinogram.shape[1]) - mid_index + position


      if position > 0:
backprojected_1 = griddata(xaxis, sinogram[number, :],
sample,method=method, fill_value=0, rescale=False)
     else:
backprojected_1 = np.flipud(griddata(xaxis,
sinogram[number, ], -sample,
method=method, fill_value=0, rescale=False))
```

```
        alfa += step
        gamma += step
        if number < limit:
    x_source = r_source * np.cos(alfa_2)
    y_source = r_source * np.sin(alfa_2)
    x_dm = r_dm * np.cos(gamma_2)
    y_dm = r_dm * np.sin(gamma_2)
source2pixel = np.sqrt(((ypr + abs(position)) -
source2center*np.sin(angular_range[number+loops]))**2.0
+(xpr -
source2center*np.cos(angular_range[number+loops]))**2.0)
normal = (xpr*(y_dm-y_source) - ypr*(x_dm-x_source) -
x_source*y_dm + x_dm*y_source)/np.sqrt((y_dm-y_source)**2 +
(x_dm-x_source)**2)
source2normal = np.sqrt(source2pixel**2.0 - normal**2.0)
    cfactor = source2normal / source2center
    sample = normal / cfactor
mid_index = (sinogram.shape[1] - shifts[number+loops])/2
xaxis = np.arange(sinogram.shape[1]) - mid_index + position
     if position > 0:
backprojected_2 = griddata(xaxis,  sinogram[number+loops,],
sample, method=method, fill_value=0, rescale=False)
```

```
else:backprojected_2 = np.flipud(griddata(xaxis,
sinogram[number+loops, ],
-sample, method=method, fill_value=0, rescale=False))


     if number==359:
plt.imsave(savePath + 'backprojected.tif', backprojected_1,
cmap='gray')
     alfa_2 += step
     gamma_2 += step
     backprojected = (backprojected_1+backprojected_2)/2
       else:
     backprojected = backprojected_1
     progress_bar(1+number*100/loops, 'RECONSTRUCTION')
     reconstructed += backprojected
     return reconstructed
```

Appendix B - Published article

Simulation of translational data acquisition scheme of X-Ray computed tomography for application in NDT

Bright K. AFORNU[1, a, *], Joseph C. ODII[2, b], Ali H. OZDIEV[3, c], Dmitry A. SEDNEV[4, d]

[1, 2, 3, 4]National Research Tomsk Polytechnic University
Russia, Tomsk, Lenin Avenue, 30, 634050

[a]email: brightafornu@yahoo.com
[b]email: monoexiton@yahoo.com
[c]email: ozdiev@tpu.ru
[d]email: sednev@tpu.ru

Keywords: X-Ray tomography, simulation, NDT, translational data acquisition scheme, reconstruction algorithms.

Abstract: The invention of computed tomography some few decades ago, coupled with its applications in the field of non-destructive testing for industrial objects inspection has revolutionized the way inspections were formerly done. Despite the conventional data acquisition scheme, which is integrated with a rotational stage in between the source and the detector, works perfectly for small and lighter objects, hence, it seems impossible to investigate complicated, bulky objects with interconnected unbalanced composites. Moreover, it will be very expensive to harness technologies into the rotational stage which can be incorporated into this conventional technique with an optimum degree of accuracy.

Therefore, this paper will consider the translational data acquisition scheme which is proven mathematically as an alternative method to the conventional technique [1]. This translational scheme takes into account the variations and the magnification of both the X-ray source and the detector around the object and then proceeded by scans from different focal distances. Python packages with necessary plugins were used in implementing the reconstructive algorithm generated in simulating and modelling a suitable image of inspected object.

1.Introduction

The embracement of X-ray computed tomography has widely gained grounds in the medical, scientific research and in the industrial field [1, 2]. Though this work is based on the translational data acquisition scheme for non-destructive testing in the industrial arena and many others. This paper cannot be complete without highlighting the conventional X-ray tomography data acquisition scheme (see Fig. 1) which prepared the foundation for other improved techniques but has its own limitations. For instance, the expensive resources that might be invested in building an advanced and bigger rotational stage to handle large-scale industrial objects, and larger flat panel screen detectors coupled with complications of technologies involved.

Despite all the effort and improvement in the conventional rotational data acquisition technique such as increasing the scan speed, most systems depend on a fan-beam type or cone beam geometry [3]. These developments enhance the acquisition of more than a slice in a single rotational scan through the test specimen. Hence, this is achieved by using multi-row or flat-panel detectors. However, there are several objects in situations which demand inspections for safety and for many reasons yet cannot be rotated due to the inaccessible positions they are located, size and many more.

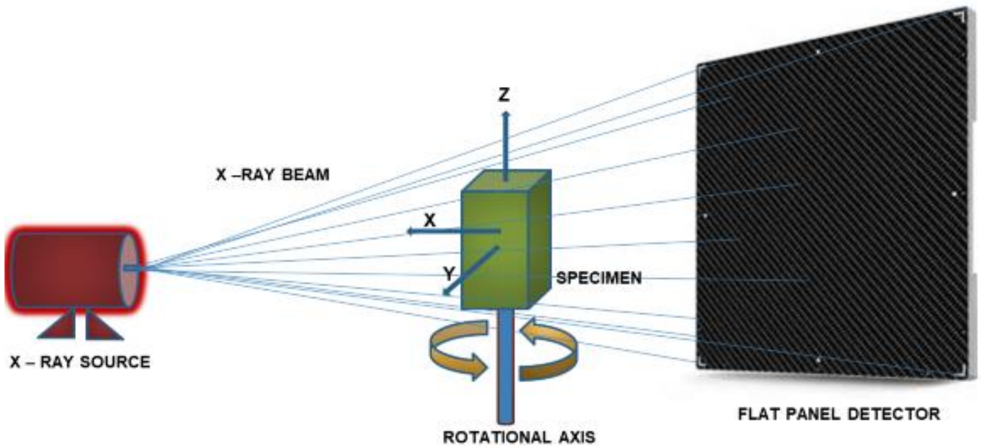

Figure 1. Scheme of the conventional data acquisition setup. During the industrial set-up of non-destructive testing, the object under inspection is mechanically rotated in between the X-ray source and the detector at specified angular interval to obtain certain angular range

2. Translational data acquisition scheme

However, these limitations come with higher expenses involved in handling large scale object using the conventional technique calls for a different technique, but similar end result known as the translational data acquisition scheme (see Fig.2) will be the core of this paper. In the translational data acquisition scheme technique, a rotational stage is not needed, since it involves the variation and changing of the focal distances and directions between the X-ray source and the detector only, hence the object under investigation is maintained in a stationary position. These are done for the purpose to obtain different ray paths and beam angles to acquire enough data for the image processing stage to give a detailed and brighter image at the end. For instance, the figure below illustrates a translational data acquisition scheme involving the linear translation of just the X-ray source.

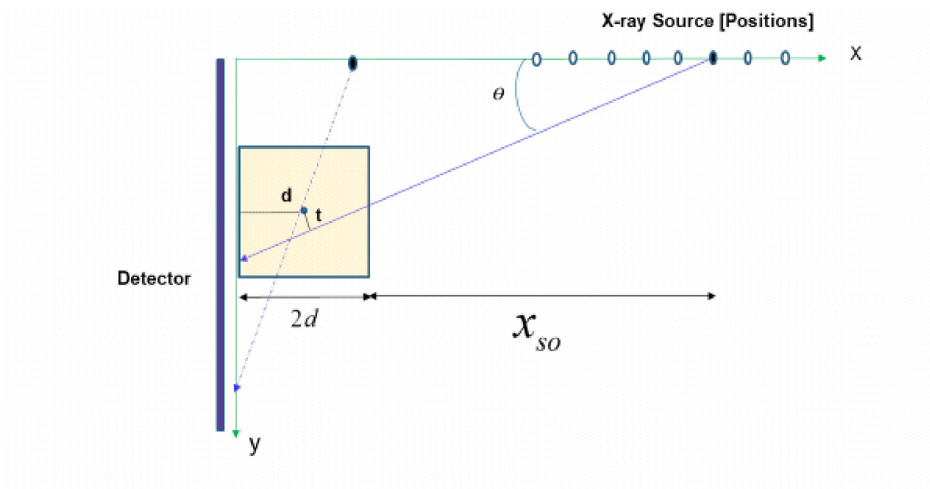

Figure 2. Scheme for translational data acquisition with linear translation involving only the source

From the scheme, scans were taken from different focal distances as well as directions as the X-ray source position was varied. This technique can be used to acquire data of larger and complicated objects compared to the classical method. The thick blue vertical line represents the detector and is positioned behind the object. The distance *d* of the object indicates the dimension of the cross-section that encompasses the measured field. Also, x_{so} represents the distance between the X-ray source and the object at a point of arrangement. However, the beam angles directed through the object varies as the source position is translated.

3. Simulation Results

Figure 3 below shows four scan images from different X-ray focal directions and the final reconstructed image. In reality, a single scan is not able to give an accurate and precise result as can be seen from the images *a*, *b*, *c*, and *d* individually. However, by adding the four separate images and reconstructing together based on pixel locations significantly yielded a more detailed and higher-quality result as can be observed from Fig. 3e. During the reconstruction of the images, a state-of-the-art python programming packages were used by implementing the filtered back-projection algorithm [4].

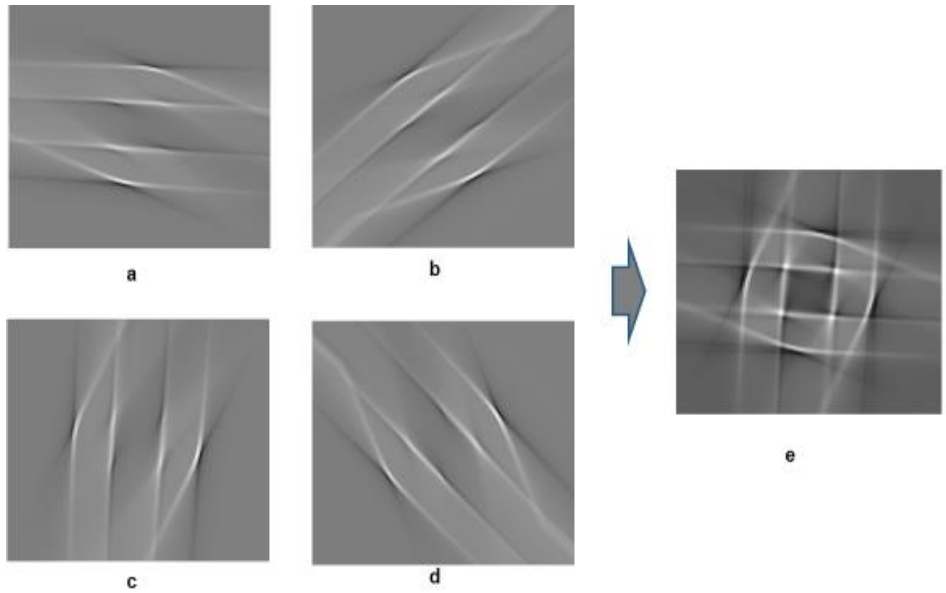

Figure 3. Reconstructions obtained from the translational data acquisition during four translations of the X-ray source only at angles of 0^0, 45^0, 90^0, 135^0 respective to the images *a*, *b*, *c*, and *d*; *e* is the resulting or reconstructed image obtained from joining the four pixel apportioning

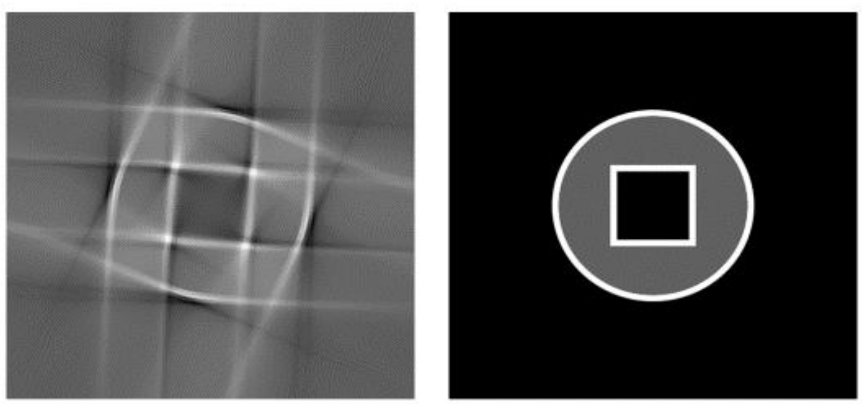

Figure 4. Schematic view of both final reconstructed image (left) and phantom (right)

Comparing the reconstructed image to the phantom as seen in Fig. 4 shows clearly that the more scans are taken from different focal directions and joined together during the reconstruction and image processing stage, the more detailed and closer the reconstructed image to that of the phantom.

4. Discussion

Figure 5 below is the schematic representation of the object under investigation which, when simulated with the simple filtered back-projection algorithms with the proposed translational based data acquisition technique, yields the simulated results as shown in Figure 3.

The filtered back-projection algorithms as an analytical reconstruction algorithm was established to overcome the limitations associated with the conventional back-projection. This reconstruction technique works well when enough data is available during the image processing stage. Also, it gets rid of blurring due to the application of vortex filters [5].

However, it considers ray sums obtained simultaneously at different angles with sine wave representations to compute the attenuation coefficients within a specified cross-section. Moreover, these computations are done and modeled using the python programming packages to generate the 3-dimensional analogue of the pixels (voxel).

There are several other ways such as the Algebraic Reconstruction Technique (ART), Fourier-domain Reconstruction Algorithm, Iterative Reconstruction Algorithm [6, 7] which can be applicable in sorting out the data and working with it to obtain an optimized algorithm which can be used to improve the reconstructed image. The ART implemented with the translational based data acquisition scheme as proposed and proven method led to a breakthrough in this approach to that of the classical method with its numerous limitations.

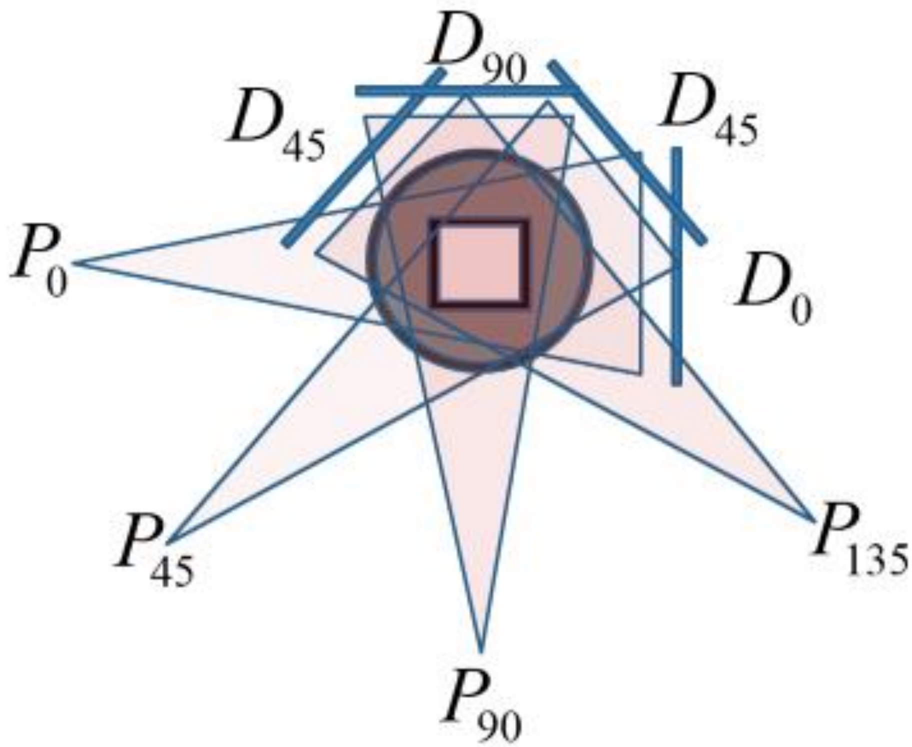

Figure 5. Schematic view of the setup involved in the translational based data acquisition technique

In Figure 5, projections were taken from four focal directions with an angular interval of x-ray beam propagation of 45^0 starting from 0^0 to 135^0. The $P_{0,}$ P_{45}, P_{90}, P_{135} are various angles the beams were directed from onto the detectors D_0, D_{45}, D_{90}, D_{135} respectively.

5. Summary

From our introductory simulations based on the filtered back-projection algorithms, it has proven to work with the translational based data acquisition scheme. However, it is projected to work perfectly involving other kinds of algorithms stated in the discussion. Therefore, our future research would be more focused on developing an alternative algorithm by combining the already existing ones to generate a mathematical model. This model would be expected to sort out acquired data better and with an optimized result of handling large-scale object using the translational based data acquisition scheme.

Acknowledgement

The reported study was partially supported by the Governmental program "Science", research project No. 11.6342.2017/8.9

References

1. Fuchs T., Schon T., Hanke R., A Translation-based Data Acquisition Scheme for Industrial Computed Tomography, ECNDT, 2010
2. Cantatore A., & Müller P., “Introduction to computed tomography”, DTU, Department of Mechanical Engineering, Denmark, 2011.
3. Avinash K., Malcolm S., “Principles of Computerized Tomographic Imaging”, [Electronic copy 1999] IEEE Press, ISBN 0-87942-198-3
4. Ozdiev, A., X-ray tomography simulation based on direct radon transform, Volume 743 KEM, 2017, Pages 445-448
5. URL: https://radiopaedia.org/articles/filtered-back-projection-1
6. Dudgeon and Mersereau (1984), “*Multidimensional digital signal processing”*Prentice-Hall.
7. A.C. Kak and M. Slaney, “Principles of Computerized Tomographic Imaging,” IEEE Press, 1988, Pages 49 – 63